Radio access mechanisms for massive machine communication in long-range wireless networks

Qipeng Song

IMT Atlantique
Bretagne-Pays de la Loire
École Mines-Télécom

UNIVERSITE BRETAGNE LOIRE

THÈSE / IMT Atlantique

sous le sceau de l'Université Bretagne Loire

pour obtenir le grade de

DOCTEUR D'IMT Atlantique

Spécialité : Informatique

École Doctorale Mathématiques et STIC

Présentée par

Qipeng Song

Préparée dans le département Systèmes réseaux, cybersécurité & droit du numérique

Laboratoire Irisa

Radio Access Mechanisms for Massive Machine Communication in Long-Range Wireless Networks

Thèse soutenue le 07 novembre 2017

devant le jury composé de :

Tijani Chahed
Professeur, Télécom SudPAris / président

Philippe Martins
Professeur, Télécom ParisTech / rapporteur

Martin Heusse
Professeur, Ensimag - Grenoble / rapporteur

Christophe Fourtet
Directeur scientifique, Sigfox - Labège / examinateur

Lina Mroueh
Maître de conférences, ISEP – Issy les Moulineaux / examinateur

Xavier Lagrange
Professeur, IMT Atlantique / examinateur

Loutfi Nuaymi
Maître de conférences (HDR), IMT Atlantique / directeur de thèse

Fabrice Valois
Professeur, Insa - Lyon / invité

I would like to dedicate this thesis to my family…

Declaration

I hereby declare that except where specific reference is made to the work of others, the contents of this dissertation are original and have not been submitted in whole or in part for consideration for any other degree or qualification in this, or any other university. This dissertation is my own work and contains nothing which is the outcome of work done in collaboration with others, except as specified in the text and Acknowledgements.

Qipeng Song
January 2018

Acknowledgements

I would like to express my deep gratitude to my supervisors Loutfi Nuaymi and Xavier Lagrange for their guidances during this thesis. They did not save any effort to scarify their skills and expertise for the benefit of my thesis. Their valuable comments and ideas have helped in enriching my thesis work and ameliorating its quality. Also, I'm very grateful to them for hosting me in ADOPNET team inside IMT Atlantique/IRISA research team in Rennes, France for three years. In this occasion, I would also like to thank all the researchers and all the members of ADOPNET team as well.

Furthermore, I would like to express my sincere gratitudes to the jury members. Their insightful questions and encouraging remarks on my work made my thesis defense a lifelong memory as well as a learning process. It is my utmost honor to have all these experts reviewing my work.

Moreover, my sincere thanks also go to my colleagues in RSM department: Saad, Francois Lemercier, Xavier Corbillon. I would never forget the days we worked together. Also, these years in Rennes, I made some very good friends like Yue Li, Yanhuang Li, Jialong Duan, Yangyang Chen, Wenjing Shuai, Yifan Zhou and Hao Lin. Because of you guys, I had a very colorful life, this would definitely be one of my best memories.

Last but not the least, I would like to thank my girl friend Yue Li, my parents Chun Song, Yufang Qi, Jinxi Li and Jing Wang, my elder sister Na Qi. No matter what decisions I have made, thank you for your endless love and support.

List of Publications

- Q. Song, X. Lagrange, and L. Nuaymi, "Evaluation of macro diversity gain in long range ALOHA networks," *IEEE Communications Letters*, 2017
- Q. Song, X. Lagrange, and L. Nuaymi, "An analytical model for S-ALOHA performance evaluation in M2M networks," in *2017 IEEE International Conference on Communications (ICC)*, pp. 1–7, May 2017
- Q. Song, L. Nuaymi, and X. Lagrange, "Survey of radio resource management issues and proposals for energy-efficient cellular networks that will cover billions of machines," *EURASIP Journal on Wireless Communications and Networking*, vol. 2016, no. 1, pp. 1–20, 2016
- Q. Song, L. Nuaymi, and X. Lagrange, "Evaluation of multiple access strategies with power control error and variable packet length in M2M," in *Wireless Communications and Networking Conference Workshops (WCNCW), 2016 IEEE*, pp. 379–384, IEEE, 2016
- Q. Song, X. Lagrange, and L. Nuaymi, "An efficient M2M-oriented network-integrated multiple-period polling service in LTE network," in *IEEE 82nd Vehicular Technology Conference, VTC Fall 2015, Boston, MA, USA, September 6-9, 2015*, pp. 1–6, 2015

Abstract

As a key step toward a smart society, apart from the Human-to-Human (H2H) communication, the future wireless networks, are expected to accommodate Machine-to-Machine Communication (also known as Machine Type Communication (MTC)). The latter is a new communication paradigm in which the devices can talk with each other without or with little human intervention. With the rapid proliferation of M2M applications, a huge number of devices will be deployed in many types of use cases such as smart metering, industry automation, e-health, etc.

However, the current wireless networks are still not ready to hold traffic from MTC. The reason is twofold. First, the evolution of the wireless network seeks for higher throughput and lower latency. Second, the special features that MTC exhibits, such as huge number of deployed devices, small payload but frequent transmission, adverse installation location, etc., lead to that the requirements by H2H are no longer required by most of M2M use cases.

From the state-of-the-art work, we find that two possible research orientations to efficiently handle M2M traffic: Low Power Wide Area Network (LPWAN) and adaption of the existing cellular networks. For both of them, the radio access mechanisms, used in Radio Access Network (RAN), is vitally important to make MTC a promising technology. From this view, radio access mechanism is the main focus of our studies. In this thesis, we present the contributions covering the aforementioned aspects: performance evaluation of ALOHA-based LPWAN networks, and a polling service that is an extension to RAN of LTE networks for periodic M2M traffic.

The contributions of this thesis are summarized on the following axis:

- We make a survey about the energy efficiency related studies in the literatures. The main contribution in this survey is to review, classify the existing research works into different categories, and compare the pros and cons between categories. We also review the advances of the LPWAN related study.
- We study the impact of transmit power level diversity and imperfect power control to the slotted ALOHA based LPWAN systems. Some insightful design guidelines are obtained by manipulating the established analytical model.

- We study the performance of LPWAN system with macro reception diversity. By stochastic geometry, we get simple closed-form formulas for the packet loss rate and spatial throughput. These formulas are very useful to analyze LPWAN networks (especially in urban areas) and to quantify the system capacity gain. By gathering several available results about the analysis of non slotted ALOHA, we finally get a synthesis framework to study the RAN of LPWAN.
- In terms of adaptations to RAN of LTE networks, we first analyze the conventional random access mechanism in LTE and identify the existing inefficiencies. We then propose a multiple period polling service for periodic M2M use cases. The proposed service is compared with conventional random access mechanism in LTE in a fluid model. The numerical results show that the proposed service dramatically reduces the consumption of system resources such as Radio Network Temporary Identifier (RNTI), Resource Block (RB) and has a higher energy efficiency due to the avoidance of random access procedure and related signaling messages.

Abstract

En tant qu'étape importante vers une société intelligente, hormis la communication d'humain à humain (H2H), les réseaux sans fil de l'avenir devraient prendre en charge la communication machine-à-machine (également connue sous le nom de MTC). Ce dernier est un nouveau paradigme de communication dans lequel les terminaux peuvent parler les uns avec les autres sans ou avec peu d'intervention humaine. Avec la prolifération rapide des applications M2M, un grand nombre de terminaux seront déployés dans de nombreux types d'applications telles que le comptage intelligent, l'automatisation de l'industrie, la télésanté, etc.

Cependant, les réseaux sans fil actuels ne sont toujours pas prêts pour écouler correctement le trafic des MTC. La raison en est double. Tout d'abord, l'évolution du réseau sans fil vise à augmenter le débit et à réduire le délai. Deuxièmement, les caractéristiques spéciales des MTC, telles qu'un nombre très élevé de terminaux déployés, une petite charge utile mais une transmission fréquente, un emplacement souvent d'installation défavorable, etc., font que les exigences de H2H ne sont pas partagés par la plupart des cas d'utilisation M2M.

À partir de l'état de l'art, nous distinguons deux orientations de recherche possibles pour gérer efficacement le trafic M2M: Low Power Wide Area Network (LPWAN) et adaptation des réseaux cellulaires existants. Pour les deux pistes, les mécanismes d'accès radio, utilisés dans le réseau d'accès radio (RAN) sont d'une importance vitale pour assurer le succès de MTC. De ce point de vue, le mécanisme d'accès radio est le principal objectif de nos études. Dans cette thèse, nous présentons les contributions couvrant les aspects susmentionnés.

Les contributions de cette thèse sont résumées dans les points suivants:

- Nous faisons état de l'art sur les études liées à l'efficacité énergétique des MTC de la littérature. La contribution principale de cette enquête est de passer en revue, classifier les travaux de recherche existants dans différentes catégories, et de comparer les avantages et les inconvénients entre les catégories. Nous parlons également des progrès de l'approche basée sur les LPWAN.

- Nous étudions l'impact de la diversité du niveau de puissance d'émission et du contrôle de puissance imparfait sur les systèmes LPWAN en slotted-ALOHA. Quelques directives de conception perspicaces sont obtenues en manipulant le modèle analytique établi.
- Nous étudions les performances du système LPWAN avec la diversité de la réception macro. En utilisant la géométrie stochastique, nous établissons des formules simples de forme fermée pour le taux de perte de paquets et le débit spatial. Ces formules sont très utiles pour analyser les réseaux LPWAN (en particulier dans les zones urbaines) et pour quantifier le gain de capacité du système. En rassemblant plusieurs résultats disponibles sur l'analyse de l'ALOHA pure, nous obtenons finalement un cadre de synthèse pour étudier le RAN de LPWAN.
- En termes d'adaptations au RAN des réseaux LTE, nous analysons d'abord le mécanisme d'accès aléatoire conventionnel dans LTE et identifions les inefficacités existantes. Nous proposons ensuite un service d'interrogation multipériodique pour les cas d'utilisation M2M périodiques. Le service proposé est comparé au mécanisme d'accès aléatoire conventionnel en LTE dans un modèle fluide. Les résultats numériques montrent que le service proposé réduit considérablement la consommation des ressources système telles que l'identificateur temporaire de réseau radio (RNTI), le bloc de ressources (RB) et a une efficacité énergétique supérieure en raison de l'évitement de la procédure d'accès aléatoire et des messages de signalisation associés.

Table of contents

List of figures xxi

List of tables xxv

Glossary xxvii

1 Introduction 1

1.1 Motivations . . . 1

1.2 Contributions and Organization of Manuscript . . . 2

1.2.1 A Survey about energy-efficiency for M2M-included wireless networks . . . 3

1.2.2 Performance evaluation of transmit power diversity and imperfect power control in S-ALOHA based LPWAN networks . . . 3

1.2.3 Performance analysis of macro reception diversity in large-scale ALOHA Network . . . 4

1.2.4 A periodic polling service in LTE network to support periodic M2M traffic . . . 5

2 M2M overview: Applications, Architecture and Energy efficiency Related Research 7

2.1 M2M Applications, Classifications and QoS requirements . . . 7

2.1.1 Classification according to reliability and quantity of connected machines . . . 9

2.1.2 Classification according to the level of mobility and dispersion . . . 10

2.1.3 Classification according to delay tolerance level . . . 10

2.1.4 Classification according to data reporting mode . . . 11

2.1.5 QoS feature for typical M2M applications . . . 11

2.2 M2M Traffic Characterization . . . 11

2.3 M2M Related Standardization Efforts . . . 12

2.4 M2M Communications architecture . . . 14
2.4.1 ETSI M2M reference architecture . . . 15
2.4.2 oneM2M reference architecture . . . 15
2.4.3 3GPP reference MTC architecture . . . 17
2.5 Low Power Wide Area network . . . 18
2.6 M2M Related Energy Efficiency Studies . . . 22
2.6.1 Cooperative Relaying . . . 22
2.6.2 Design of energy efficient signaling and operation . . . 26
2.6.3 Radio resource allocation and packet scheduling strategies . . . 27
2.6.4 Energy-efficient random access procedure and MAC . . . 28
2.7 Summary . . . 31

3 Performance Evaluation of Transmit Power Diversity in S-ALOHA based Systems 33
3.1 Introduction . . . 33
3.2 Related work . . . 34
3.3 System Model . . . 35
3.3.1 Retransmission Mechanism . . . 35
3.3.2 Transmission Power Diversity Strategy . . . 35
3.3.3 Capture Effect . . . 36
3.3.4 Performance Metrics . . . 37
3.4 Ideal systems with perfect power control . . . 38
3.5 Wide band Systems with Imperfect Power Control . . . 39
3.6 Narrow band Systems with Imperfect Power Control . . . 42
3.7 Simulation results and discussion . . . 44
3.7.1 Accuracy of proposed models . . . 44
3.7.2 Evaluation for wide band systems with imperfect power control . . . 45
3.7.3 Evaluation for narrow band systems with imperfect power control . . . 51
3.8 Summary . . . 51

4 Performance Evaluation of macro reception diversity in large-scale ALOHA networks 57
4.1 Introduction . . . 57
4.2 State of the Art . . . 59
4.2.1 Fundamental Concepts and Theorems of Stochastic Geometry . . . 59
4.2.1.1 Point process and Poisson point process . . . 59
4.2.1.2 Useful theorems . . . 61

4.2.2 Use of stochastic geometry for the performance analysis of wireless networks . . . 62
4.3 System model . . . 63
4.3.1 Distribution of Nodes and Traffic Model . . . 63
4.3.2 Slotted ALOHA and Pure ALOHA . . . 63
4.3.3 Random Channel and Capture Effect . . . 64
4.3.4 Association Policy and Displacement Theorem . . . 65
4.4 Link-level Transmission Success Probability . . . 65
4.4.1 Slotted ALOHA . . . 66
4.4.2 Pure ALOHA, average interference . . . 67
4.4.3 Pure ALOHA, maximum interference . . . 67
4.4.4 Generalized model . . . 67
4.5 Network Level Performance Without Retransmission . . . 68
4.5.1 Best BS attach method . . . 69
4.5.1.1 With background noise and γ=4 . . . 69
4.5.1.2 Without Background Noise . . . 69
4.5.2 Nearest BS attach method . . . 70
4.5.3 Selective Combining Macro Diversity . . . 73
4.5.3.1 With Background Noise and $\gamma = 4$ . . . 74
4.5.3.2 Without Background Noise . . . 74
4.5.4 Maximum Ratio Combining Macro diversity . . . 75
4.5.4.1 A special case, $\gamma = 4$, without background noise . . . 78
4.5.5 Simulation Results and Discussion . . . 79
4.5.5.1 Packet loss Rate . . . 79
4.5.5.2 Maximum Normalized Load . . . 82
4.5.5.3 Spatial Throughput . . . 82
4.6 Network Level Performance with Outage Probability Constraint . . . 83
4.6.1 Best BS Attach . . . 84
4.6.2 With background noise, $\gamma = 4$ . . . 84
4.6.3 Without background noise . . . 85
4.6.4 Selective Combining Macro Reception Diversity . . . 85
4.6.5 Numerical Results and Discussion . . . 86
4.7 Network Level Performance with Retransmission Mechanism . . . 88
4.7.1 Selective Combining based Macro Diversity . . . 90
4.7.2 Numerical Results and Discussions . . . 90
4.8 Summary . . . 91

5 M2M-oriented network-integrated multiple-period polling service in LTE networks **93**
5.1 Introduction . . . 93
5.2 Related work and motivation . . . 94
5.3 MTC device data upload procedure in LTE . . . 95
5.3.1 Random access procedure . . . 97
5.3.2 Transmission of data packet . . . 98
5.3.3 RRC Connection Release . . . 98
5.4 Network integrated M2M-oriental polling service . . . 98
5.4.1 Terminology Related to the Proposed Service . . . 99
5.4.1.1 LSFN . . . 99
5.4.1.2 PRD-RNTI . . . 99
5.4.1.3 Polling period . . . 100
5.4.1.4 Polling window . . . 100
5.4.2 Multiple-period polling mechanism . . . 101
5.4.2.1 Registration stage . . . 101
5.4.2.2 Periodic polling stage . . . 101
5.4.3 RNTI allocation algorithm . . . 101
5.4.4 An example . . . 103
5.5 Performance Analysis . . . 104
5.5.1 System model . . . 105
5.5.2 Lower bound of RNTI Consumption . . . 106
5.5.2.1 Our proposal . . . 106
5.5.2.2 Random access method . . . 106
5.5.3 Resource Blocks Consumption . . . 108
5.5.3.1 Downlink Resource Block Consumption . . . 109
5.5.3.2 Uplink Resource Block Consumption . . . 111
5.5.4 Uplink Energy efficiency ratio . . . 112
5.6 Numerical results and Discussions . . . 113
5.6.1 RNTI consumption . . . 114
5.6.1.1 Log-normal distribution . . . 114
5.6.1.2 Uniform distribution . . . 114
5.6.1.3 Traffic Model [6, Annex E] . . . 115
5.6.2 Resource Block Pairs Consumption . . . 116
5.6.2.1 Downlink RB pairs consumption . . . 116
5.6.2.2 Uplink RB pairs consumption . . . 118

5.6.3 Uplink Energy Efficiency Ratio 118
5.7 Summary 120

6 Conclusions and Future Work 123
6.1 Major Contributions 123
6.1.1 A Survey about energy efficiency for M2M-included wireless networks 123
6.1.2 Performance of transmit power diversity and imperfect power control in S-ALOHA based LPWAN networks 124
6.1.3 Performance analysis of macro reception diversity in large-scale ALOHA Network 124
6.1.4 A periodic polling service in LTE network to support periodic M2M traffic 125
6.2 Future Works 126
6.2.1 Optimum transmit power diversity strategy and topology-aware modeling 126
6.2.2 Extension of analysis about macro reception diversity 126
6.2.3 Advanced RNTI or radio resource allocation algorithm 126

References 129

Appendix A Proof of Lemmas and theorems used in this thesis 139

Appendix B Mécanismes d'accès radio pour la télécommunication de type machine massive dans les réseaux sans fil à longue portée 145
B.1 Contexte de la thèse 145
B.2 Contributions 146
B.3 Analyse de la diversité de la puissance d'émission dans S-ALOHA LPWAN 147
B.4 Analyse de la diversité macro dans les réseaux LPWAN 149
B.5 Service d'interrogation multi-périodes dédié à M2M périodique dans les réseaux LTE 150

List of figures

1.1 Global Mobile M2M Connections by 2G, 3G, 4G+ and LPWA. Source: [7] 2

2.1 Coexistence of MTC and HTC in the future LTE networks 8
2.2 M2M applications taxonomy by mobility and dispersion. Source: [8] 10
2.3 ETSI reference M2M communication architecture. (Modified based on [9]) 16
2.4 oneM2M reference functional M2M architecture. Source: [10] 17
2.5 3GPP reference MTC architecture. (based on [11]) 18
2.6 LoRaWAN network architecture. (based on [12]) 20
2.7 Illustration of M2M devices clustering 24
2.8 Un-peer2peer cellular MTC architecture with M2M Facilitator. Source: [13] 25

3.1 The transition of transmission power level diversity 36
3.2 Packet loss rate with different transmit power diversity strategies and capture ratios in S-ALOHA based ideal systems 46
3.3 Packet loss rate with different transmit power diversity strategies and capture ratios in S-ALOHA wide-band systems 46
3.4 Packet loss rate with different transmit power diversity strategies and capture ratios in S-ALOHA networks that suffer from fading and imperfect power control 47
3.5 Performance comparison with different transmit power diversities and power control precisions in wide band systems. SINR threshold 3 dB 48
3.6 Performance comparison with different transmit power diversities and power control precisions in wide band systems. SINR threshold 0 dB 49
3.7 Performance comparison with different transmit power diversities and power control precisions in wide band systems. SINR threshold -3 dB 50
3.8 Performance comparison with different transmit power diversities and power control precisions in narrow band systems. SINR threshold 3 dB 52

3.9 Performance comparison with different transmit power diversities and power control precisions in narrow band systems. SINR threshold 0 dB 53
3.10 Performance comparison with different transmit power diversities and power control precisions in narrow band systems. SINR threshold −3 dB 54

4.1 Selective Combining (SC) Macro Reception Diversity Scheme Illustration. Each BS is equipped with a packet decode function. The decoded packet is sent to the core network and the latter is in charge of duplicated packets . . 58
4.2 Maximum Ratio Combining (MRC) Macro Reception Diversity Scheme Illustration 59
4.3 A realization of Poisson point process 61
4.4 Comparison between approximation formula (4.21) and Monte-Carlo simulation result. 72
4.5 Network packet loss rate with respect to normalized load $p\lambda_m/\lambda_b$ (ANA=analytical, SIM=simulation) for slotted ALOHA 80
4.6 Network packet loss rate with respect to normalized load $p\lambda_m/\lambda_b$ (ANA=analytical, SIM=simulation) for pure ALOHA with advanced transmission techniques. 81
4.7 Network packet loss rate with respect to normalized load $p\lambda_m/\lambda_b$ (ANA=analytical, SIM=simulation) for pure ALOHA without advanced transmission techniques. 81
4.8 Spatial throughput with respect to normalized load 83
4.9 Minimum BS spatial density with respect to network load. The target packet loss rate and outage probability threshold are both 10%. 88
4.10 Minimum BS spatial density with respect to network load. The target packet loss rate is 10% and outage probability threshold is 1%. 89
4.11 Network packet loss rate with respect to fresh normalized load $p\lambda_m/\lambda_b$ for pure ALOHA. Each packet is always transmitted $N_{\max}$ times. 91

5.1 Periodic M2M application work flow 95
5.2 Conventional random access and data upload procedure in LTE networks . . 96
5.3 Construction of LSFN 99
5.4 Illustration of Polling window in time domain 100
5.5 Proposed polling service work flow 102
5.6 Illustration of RNTI allocation result 104
5.7 The studied hexagonal grid network topology 105
5.8 Comparison of RNTI required for case of log-normal distribution 114
5.9 Comparison of RNTI required for case of uniform distribution 115

5.10 Comparison of RNTI required for the traffic model proposed by 3GPP . . . 115
5.11 Signaling overhead in terms of consumed RB pair number with respect to uplink reporting packet size . . . 119
5.12 Average RB occupation ratio within a traffic model [6, Annex E] . . . 119
5.13 Energy efficiency ratio with respect to uplink reporting packet size . . . 120

B.1 Comparaison de performances entre différentes stratégies de diversités de puissance de transmission dans des systèmes à large bande. SINR seuil 3 dB 148
B.2 Illustration de diversité de réception macro de type combinaison sélective (SC). Chaque BS est équipée d'une fonction de décodage de paquet. Le paquet décodé est envoyé au coeur du réseau et ce dernier est en charge des paquets dupliqués . . . 149
B.3 Illustration de diversité de réception macro de type combinaison de taux maximum (MRC) . . . 150
B.4 Illustration du service d'interrogation proposé . . . 152

List of tables

2.1 MTC applications categorization (Non-exhaustive) according to [14][15][16] 8
2.2 Typical M2M applications and their QoS Requirements 12
2.3 Difference Between MTC and HTC 13
2.4 The comparison among LPWAN solutions (All solutions are on ISM band, extracted from [17]) 19
2.5 Categorization and comparison of energy/power saving-related proposals . 23

3.1 Packet loss rate ratio between simulation and analytical results. Capture ratio: 3 dB. P_{sim}:packet loss rate by simulation. P_{ana}: packet loss rate from analytical model 45

4.1 Maximum normalized load under packet loss rate 10% and corresponding diversity gain with 8 dB shadowing 82
4.2 Parameter values for numerical results 87

5.1 Polling window allocation resume 104
5.2 Transport block size with respect to TBS index and number of RB pair. Source: [18, Tab. 7.1.7.2.1-1] 109
5.3 Parameter Values for Numerical Results 113
5.4 RRC messages exchanged between UE and the eNB (unit: bit) 116
5.5 SNR threshold and distance for message *ConnectionReconfiguration* 117
5.6 RB pairs number and relative distance interval for message *ConnectionReconfiguration* 118

Glossary

3GPP 3rd Generation Partnership Project.

BPP Binomial Point Process.

CDF Cumulative Distribution Function.

D2D Device-to-Device Communication.

ETSI European Telecommunications Standards Institute.

GSM Global System for Mobile communication.

H2H Human-to-human Communication.

HTC Human Type Communication.

LPWAN Low Power Wide Area Network.

LT Laplace Transformation.

LTE Long Term Evolution.

LTE-A Long Term Evolution Advanced.

M2M Machine-to-machine Communication.

mMTC Massive Machine Type Communication.

MTC Machine-to-Machine Communication.

OFDMA Orthogonal Frequency-Division Multiple Access.

PDCP Packet Data Convergence Protocol.

PDF Probability Density Function.

PGFL Probability Generating FunctionaL.

PPP Poisson Point Process.

PRD-RNTI Periodic Radio Network Temporary Identifier.

QoS Quality of Service.

RAN Radio Access Network.

RB Resource Block.

RNTI Radio Network Temporary Identifier.

RRC Radio Resource Control.

SDO Standard Development Organization.

SINR Signal to Interference Noise Ratio.

TTI Transmission Time Interval.

uMTC Utra-reliable Machine Type Communication.

Chapter 1

Introduction

1.1 Motivations

Machine-to-machine Communication (M2M), also known as Machine-to-Machine Communication (MTC) in 3rd Generation Partnership Project (3GPP)'s terminology, is an emerging technology allowing devices to mutually communicate without (or only limited) human intervention. It is expected to become more popular in the next decade and be an integrated part of future wireless networks [14][19]. As an example, Ericsson estimates that 50 billion MTC devices will be connected to wireless networks by 2020, among which 2 billion will be served by cellular networks [20].

In opposite to the traditional H2H or Human Type Communication (HTC), MTC presents lots of its own special characteristics. These features are uplink-centric applications, short but more frequent transmission, large number of devices, difficulty to change battery and so on [21]. The aforementioned characteristics pose problems for current deployed wireless systems to handle the traffic from MTC. For example, large number of deployed devices can quickly congest the radio access network, leading to high collision and retransmission rate and low energy efficiency. However, theses devices usually has no power supply and cannot be easily replaced with new battery. Hence, how to efficiently support a huge amount of devices is of a paramount concern for the mobile network operators.

Nowadays, the research efforts to tackle with MTC traffic in the future wireless networks, can be broadly classified into two categories:

- Design from scratch of M2M-dedicated wide area networks, i.e., the emerging Low Power Wide Area Network (LPWAN). A representative example is the LoRaWAN [12] proposed by LoRa Alliance [22];

- Evolution from existing wireless networks, which consists in adapting 3GPP cellular networks to support MTC traffic in addition to H2H traffic, for example the LTE-M [23].

According to Cisco's forecast [7], LPWAN[1] and evolved 3GPP networks will have a dominant role for handling MTC traffic in future. It is expected that 29% of MTC devices will be served by LPWAN networks and 71% of MTC connections will be served by 3GPP networks (including 2G/3G/4G, shown in Fig. 1.1). Actually, both solutions have their own advantages and shortcoming. 3GPP cellular networks, compared with LPWAN networks, have ubiquitous coverage, largely deployed infrastructure, mature user subscription/management system and so on, but they are not easy to be adapted to handle MTC due to compatibility to the H2H. LPWAN networks are designed for MTC and thus energy efficient compared with cellular networks, but need huge investment to deploy the dedicated MTC infrastructure. Both types of networks will coexist for a long term.

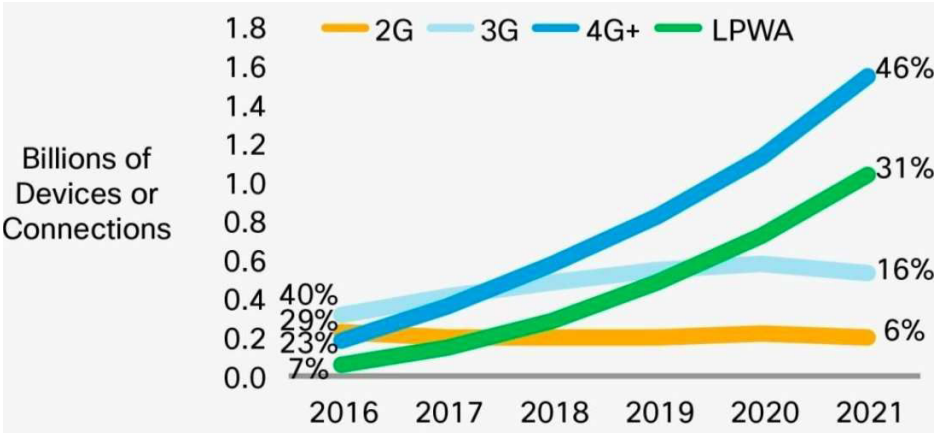

Fig. 1.1 Global Mobile M2M Connections by 2G, 3G, 4G+ and LPWA. Source: [7]

No matter for which research direction, the performance of radio access mechanism, used in Radio Access Network (RAN), is vitally important to guarantee lower collision rate and higher energy efficiency. Hence, the performance of radio access mechanism in M2M-compatible wireless networks is the main focus of our studies.

1.2 Contributions and Organization of Manuscript

To efficiently supporting the huge number of MTC devices in wireless networks, it is necessary and meaningful to establish not complicated but still accurate analytical models. The

[1] The abbreviations LPWAN and LPWA are interchangeably used in this thesis

latter allows to evaluate the performance of RAN and derive some insightful design guidelines for M2M-included wireless networks.

From our studies, we try to answer the questions including but not limited to: for cellular networks, how to leverage the widely deployed LTE/LTE-A system to support energy efficiency constraint M2M application? Given that LPWAN system leverages macro reception diversity[2] but use non slotted ALOHA, what is the performance gain compared with slotted system? If the transmit power are different between transmissions, what's the performance gain in slotted ALOHA based LPWAN? Which is the better choice for M2M systems? These issues are still not fully investigated in the literature. The contributions of this thesis can be summarized into four parts described in the following.

1.2.1 A Survey about energy-efficiency for M2M-included wireless networks

We make a survey that provides a global view of the network technologies for M2M in wireless networks. In this survey, we study the classifications of M2M applications and compare traffic characteristics between M2M and H2H. Quality of Service (QoS) requirements for typical M2M applications are resumed. The advances of reference M2M network architectures proposed by the Standard Development Organization (SDO) are investigated. As the main part of this survey, we review, compare and categorize the proposals related to energy issues of cellular M2M mainly over the period from 2011 to 2016. We also present the development of LPWAN networks. Finally, we observe that the cooperative relaying, the design of energy-efficient signaling and operation, the new radio resource allocation schemes, and the energy-efficient random access procedure are the main points of improvement. Besides, it is also necessary and meaningful to leverage mathematical tools, such as game theory, stochastic geometry, etc., for topology-aware modeling, analysis and design of future M2M-included wireless networks. This part of work has been published in the journal EURASIP [3] and presented in Chapter 2.

1.2.2 Performance evaluation of transmit power diversity and imperfect power control in S-ALOHA based LPWAN networks

The S-ALOHA (i.e. slotted-ALOHA) protocol is recently regaining interest in the study of Low Power Wide Area Networks (LPWAN) to handle M2M traffic. Despite intensive studies since the birth of S-ALOHA, the special features of M2M traffic and requirements

[2]This concept will be explained in detail in Chapter 4.

highlight the importance of analytical models taking into account performance-affecting factors and giving a thorough performance evaluation.

Our contribution is to fulfill such a necessity: we jointly consider the impact of capture effect, diversity of transmit power levels with imperfect power control. We propose a low-complexity but still accurate analytical model capable of evaluating S-ALOHA in terms of packet loss rate, throughput, energy-efficiency and average number of transmissions. The proposed model is able to facilitate dimensioning and design of S-ALOHA based LPWAN. The comparison between simulation and analytical results confirms the accuracy of the proposed model.

Some design guidelines about S-ALOHA based LPWAN deduced from our model are: the imperfect power control can have positive consequence with capture effect and appropriate transmit power diversity strategy. The transmit power diversity strategy should be determined by jointly considering network load level, power control precision and SINR threshold to achieve optimal performance of S-ALOHA. This work has been published in ICC 2017 [2] and is presented in Chapter 3.

1.2.3 Performance analysis of macro reception diversity in large-scale ALOHA Network

In cellular networks, the packet is sent in unicast mode: the destination Base Station (BS) is indicated by the terminal. However, it also could be sent in broadcast mode, and benefit from macro reception diversity. The latter is a capability that a wireless network has, allowing each device transmit messages in an omni-direction way without attach procedure. All the BS are the potential receivers of any sent message. Each BS autonomously demodulates and decodes the packets. The network is able to remove the duplicated received messages.

Due to its advantages, BS reception diversity has been applied by some Lower Power Wide Area Networks, such as Sigfox and LoRaWAN [24]. We propose a tractable model to evaluation the gain brought by this capability, under fading and shadowing effect, in large wireless network with stochastic geometry. We get simple closed-form formulas for the packet loss rate. These formulas are very useful to analyze LPWAN networks and to quantify the gain brought by macro-diversity. Secondarily, we gathered several available results about the analysis of ALOHA. This synthesis can be interesting for the scientific community. This work has been published in IEEE Communication Letters [1] and is presented in Chapter 4.

1.2.4 A periodic polling service in LTE network to support periodic M2M traffic

The last contribution is a proposal in LTE/LTE-A networks to handle MTC traffic. It is known that LTE/LTE-A networks are designed to well meet the human-to-human (H2H) communication. Unfortunately, current LTE random access procedure is not able to efficiently handle MTC traffic.

As a first step, we analyze traditional random access procedure and identify its inefficiency for M2M use case. We then propose a polling service that avoids contention. This service is integrated into LTE access network, fully compatible with the standard access mechanism and able to manage a large range of polling periods (typically from 1 minute to 28 days). This proposed service reduces the transmission overhead and thus improves the energy efficiency for MTC devices. It also reduces access network overload in radio access network by avoiding random access.

Traditional random access mechanism and our proposal are compared in terms of RNTI (Radio Network Temporary Identifier) and RB (Resource Block) consumption. The numerical results show that with the proposed service one eNodeB (eNB) can easily support up to 15000 MTC devices without network access collision. In terms of RB consumption, during each message upload, our proposal saves 5.76 pairs of RB for the downlink signaling and 3 pairs of RB for uplink signaling. This work has been presented in VTC Fall 2015 [5] and is presented in Chapter 5.

Chapter 2

M2M overview: Applications, Architecture and Energy efficiency Related Research

In this chapter, we present the state-of-the-art work of this thesis. Therefore, the objective of this chapter is to give an overview about M2M, compare and categorize existing M2M-related energy efficiency proposals before presenting out contributions. We also review the advances of Low Power Wide Area networks, which are MTC-dedicated networks, and today are experiencing a rapid development. The rest of this article is organized as follows. Section 2.1 presents the typical cellular M2M applications and several classifications according to different criteria, introduces a QoS requirement table for some typical cellular M2M applications. Section 2.2 compares the differences between H2H and M2M in terms of traffic characteristics. Section 2.4 first talks about conventional M2M solutions in cellular networks then presents the advance of reference M2M network architecture. Section 2.5 resumes the development of Low Power Wide Area networks. Section 2.6 presents, categorizes and compares all found proposals related to energy issues for MTC in cellular networks. Section 2.7 gives the conclusions obtained from this survey.

2.1 M2M Applications, Classifications and QoS requirements

M2M communication is expected to be an integrated part of the future wireless networks. For example, a future LTE network will see the coexistence of MTC and HTC as what is shown in Fig. 2.1. The types of M2M applications are varied, including but not limited to

security, intelligent transport system, payment, health, remote maintenance/control, metering, bicycle sharing system [8], logistics application, insurance [8]. In Tab. 2.1, we resume the M2M applications listed by 3GPP.

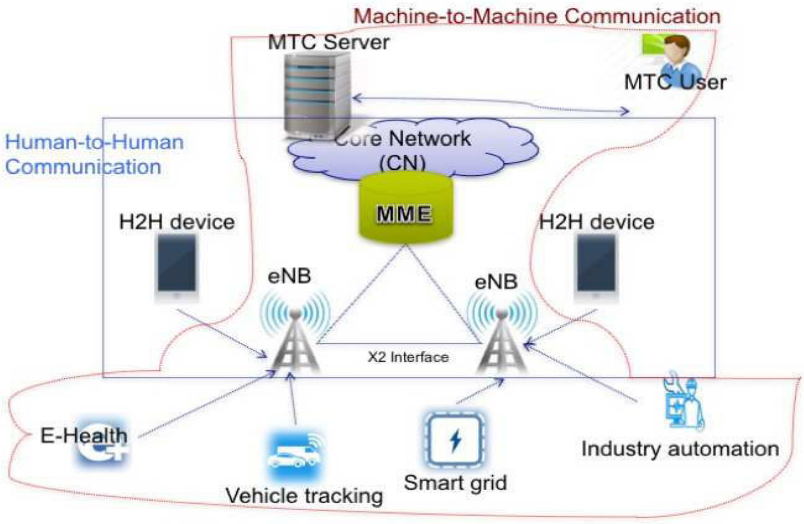

Fig. 2.1 Coexistence of MTC and HTC in the future LTE networks

Given that M2M applications are so varied, it seems very difficult to end up with developing a unique platform to support all these applications in an economical way. For example, the metering device is desired to be simple but the video surveillance device needs different and powerful codec, different protocols and should have different radio capabilities. If only one solution or hardware platform is adopted for all the services, the consequence is a MTC machine with the high complexity, which is like a smart phone today [25]. Thus, it is important to classify the existing M2M applications and propose improvement according to different requirements. In addition, an appropriate M2M classification helps identify QoS features and other works. In this section, we present all classification schemes found in the literature, each of which may serve for specific research purpose.

Table 2.1 MTC applications categorization (Non-exhaustive) according to [14][15][16]

service area	MTC applications
Security	Surveillance systems Backup for landline Control of physical access Car/driver security
Intelligent Transport system	Fleet management

	Assess tracking Navigation Traffic information Road tolling
Payment	Point of sales Vending machine Gaming machines
Health	Monitoring vital signals Supporting the aged or handicapped Web access telemedicine points Remote diagnostics
Remote maintenance/control	Elevator control Lighting Pumps Industrial automation Vehicle diagnostics
Metering	Power/Gas/Water Heating Grid control Industrial metering
Other futuristic applications	Information ambient society Robotic applications Environment monitoring

2.1.1 Classification according to reliability and quantity of connected machines

According to reliability and quantity of connected machines, the project METIS divides M2M applications into two categories: Massive Machine Type Communication (mMTC) and Utra-reliable Machine Type Communication (uMTC) [26]. mMTC refers to massive MTC and provides connectivity for a large number of cost and energy-constrained devices. Sensor and actuator deployments can be in a wide-area for surveillance and area-covering

measurements, but also co-located with human users, as in body-area networks. The main attribute of this service is the massive number of connected devices, where the required rates decrease as the number of devices grows significantly. uMTC addresses the needs for ultra-reliable, time-critical services, e.g., V2X (Vehicle-to-Vehicle/Infrastructure) applications and industrial control applications. Both examples require reliable communication and V2X additionally requires fast discovery and communication establishment. The main attribute is high-reliability, while the number of devices and the required data rates are relatively low.

2.1.2 Classification according to the level of mobility and dispersion

According to the level of mobility and dispersion, M2M applications also could be categorized into four categories: dispersed and fixed application, dispersed and mobile application, concentrated and fixed application, concentrated and mobile application [8]. The dispersion refers to the area that the M2M devices are spread out over. The mobility measures whether the device is stationary or whether it needs to move around. The typical example for dispersed and fixed application is smart grid where sensors are deployed in a large scale at a fixed location. Logistic applications are representative for dispersed and mobile application. For example, the sensors to track the cargo in the container may spread and move anywhere. Fig. 2.2 shows the result of classification for some typical M2M applications according to this criterion.

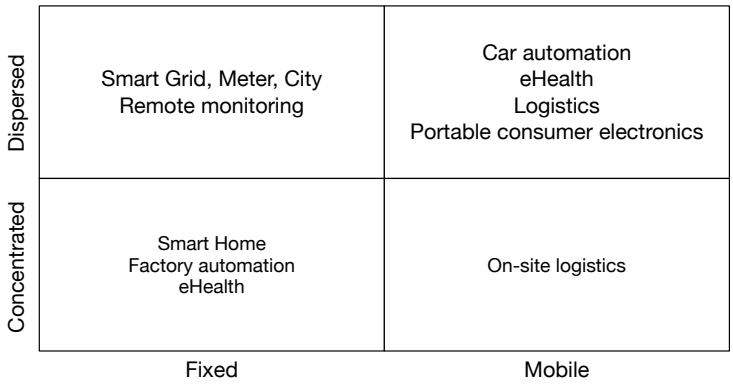

Fig. 2.2 M2M applications taxonomy by mobility and dispersion. Source: [8]

2.1.3 Classification according to delay tolerance level

According to delay tolerance level, M2M applications can be divided into 4 classes: Class 1 (Elastic applications), Class 2 (Hard real-time applications), Class 3 (Delay-adaptive ap-

plications), Class 4 (Rate-adaptive applications [27]. The Class 1 applications are generally rather tolerant of delays, for example, file downloading of remote MTC devices from MTC servers. The Class 2 applications need their data to be served within a given delay constraint. The typical example of class 2 application is vehicle and asset tracking. Similar to class 2, the class 3 applications are usually delay sensitive, but most of applications of class 3 can be made rather tolerant of occasional delay-bound violation and dropped packets. The class 4 applications adjust their transmission rates according to available radio resources while maintaining moderate delays.

2.1.4 Classification according to data reporting mode

According to data reporting mode, M2M applications are classified into five categories: time-driven, query-driven, event-driven, continuous based and hybrid-driven [28–30]. Time-driven M2M applications refer to those applications where machines periodically turn on their sensors and transmitters to transmit the collected data. Query-driven applications reply to certain instructions from MTC servers by transmitting data. This type of applications allows packet omissions, as adjacent data reports usually contain redundant information. Event-driven applications react to certain critical query or event. Normally, applications fall into this category when they use priority alarm messages (PAM). Continuous based M2M applications make the devices send their data continuously to the remote server at a prespecified rate. Hybrid-driven is a combination of aforementioned types.

2.1.5 QoS feature for typical M2M applications

In Tab. 2.2, a QoS requirement table in terms of data rate, latency and message priority is given for some representative cellular M2M applications, based on different references found in the literature. It should be noted that in Tab. 2.2, we give only indicative values.

2.2 M2M Traffic Characterization

A comprehensive comparison between MTC and HTC is resumed in Table 2.3. The illustration of this difference helps to rethink the design of some principles and the optimization guidelines. Some explanations about Table 2.3:

- First, the representative device in H2H communication is smartphone, which is equipped with more and more computational capacity. The complexity of M2M devices vary with respect to M2M applications. For M2M applications such as remote monitoring, a M2M

Table 2.2 Typical M2M applications and their QoS Requirements

M2M service	Data rate	Latency	Priority
Surveillance system	64.000 bits/s[31]	small	Medium
Urgent notification	small	less than 1 s	High
Fleet management	less than 500 bytes	very small	High
Pay as you pay	small	very small	High
Smart metering	500-1000 bytes per message	15 sec - 15 min [32]	Low
Grid automation	10-100 kps[33]	0.1-2 sec[33]	High
Monitoring vital signals	less than 200 bytes per message [34]	small	High
Monitoring in emergency	less than 200 bytes per message [34]	small	High
Industrial automation	small	less than 5 ms [35]	High
Vending machine control	small	small	Medium

device has low complexity: it could be in format of sensor with transceiver and simplified processor. For other use cases such as Intelligent Transport System (ITS), a M2M device can be very powerful. It could be regarded as a smartphone without screen.

- Second, the experiment results in [21] reveal that compared to H2H communication, cellular M2M traffic suffers from a higher packet loss ratio, and the reason may be the adverse deployment location and the lack of UI (e.g., screen) to show the signal strength in its place.
- Third, since at present, a majority of cellular M2M applications are based on GSM/UMTS technologies, MTC mainly supports SMS or data reporting service. We could imagine more innovation M2M services when 4G networks even 5G networks are largely rolled out.

Not all MTC applications have the same characteristics and not every optimization is suitable to all applications; therefore, features are defined to provide some structure to the customer and the network is then tuned accordingly to needs.

2.3 M2M Related Standardization Efforts

To address the difficulties for well supporting cellular MTC, the Standardization Developing Organizations (SDO) have launched their activities in their own fields. The dominant players in M2M landscape are ETSI M2M and 3GPP LTE. 3GPP is very active in M2M landscape. The focus of 3GPP is the improvement of radio access and core network to facilitate MTC over 3GPP networks. The first 3GPP report related to M2M [40] issued in 2007 indicates a huge market potential for M2M beyond the current market segment. During the age of 3G, there have been little developments about MTC, since CDMA-based 3G systems

Table 2.3 Difference Between MTC and HTC

Item	M2M	H2H
Delay range	10 ms $\sim$ several minutes [36]	250 ms (voice) to few seconds (email for example)
Device composition	GSM/UMTS/LTE module, extension slots, USB, memory, CPU, etc.	GSM/UMTS/LTE/Wifi module GPS, Bluetooth, USB, memory, CPU, flash storage,etc.
Packet loss radio	Relatively high [21]	Low
Mobility	Most of the M2M devices (90% according to [37]) are stationary.	Human are very rarely considered fixed in practical mobile networks
Support service	Mainly SMS or data reporting	SMS/Voice/Web/Multimedia, etc.
Session duration /frequency	Short but more or less frequent [38], depending on the applications: monitoring, transport or others	Long but less frequent
Uplink	MTC traffic is mainly generated in uplink	Traditionally less traffic in uplink but increase rapidly with the flourishing of interactive applications such as social network
Downlink	Less traffic except for some application requiring interaction between sensors and MTC servers, for example consumer electronics use case	Currently most traffic, for instance, web browsing and multimedia
Message size	Generally very short. In some cases could increase, for example, if video sequences are uploaded	Typically big, especially for multimedia and real-time transmission
Number of devices	Hundreds or thousands of devices per Base Station	At most hundreds of UE, typically tens of UEs per base station [39]
Battery life requirement	Up to a few years, especially for deployment locations with difficult access	Order of days or weeks, Human could easily recharge their device
Key metrics for user experience	Energy efficiency, latency	Delay, throughput, packet loss

are not suitable for low power operations. With the emergence of OFDM-based LTE, cellular M2M has become of interest and a set of further documents has been issued. MTC features and service requirements are defined in [14]. An architectural reference model for MTC, key issues and possible solutions, are presented in [11]. Recently, 3GPP also study to introduce a new class of User Equipment (UE) with low-cost feature in Release 13 [41]. In addition, 3GPP also aligns with ETSI Technical Committee M2M work. ETSI M2M is composed by various manufacturers, operators and service providers, among others. To enable interoperability between M2M services and networks, ETSI established a Technical Committee (TC) in 2009 focusing on M2M service level and defined a M2M reference architecture and interfaces specification [9].

Besides, there are some international projects for facilitating MTC over 3GPP cellular networks. The EXALTED project (Expanding LTE for Devices, 2010-2013) [42], a Europe FP7 project, is one of the flagship projects in M2M landscape. The main goal of this project is to develop a cost-, spectrum-, and energy-efficient radio access technology for M2M applications, the so-called LTE-M overlay, adapted to coexist within a high-capacity LTE network. Special attention was paid to scalability issues (to, e.g., avoid congestion in the random access procedures) and cost aspects, to ensure affordability of LTE M2M modules. Within this project, a lot of specific issues related to M2M communication in cellular network are studied, including radio resource allocation, relaying, security, PHYsical Layer, coding, emergency and rescue networks along with important standardization activity [43][44]. The METIS (Mobile and Wireless Communications Enablers for the Twenty-Twenty Information Society) is a Europe FP7 project from 2012 to 2015. Its global objective is to lay the foundation for the 5G system. With regard to MTC, they focus how to efficiently support Massive Machine-Type Communication (mMTC) and Utra-reliable Machine-Type Communication (uMTC) in the future 5G, by studying technologies about radio Links, multi-node/multi-antenna transmission and so on. LOLA (Achieving Low-Latency in Wireless Communications) [45] project focuses on physical and MAC layer techniques aimed at achieving low-latency transmission in cellular (LTE and LTE-A) and wireless mesh networks.

2.4 M2M Communications architecture

Given that there is not a consensus about MTC reference architecture, standardization developing organizations (SDO) and research community have proposed a few of proposals about standardizing M2M reference architecture. ETSI provides a general M2M reference architecture with purpose of designing an access and transmission technology independent ser-

vice middle layer [9]. Nowadays the architecture-related works are transferred to oneM2M. The project oneM2M published their reference architecture at the beginning of 2015, which is similar but different than that of ETSI M2M. 3GPP proposes a MTC reference architecture with focus on improvement of core network [11]. IEEE 802.16p gives an overall architecture for M2M [46]. Since the reference architectures of 3GPP and IEEE 802.16p are functionally equivalent, mainly the efforts of ETSI, oneM2M and 3GPP are presented.

2.4.1 ETSI M2M reference architecture

The ETSI proposes a high level reference architecture for M2M communication, which is illustrated in Fig. 2.3 and composed by a device-and-gateway domain and a network domain [9]. This architecture consists of the following components:

- M2M-D, a device running M2M applications usually embedded in a smart device and replies to requests or sends data;
- M2M area network, a capillary network (e.g. small-scale home environment) composed by individual M2M-D leveraging short-range communication technologies (e.g. IEEE 802.15.1, Zigbee, Bluetooth, etc.)
- M2M-G, a proxy responsible for interworking for M2M area network and Network domain.
- Access Network, a network that provides access to the core network for devices (i.e. M2M-D and M2M-G) in device-and-gateway domain. It can be, among others, in form of the access network of 3GPP, xDSL, satellite and WiMAX.
- Core Network, a network that provides various services such as IP connectivity, network control, interworking, roaming and so on between M2M-A and M2M-D. It includes, but is not limited to, 3GPP CN, ETSI TISPAN CN and 3GPP2 CN.
- M2M-A, M2M Applications, application services that run the service logic and use M2M-SC via application programming interfaces.
- M2M-SC, a network node providing M2M functions to M2M-A and hiding network specificities for M2M application development.

2.4.2 oneM2M reference architecture

Apart from the efforts of ETSI M2M, other regional SDOs conduct standardization activities. To avoid the risks of divergence, the oneM2M partnership project was established in 2012 by leading regional SDOs such as ETSI (Europe), TIA and ATIS (North America), CCSA (China), TTA (Korea), ARIB and TTC (Japan). The objective of oneM2M is to prepare,

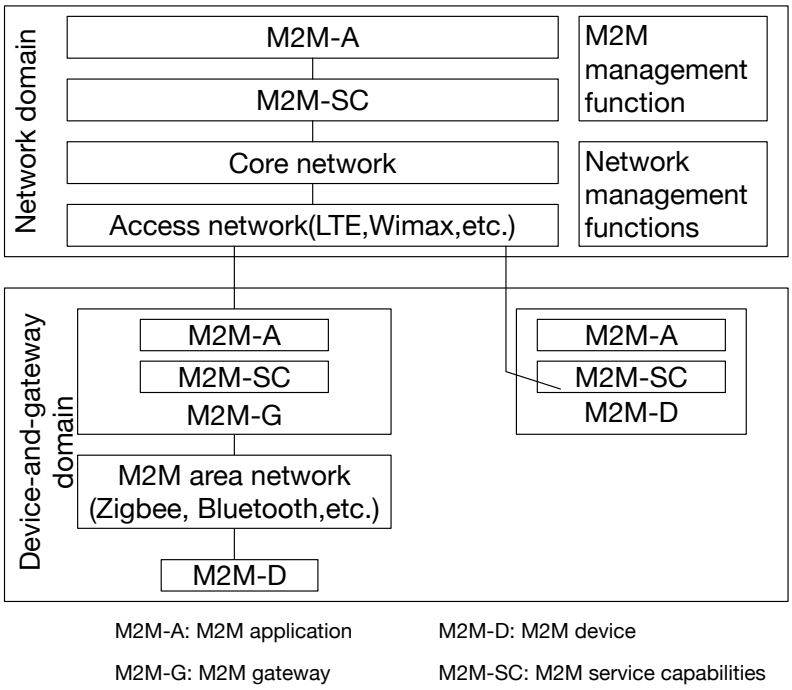

Fig. 2.3 ETSI reference M2M communication architecture. (Modified based on [9])

approve and maintain globally applicable, access-independent technical specifications and reports related to M2M solutions, with initial focus on the Service Layer. The functional architecture of oneM2M is shown in Fig. 2.4. There exist mainly three functions: Application Entity (AE), Common Services Entity (CSE) and Network Services Entity (NSE). Application Entity is an entity in the application layer that implements an M2M application service logic and equivalent to the M2M-A in ETSI reference architecture (shown in Fig. 2.3). The Common Services Entity represents an instantiation of a set of *common service function* (i.e. M2M service subscription management, device management, etc.) A Network Services Entity hides the implementation of underlying communication networks and provides services to the CSEs. The oneM2M reference architecture reuses principles and solutions from ETSI M2M: the entity AE is like the M2M-A in Fig. 2.3. The CSE is equivalent to the M2M-SC in Fig. 2.3. The infrastructure is similar to the ETSI network domain and the field domain is like the device and gateway domain of ETSI.

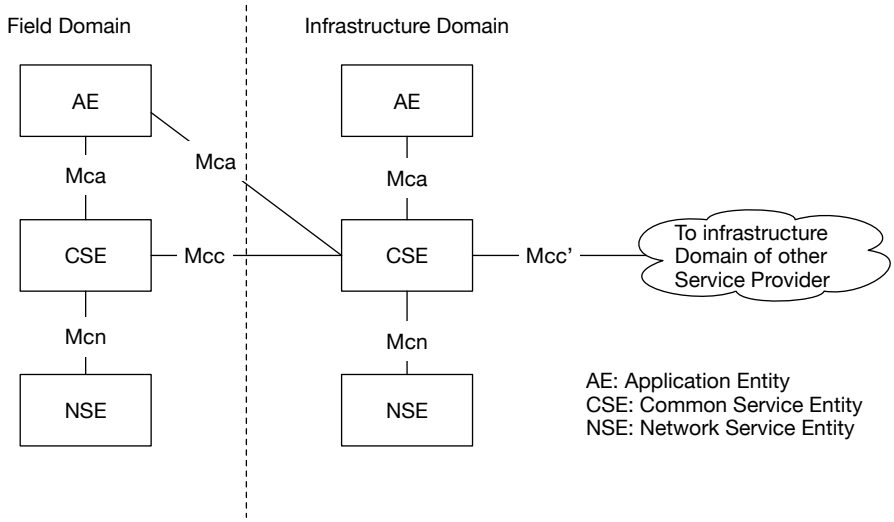

Fig. 2.4 oneM2M reference functional M2M architecture. Source: [10]

2.4.3 3GPP reference MTC architecture

The main contribution of ETSI M2M overall architecture is to standardize the resource structure representing the information contained in M2M-SC, but ETSI has not specified the standardization for M2M area network, access network and core network. The efforts of 3GPP about MTC architecture are summarized in [47, 11]. Different from that of ETSI, the focuses of 3GPP are mainly cellular wireless network, especially the access and core network. The proposed reference architecture is shown in Fig. 2.5. The enhancement made by 3GPP supports the device trigger function. To this end, two new network nodes (MTC-IWF and SCS) and a series of reference points related to these two nodes are introduced. The first node, MTC Interworking function (MTC-IWF), hides the internal PLMN (Public Land Mobile Network) topology and relays or translates signaling protocols used over Tsp (shown in Fig. 2.5) to invoke specific functionality in the PLMN. The main functions of MTC-IWF are: to authorize the SCS before communication establishment with the 3GPP network, receive a device trigger request from SCS, select the most efficient and effective device trigger delivery mechanism, etc. The SCS is an entity that connects to the 3GPP network to communicate with MTC devices and the MTC-IWF in the HPLMN. This entity offers capabilities to be used by one or multiple MTC Applications, and is controlled either by the mobile operator or a MTC Service Provider.

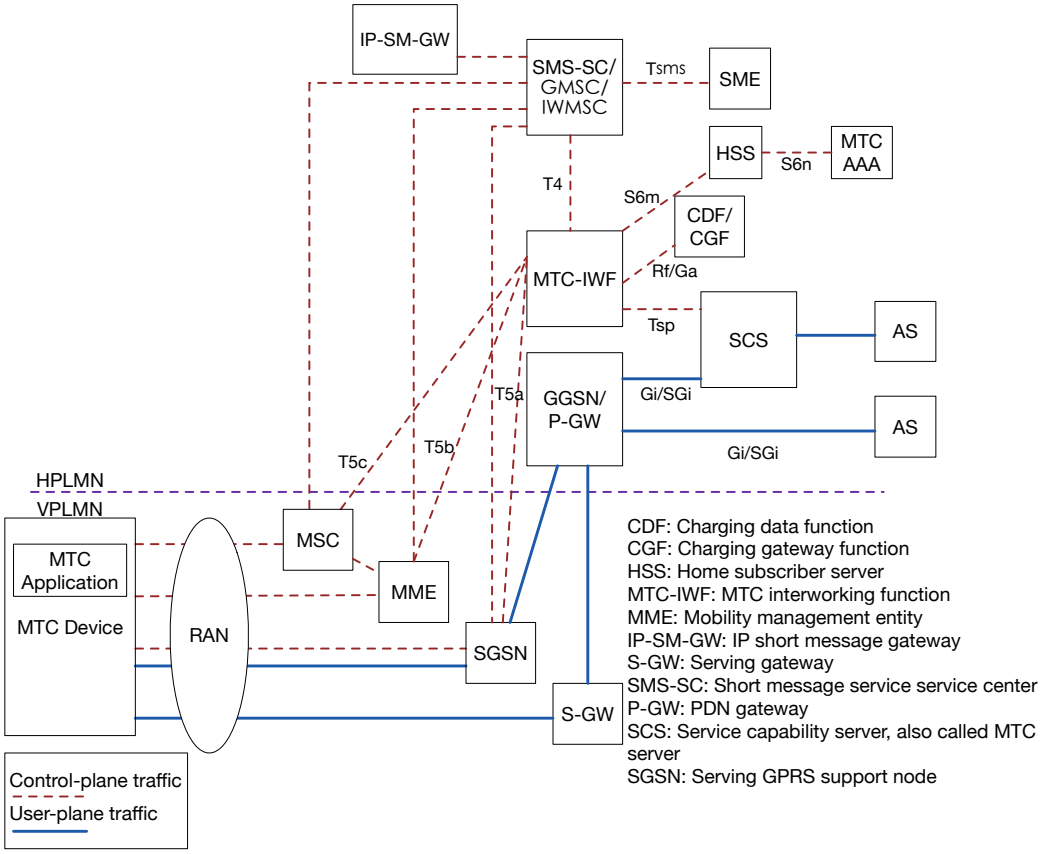

Fig. 2.5 3GPP reference MTC architecture. (based on [11])

2.5 Low Power Wide Area network

The term Low Power Wide Area network (LPWA) refers to a network relying on low power and wide area connectivity technology that simultaneously supports low batter energy consumption and wide coverage area. The LPWA network is dedicated to serve battery-powered applications characterized by low throughput, delay-tolerant and being event-driven such as water-meter monitoring. Unlike the other technologies that are adapted for IoT, LPWA networks are purposely designed from scratch to meet wide-area IoT application.

LPWA technologies are typically narrow-band (with some exceptions) and operate in the ISM license-exempt spectrum bands. Faced with a potential huge market, lots of players propose their solutions. Some typical and already deployed proprietary technologies of LPWA network are LoRaWAN, Sigfox, Weightless, OnRamp, etc. A comprehensive comparison about these existing LPWA solutions is shown in Tab. 2.4. LoRa alliance has issued their first vision of LoRaWAN specification [12] in January 2015, which is regarded as a major step towards international standardization in field of LPWA networks. Thus, LoRaWAN (LoRa Wide Area Network) technology is taken as a concrete example to give a general

Table 2.4 The comparison among LPWAN solutions (All solutions are on ISM band, extracted from [17])

	LoRaWAN	NWave	OnRamp	Sigfox	Telensa	Weightless-N	Weightless-P	Amber Wireless
Range (km) (Caveat)	15-45 flat; 15-22 suburban; 3-8 urban	10	4 (but claims 25X competition)	50 rural; 10 urban	up to 8	5+	2+ urban	up to 20
Band (MHz)	spread; varies by region	sub-GHz	2.4 GHz	868;902	868/915 470 (China)	sub-GHz	sub-GHz	434, 868, 2.4GHz
Symmetric up/down	depends on mode. Can be	no	no(4:1)	no	yes	uplink only	not yet determined	
Data rate	0.3-50 kbps (adaptive)	100 bps	8 bps - 8 kpbs	100 bps	low	30-100 kbps	up to 100 kpbs	up to 500 kbps
Max nodes (Caveat)	depends; millions/hub	million/base	"10s of 1000s"	millions/hub	150,000/server (moving to 500,000)		32767 NWs, 65535 hubs each, 16 M edge device per NW	255 network of 255 nodes
Operational model	public or private (expect 80% public)	public or private	public or private	private	public	public or private	public or private	
Standard status (if any)	LoRa: proprietary LoRaWAN: yes	Weightless-N	no	no	no (perhaps in future)	yes	in process	

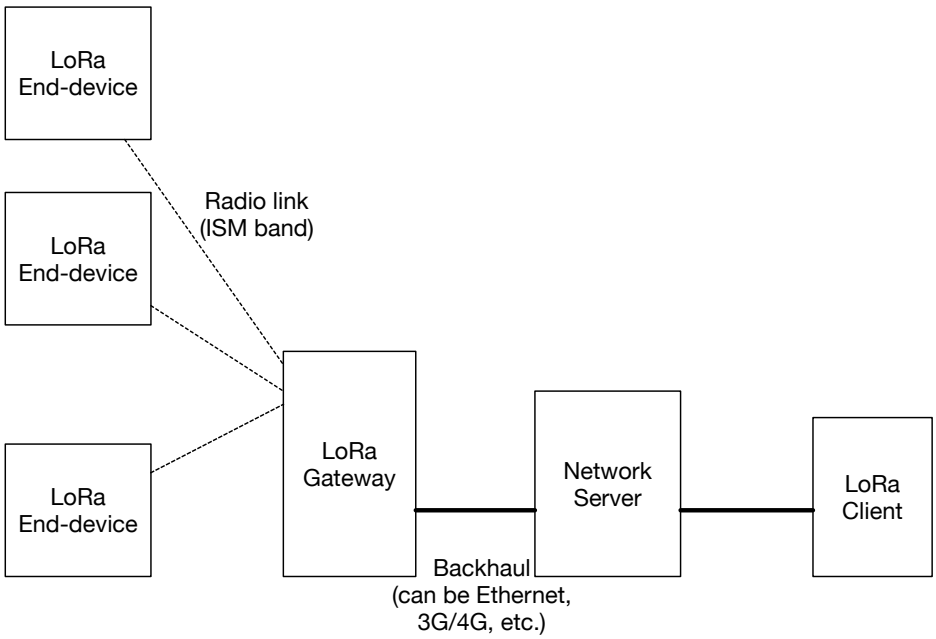

Fig. 2.6 LoRaWAN network architecture. (based on [12])

view about LPWA networks. The network architecture is illustrated in Fig. 2.6, which is a star-of-stars topology. A LoRaWAN network consists of the following components [12]:

- End-device: the end-device is the element in a LoRaWAN network, which is responsible for collecting and uploading information to remote network server. LoRa supported functionalities can be classified to three classes: Class A (unidirectional end-devices), Class B (Bi-directional end-devices with scheduled receive slots) and Class C (Bi-directional end-devices with maximal receive slots). All LoRaWAN end-devices at least support Class A. According to applications, end-devices can optionally support Class B and Class C.

- LoRa air interface: The LoRa air interface provides the connectivity between LoRa end-devices and gateway. It is on ISM (Industrial Scientific Medical) band and based on LoRa modulation, which is a proprietary modulation scheme. The LoRa data rate ranges from 0.3 kbps to 50 kbps. The selection of data rate is a trade-off between communication range and message duration, and communications with different data rates do not interfere with each other.

- LoRa gateway: the LoRa gateway receives the communications from the LoRa end-devices and then transfers them to network server via the backhaul system. Note that LoRa gateways may be co-located with a cellular base station. In this way they are able to use spare capacity on the backhaul network.

- Network server: the LoRa network server manages the network. The network server acts to eliminate duplicate packets, schedules acknowledgment, and adapts data rates (Adaptive Data Rate scheme). The communication between LoRa gateway and network server is IP-based, and the underlying carrier networks can be wired or wireless, Ethernet or 3GPP cellular, public or private networks.

In order to answer the huge expected demand of cellular M2M coverage, the standardization organizations embarked on a process of standardizing narrow-band technology for use in mobile spectrum. Two possible tracks are addressed by the 3GPP. The first track is the evolution of LTE 3GPP cellular system with the objective of reducing the occupied bandwidth but still reusing the basic LTE principles. The second track is to propose a clean slate solution, which features narrow-band (NB) technologies and leverage the existing cellular infrastructure. One major difference between these two tracks relies in that whether it should redesign the radio interface and multiple access control mechanism for cellular M2M networks.

As an effort in the first track, the 3GPP developed LTE-M specification in Rel-12 [48] with introduction of a new low complexity device category (Cat-0). The device complexity of Cat-0 is 50% of the previously defined Cat-1, which is the basic LTE terminal defined in the first LTE Release (Rel-8). Nowadays, 3GPP is considering to further optimize LTE-M in Rel-13: 1) bandwidth of 1.4 MHz and less complexity [48]; 2) a narrow-band evolution of LTE-M with bandwidth 200 kHz [23].

For the clean slate solutions, the main idea is to sacrifice the data rate in order to gain energy efficiency and coverage extension. They are supposed to satisfy the following requirements: deployment in a small bandwidth (e.g. 200 kHZ), ultra low-cost terminal (less than 5 dollars), ultra-long battery life and coverage extension of 20 dB with existing cellular technologies. The typical solutions include Narrow Band IoT (NB IoT), Narrow Band OFDMA, Cooperative Ultra Narrow Band (C-UNB) [6]. The deployment options include re-farming GSM spectrum, LTE band guard and leftover fragments of spectrum during re-farming of 2G/3G to 4G.

When these standards will be available, the cellular M2M connectivity solutions may be more competitive, since they not only fulfill the requirements of extended coverage and long battery life, but also have the advantage of being able to operate in currently existing cellular network, thus requiring no additional deployment of antennas, radio, or other hardware. On the contrary, the proprietary (at least for the time-being) technologies such as Sigfox, On-Ramp and LoRaWAN require a dedicated network and maintenance team to deploy and maintain their services, which increases operational complexity for the operator. However, their M2M solution is currently available for the operators and start to occupy some share of

the market. In addition, some of the proprietary technologies such as LoRa, have the plan to adapt their technology running on licensed spectrum and submitted to GERAN [49] to keep its competitiveness.

2.6 M2M Related Energy Efficiency Studies

To achieve energy efficiency at device side, the research community has done lots of efforts. In this section, we present, categorize and compare all found proposals related to energy issues for MTC in cellular networks. The energy issues may refer to energy saving, energy efficiency or power efficiency/saving. The result of classification and comparison among the proposals presented in this survey is resumed in Tab. 2.5.

2.6.1 Cooperative Relaying

Cooperative relaying, also called cooperative design [43], can be interpreted as the process of devices helping each other to jointly achieve a goal more efficiently than each device could do on its own. The first possible form is group-based and relay (in fact, at most 2 hops) mechanism, which is very useful for energy saving, massive access control. A general and common description about group-based and relay transmission is illustrated in Fig. 2.7: all MTC devices (MTCD) are classified into several groups (some references call group as cluster). A certain device in each group is selected as coordinator (also can be called cluster header, group head) according to some criteria (e.g., QoS requirements [36], link quality or location). The MTC devices other than coordinators transmit packets to their allocated coordinators, which relay the received packets to the BS (multiple-hop communication). In this model, there exist two links: MTCD-to-Coordinator (actually MTCD-to-MTCD link, since the coordinator is by nature still a MTC device) and Coordinator-to-BS. A basic issue is the interference between the two aforementioned links. This problem can be addressed by interference-based topology control algorithm [67], specific scheduling, use of different frequencies between the two communications (but this is pricey in frequencies) or even using two different protocols as proposed in [52]. In addition, how to enable and make the MTCD-to-MTCD link efficient is addressed by D2D communication [68][69].

The idea of group-based communication is presented in [50] but without clarifying grouping/clustering algorithms. In fact, the algorithms of device grouping and coordinator are a key factor influencing energy efficiency. A series of K-means (K-means clustering aims to partition n observations into k clusters in which each observation belongs to the cluster with the nearest mean) derived grouping and coordinator selection algorithms are

Table 2.5 Categorization and comparison of energy/power saving-related proposals

Category	Subcategory	Reference	Principle for energy saving	Drawback	Notes
Cooperative design	Clustering and relay	[50] [51] [52] [53]	Group devices into clusters; Cluster head relays the messages for other cluster member in the same group	High energy consumption for cluster head; Scheduling and resource issues in order to manage the interference; Delay increase cause of relay	It is possible to combine cooperative relaying with other emerging technologies for the device-to-device link
	Cooperation between MTC server and MTC devices	[29]	Adjust MTC device setting according to context	High complexity for MTC devices	
	M2M gateway	[25] [54] [13]	Similar to clustering and relay, except that M2M gateway is a special network node instead of a MTC device	Installation and deployment cost of M2M gateway for operators	Reduce implementation complexity for MTC device. Possible to use LoRa gateway as M2M gateway.
Design of energy efficient signaling and operation	Modified DRX and Idle state	[55] [56]	Make MTC devices stay in low power mode as long as possible	High delay	Simple method to achieve energy saving
	Extending paging cycle	[14] [19] [57]	Make MTC devices stay in low power mode as long as possible	High delay	
	Reduction of RRC Inactivity timer	[58]	Make MTC devices stay in low power mode as long as possible	Impact on H2H service	
	Group-based and M2M- dedicated paging mechanism	[59]	Group paging for MTC devices	May reduce the paging capacity of H2H; Scalability and bacward-compatibility issues.	
	Removal of unnecessary activities	[59]	Remove activities related to mobility management (MM) for MTC Device	Applicable uniquely for M2M application with no or low mobility	Reduce the cost of MTC device and energy consumption
	Disconnect MTC-device from network when inactive	[60]	Instead of staying in low power mode, turn devices radio off	High delay	
Radio resource allocation and packet scheduling	Formulation of optimization problem	[61] [62]	Convert radio resource allocation into an optimization problem with constraints	High complexity; Scalability issues; Possible impact for human users.	
	Optimized with periodicity	[63] [64]	Leverage the periodicity of MTC	Applicable uniquely to periodic M2M applications; Not easy applied in the presence of different period values.	
	Packet scheduling	[44] [65]	Propose packet scheduling adapted for cellular MTC context	Compatibility with H2H; May need modifications of the specification	Ensure QoS requirements
Energy efficient random access and MAC	New random access protocol	[39]	ALOHA-based random access protocol is not the best option for MTC	It may be difficult to find a specified random access protocol suitable for all cellular users	
	Fixed time alignment	[66]	Leverage the low mobility of MTC	Only applicable for M2M with no mobility	Reduce the access collision
	Transmit message in MAC PDU or preamble	[25]	Transmit message directly in access reservation stage	Scalability issues	Reduce the signaling overhead

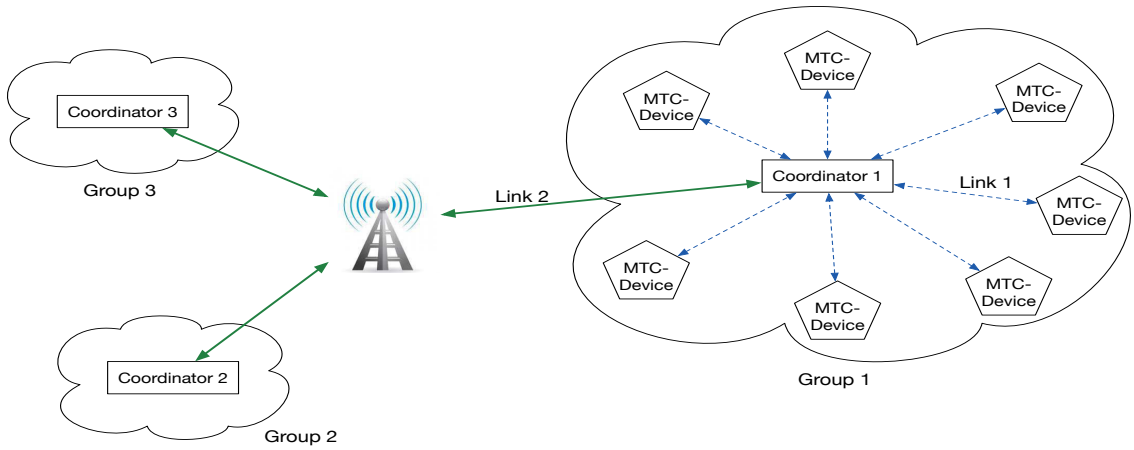

Fig. 2.7 Illustration of M2M devices clustering

proposed in [51]. Ho et al. [52] propose a two-stage mechanism to minimize the energy consumption of all MTC devices. The first stage consist of MTC devices grouping, coordinator selection. The criteria for grouping and coordinator selection in each group are the minimization of energy consumption of this group. The second stage is that BS performs power allocation for each coordinator to further reduce energy consumption. However, it is difficult to obtain the closed-form solution for the formulated problem, the proposal of [52] could achieve suboptimal result. An implementation of clustering and relay is presented in [53]: Intra-cluster communication uses CSMA/CA protocol with multiple-phases while resource reservation based protocol is used for communication between cluster head and BS. The drawback of the group-based and relay design relies in that:(i) although it is globally energy efficient for all the MTC devices, the cooperative relaying causes the cluster head to consume more energy than others; (ii) each MTC device should be equipped with multiple transceiver (e.g. OFDMA transceiver for Coordinator-to-BS link, TDMA transceiver for MTCD-to-Coordinator link), since every device is possible to be selected as coordinator.

The second form of cooperation is to introduce M2M gateway (may be called proxy [25]). The M2M gateway serves as an intermediary node to collect and process data for neighbor MTC devices. Thus, topologically, M2M gateway is very similar to the aforementioned cluster header, except that M2M gateway does not have its own data to transmit and may have a permanent energy source. It is preferred to use half-duplex M2M gateway to avoid self-interference and reduce implementation complexity [27]. The use of M2M gateway helps reduce the number of accessing devices, signaling overhead and contention thus helps improve energy efficiency. Chen et al. [25] give a simple work flow for MTC with M2M gateway. Pereira et al. [54] consider to use smartphones as M2M gateway between Base Station and MTC devices. The existing scheduled airliners used as relays between ground

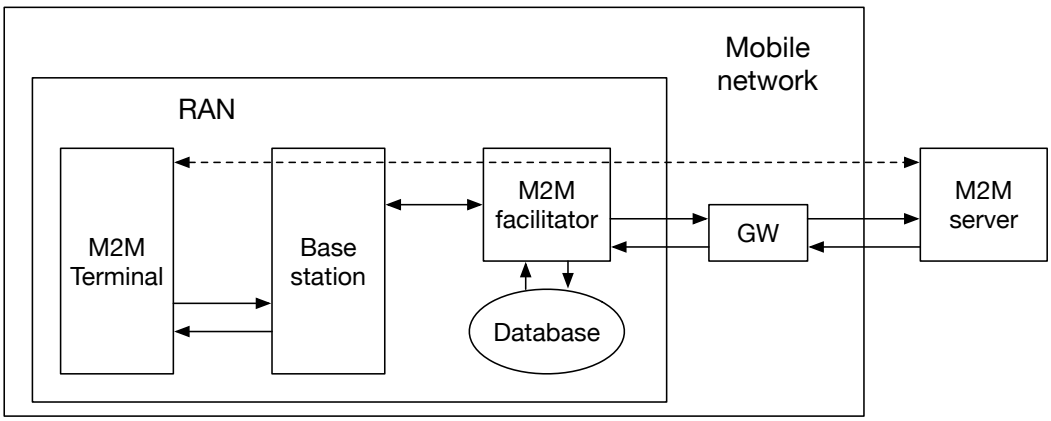

Fig. 2.8 Un-peer2peer cellular MTC architecture with M2M Facilitator. Source: [13]

devices and satellites are presented in [70]. It is also possible to add a gateway-like element node called M2M facilitator [13] between 3GPP RAN and Core Network, which is shown in Fig. 2.8. M2M devices nominally communicate with M2M server. However, the M2M devices only communicate with base station and enter in sleep mode after the session with base station. Base station then transfers received data to M2M facilitator. Finally M2M facilitator is in charge of data transmission, retransmission and session termination with M2M server. Since the devices communicate only with M2M facilitator and the latter has no energy constraint, the protocol stack at device side can be significantly simplified to save energy consumption. The cost is that a fraction of protocol stack complexity is transferred to M2M facilitator. The inconvenient points of M2M gateway related proposals are:(i) operator should deploy M2M gateways to serve MTC devices, which may be of high cost; (ii) not flexible and dynamic compared with clustering-based group. Compared with group-based and relay mechanism, the use of M2M gateway may be more energy efficient for devices. This is actually due to that a part of energy consumption of MTC devices is transferred to M2M gateway, which may have a permanent energy source.

The third possible form of cooperation mechanism is context-based communication between MTC servers and MTC devices. The philosophy of this axis is: intelligent algorithms can be deployed at application level to help M2M devices and overall network adjust their settings to improve energy efficiency. According to this philosophy the authors propose a context-aware framework based on context concept in [29]. M2M devices send context-related information to MTC server, MTC server judges the data reporting mode(time-driven, query-driven, event-driven or hybrid) and QoS feature (real-time, priority and accuracy) then returns a set of output useful for setting device's behavior. This output involves inter-arrival time, average packet size, transmitting power, packet omission, etc. that could extend the operative lifetime of M2M devices.

2.6.2 Design of energy efficient signaling and operation

An intuitive solution to achieve energy-efficiency for MTC is to design energy efficient signaling and simplify the operations leading to energy wasting. The key philosophy is to maximize the duration in low power state and reduce or even delete all operations unnecessary for MTC. The improvement possibilities are summarized as follows:
(1) Adaption of DRX and Idle state: 3GPP has incorporated some energy/power saving mechanisms into their specification for H2H devices: for instance, Discontinuous Reception (DRX) [71]. Due to long inter-arrival time between traffic sessions, MTC devices stay in LTE Idle states most time as it is designed as a low power state. In Idle state, MTC devices go to sleep to save battery and wake up periodically to inquire any system information (SI) update or downlink packet arrival via paging mechanism. However, the aforementioned mechanisms are still insufficient for MTC device, DRX and Idle state are adapted to improve device power saving in [55]. The potential of trading high delay for reducing MTC devices battery consumption is studied in [56];
(2) Extending paging cycle: 3GPP considers to extend paging cycle for M2M devices [14, 19, 57], but simulation results show that Extending Paging Cycle beyond 2.56 seconds reduces the power consumption significantly for M2M traffic with small or medium values of inter-arrival time, but has no effect when the paging cycle is more than a limit [58]. In addition, extension of Paging Cycle always increases the packet buffering delay;
(3) Reduction of RRC Inactivity timer: The network keeps MTC device in Connected mode even after the last packet delivery due to the RRC Inactivity timer in which MTC device still keep a high power, thus the impact of variation of RRC Inactivity Timer is explored and proved to be better than extending paging cycle [58];
(4) Group-based and M2M-dedicated paging mechanism: To increase paging capacity multiple terminals are allocated with the same paging occasion (PO). H2H and M2M terminals may occupy the same certain paging occasion. If both are paged together, a large number of H2H terminals and MTC devices need to wake up at the same PO, which results in terminal power wasting. The solution to avoid this kind of power wasting is paging targets with group ID or device ID at dedicated paging occasion allocated uniquely for M2M devices [59];
(5) Removal of unnecessary operations: Even in Idle state, the MTC devices are not actually inactive: they are supposed to run activities related to mobility management (e.g., TAU procedure for LTE). Since MTC presents low mobility feature, it is possible to remove these unnecessary operations (Periodic AS measurement and NAS LAU/RAU/TAU procedure) for power saving [59];
(6) Disconnect MTC device from network when inactive: Since the device power consumption in Idle state is not negligible, it is possible to turn LTE radio off (i.e. disconnect the

device from network) to obtain further power saving [60] and this is proved to be outperforming than approach of reducing RRC Inactivity timer. However, the gain of power saving is with cost of higher delay related to downlink packet. In addition, the network may also need to store the downlink data and the MTC device identities if the MTC device is off.

2.6.3 Radio resource allocation and packet scheduling strategies

Radio resource allocation and packet scheduling strategies play a key role in the overall performance of OFDMA-based wireless networks [72]. Most of research efforts in this field are about the downlink, which can for example improve network throughput and mitigate inter-cell interference [73, 74]. However, they have limited effectiveness about energy efficiency on MTC device side. In addition, MTC applications are usually uplink-centric, thus, it is import to design new radio resource allocation and packet scheduling schemes to achieve energy-efficiency.

Zheng et al. [27] study the radio resource allocation scheme for the five possible links in M2M and H2H co-existence scenario: the eNB-to-UE link, the eNB-to-MTCD link, the eNB-to-MTCG link (MTCG refers to MTC gateway), the MTCG-to-MTCD link and the MTCD-to-MTCD link. They first design a new radio resource partition scheme and then propose efficient radio resource allocation algorithms in each partition to mitigate co-channel interference and enhance network efficiency, which is useful for energy-efficiency, but they just consider the data rate when allocating resource for both UE and MTC devices.

Given that MTC usually features low data rate and emphasizes the delay requirement, Aijaz et al. [61] extend the work [27] by formulating a bits-per-joule capacity maximization optimization problem. The resource constraint for UE is the minimum data rate and maximum tolerable packet delay for MTC devices. They propose two heuristic algorithms based on steepest descent approach to solve the optimization problem. Aijaz et al. [62] further extend [61] by introducing the notion of statistical QoS (i.e., probability of exceeding a specific delay threshold) and solve the optimization problem with Canonical Duality Theory (CDT).

Radio resource allocation scheme can also leverage the periodicity of MTC, since a considerable of M2M users repetitively access to the networks to transmit collected data. Zhang et al. [63] propose to use persistent resource allocation for periodic M2M applications and indicate the condition for multiplexing multiple MTC devices with different reporting periods. Madueno et al. [64] propose a periodically occurring pool of resources that are reserved for M2M communications and shared for uplink transmission by all MTC devices. Song et al. [5] propose a multiple-period polling service in LTE transport network to avoid random access procedure by leveraging the periodicity feature of M2M.

Group-based feature can be leveraged when designing M2M-compatible radio resource allocation strategies. Since MTC devices in the same cluster are assumed to have exactly the same QoS requirements, a grouping-based radio resource allocation algorithm [65, 36] is proposed for LTE-A base stations according to packet arrival rate and maximum jitter. The access grant time interval (AGTI) is periodically allocated for each MTC device cluster according to cluster priority. All the MTC devices of a same cluster occupy an equal number of Resource Block (RB) in allocated AGTI. The shortcomings of this proposal are:i) the number of served MTC devices is limited due to the inefficient utilization of resource; ii) the base station only supports a unique packet size for all MTC devices; iii) the proposal is not scalable since BS has to know in advance how many clusters in its coverage; iv) the supported QoS classes are limited.

Since the packet delay employed in [65] is a deterministic bound, Gotsis et al. [44] extend work of [65] by using a statistical QoS (also used in [61]), which refers to the probability of exceeding a specific delay threshold. They propose an analytical model to study the performance of period scheduling algorithm in terms of statistical QoS metric with modeling the arrival traffic as Poisson process. They also enhance the periodic scheduling in [65] with queue-awareness in which devices with larger queues than others are first granted access to the scheduled AGTI with an extra cost in complexity and signaling.

To overcome the issue of QoS classes, two uplink packet scheduling strategies are proposed in [75], which take into account both the channel conditions and the maximum allowed delay of each device, however, it suffers from increased signaling requirements and is just able to serve limited number of MTC devices. In [52] a resource allocation scheme (i.e., optimal transmit power allocation over RBs) for M2M traffic over OFDMA frames is proposed, assuming a two-hop access to the LTE network though a coordinator. This work achieves the reduction of energy consumption, but does not take into account QoS issue of MTC such as the delay requirements.

2.6.4 Energy-efficient random access procedure and MAC

The currently standardized random access procedure, for example, in LTE networks, is designed and optimized for large amount of data transmission and limited UEs, thus it suffers from random access overload issue which leads to high collision probability and waste of energy. The improvement works about random access procedure have been attracting the attention of research community. Current random access optimization research efforts can be resumed into two categories:i) improvement for currently employed ALOHA-like random access procedure; ii) designs of non-ALOHA procedure.

For the first category, the focus is to reduce either signaling overhead for small data transmission or contention probability, since both reduce the transmitted bits for MTC devices thus help energy saving. For MTC with lots of fixed location machines, Ko et al. [66] propose a novel random access scheme based on fixed TA (timing alignment) for OFDMA-based cellular system. The proposal is based on the assumption that the TA value between each fixed location machine device and eNB is fixed and unchanged, the MTC devices store the TA value acquired from the initial RA access and compare it with the TA values obtained from the subsequent random access procedure. In case of mismatch of TA values, MTC devices directly start retransmission procedure to avoid possible collision after waiting a randomly selected backoff time. Otherwise, the devices continue the conventional procedure. However, this proposal is only applicable to M2M with stationary devices and has limited effect on energy-efficiency.

For M2M applications with small data transmission, establishing RRC connection, network connection to transmit several bits is deemed as wasteful. Thus, Chen et al. [25] suggest either i) use the MAC PDU that should carry the RRC signaling to carry the data; ii) define special preamble to transmit coded data. The drawbacks of [25] are:i) the solution based on the preambles is not very scalable due to the limited amount of available preambles; ii) for a long term view, the transmission of data in control plane violate the principle of separation between control plane and data plane. Wiriaatmadja et al. [76] propose to simplify the data communication procedure by allowing MTC devices to send data right after preamble transmission without explicitly establishing a connection.

For the congestion in random access, Physical Downlink Shared Channel (PDSCH) resources of LTE are deemed sufficient in most communication scenarios. To ease the congestion on the air interface, those downlink assignments and uplink grants for MTC devices, which cannot be served by Physical Downlink Control Channel (PDCCH), can be aggregated into a transport block on PDSCH identified by a special Radio Network Terminal Identifier (RNTI) called MTC-RNTI [77]. MTC devices monitor PDCCH channel with their own cell RNTI and MTC-RNTI simultaneously. Game theory has been used for the context of cellular M2M to optimize preamble allocation [78]. In addition, a detailed random access related proposals are summarized in [39], which can be a complement of our categorization.

Random access protocols can be categorized into two families: ALOHA family and tree family [79]. Andres et al. [39] claim that ALOHA based RACH procedure is not suitable for MTC. Instead they mention that RACH procedure based on distributed queuing (DQ) is more promising. The concept of DQ [79] was proposed twenty years ago and then demonstrated in other literatures in terms of stability and near optimum behavior. DQ is based on

the combination of a M-array tree splitting algorithm with a smart set of simple rules that allow organizing every device in one out of two virtual queues. Due to the rules of DQ, it behaves as a random access method for low traffic loads, and it switches smoothly and seamlessly to a reservation access method as the traffic load increases. The authors conduct some ongoing research efforts applying DQ ideas within LTE/LTE-A systems. Dhillon et al. [80] suggest to implement a load dependent access scheme wherein uncoordinated strategy for light load and coordinated strategy for heavy load. Bontu et al. [81] propose a new UL physical, transport and logical channel: Common Traffic Channel (CTCH), UL simultaneous-access shared channel (UL-SSCH) and physical uplink simultaneous access shared channel (PUSSCH). Aforementioned channels enable M2M devices to simultaneously transmit data packet in the same radio resource. They also propose to transmit control signaling through in-band transmission in the user plane control.

In addition, there also exist mathematical works that are not categorized into Tab. 2.5, but they provide useful design guidelines to help improve device side energy efficiency. For example, in [82], the transmission energy is modeled as a function of transmission power, packet size and link capacity. A cumulative distribution function (CDF) of energy consumption for large-scale MTC is derived by using stochastic geometry. In [80], the comparison in terms of energy and power efficiency between uncoordinated and coordinated multiple access strategies are conducted. In [4], we extend the work of [80] by considering various packet size and imperfect power control. We find that coordinated FDMA is more resistant to various packet lengths of M2M devices packets in terms of power efficiency and is not influenced by imperfect power control. Thus coordinated multiple strategies, especially FDMA, are more suitable for the future M2M-compatible cellular networks and deserve further optimization works. With respect to uncoordinated CDMA, it is still a considerable choice due to its simplicity and no signaling overhead, when the BS load intensity is not high and the power control is accurate.

In fact, the cellular networks evolution trend is always to seek for a trade off between diverse performance metrics such as energy efficiency, packet delay, user data rate, etc. Hence, the gain of energy efficiency is inevitably with cost of a certain degradation of other performance metrics. For example, the cooperative relaying achieves energy efficiency with more packet delay due to multiple-hop transmission. The design of energy efficient signaling and operation, such as disconnection MTC devices from network when inactive, surely saves energy consumption but introduce higher delay for downlink packet, and the effort in this direction is not systematic. The energy efficient uplink radio resource allocation and packet scheduling schemes provide a systematic manner to gain energy efficiency for MTC, but they may lead to either serving less number of MTC devices and supporting limited QoS

classes or bringing more signaling messages in radio access networks. More importantly, it is difficult to design schemes simultaneously satisfying the QoS provisioning for both human and MTC users. The random access can be designed to reduce the retransmission probability for MTC users, but human users may suffer from degradation of service, due to the limited radio access resources. Therefore, it is very important to jointly apply the aforementioned approaches to gain device side energy efficiency and seek for a trade off with other system performance. For example, the random access procedure can be optimized by applying cooperative relaying to reduce the direct links towards the base station. The energy efficient uplink radio resource allocation algorithms can be jointly designed with random access procedure: allocate more resources for PRACH in case of overload or limit the number of access devices when no radio resource for data transmission, etc.

2.7 Summary

The arrival of billions of connected machines in the short and mid term is a huge challenge for wireless networks, especially at the RAN level. LPWA technologies and cellular 3GPP solutions will be the main support used for M2M applications. In this chapter, we describe the present state of these technologies and the evolutions as expected today.

We propose a synthesis for the QoS demands and the difference of characteristics between H2H and M2M. We then review the proposals for radio coverage and service of these machines. We identify the advantage of cellular networks for this expected service. The 3GPP cellular networks have a mature infrastructure to provide wide coverage, high-availability service and user subscription/management system but the shortcomings of 3GPP networks are relatively high energy consumption level and cost of hardware with regard to LPWA networks. These challenges are addressed by some research proposals that we summarize in this article. In terms of LPWA network such as LoRaWAN, their significant advantage is their low energy consumption design and low-cost hardware. However, their disadvantage is that the operators should deploy dedicated infrastructure for providing LPWA-related service.

According to our survey, to improve the device side energy efficiency in the future cellular networks, we get some design guidelines as follows:

- The possible approaches to improve device side energy efficiency for cellular MTC include: cooperative relaying, design of energy efficient signaling and operation, radio resource allocation and packet scheduling strategies and Energy-efficient random access procedure and MAC;

- It is a better solution to employ cooperative relaying, since it can be combined with other emerging technologies such as D2D communication, ad hoc networks research results and LoRa technology, etc.
- The radio resource allocation and packet scheduling schemes allows to get energy efficiency while keeping a certain level of QoS, however it is difficult to design this kind of schemes simultaneously satisfying the QoS provisioning for both human and MTC users.
- No matter by which approach, to gain energy efficiency is always with sacrifice of other system performances such as packet delay. Thus it is important to jointly use the aforementioned approaches, for example joint design of random access control and radio resource allocation, to seek for a trade off between energy efficiency and other system performances.
- It is always useful and necessary to rethink design of the radio access network. Thus, it is necessary to study the performance via analytical system models with mathematical tools such as stochastic geometry.

Chapter 3

Performance Evaluation of Transmit Power Diversity in S-ALOHA based Systems

3.1 Introduction

Machine Type Communication (MTC) is expected to gain more popularity in the next decade. Low Power Wide Area Network (LPWAN) networks are regarded to be an attractive option for MTC [83]. Due to its simplicity, the S-ALOHA (i.e. slotted-ALOHA) protocol is recently regaining interest in the study of LPWAN.

Despite intensive studies since the birth of S-ALOHA [84], the objectives of the existing related studies are usually analyzing throughput, packet loss rate, etc. In a radio communication system, factors such as capture effect, diversity of transmit power levels, power control precision, among with others, have a significant impact on ALOHA-like multiple access protocol.

The special features of M2M traffic and requirements highlight the importance of analytical models taking into account performance-affecting factors and giving a thorough performance evaluation. Fulfilling this necessity is the main focus of this chapter: we jointly consider the impact of capture effect, diversity of transmit power levels with imperfect power control. We propose a low complexity but still accurate analytical model capable of evaluating S-ALOHA in terms of packet loss rate, throughput, energy efficiency and average number of transmissions. The proposed model is able to facilitate dimensioning and design of S-ALOHA based LPWAN. The comparison between simulation and analytical results confirms the accuracy of our proposed model. The design guide lines about S-ALOHA

based LPWAN deduced from our model are: the imperfect power control can be positive with capture effect and appropriate transmit power diversity strategy. The transmit power diversity strategy should be determined by jointly considering network charges level, power control precision and SINR threshold to achieve optimal performance of S-ALOHA.

The rest of this chapter is organized as follows: Sec. 3.2 talks about the related work and motivation of this work. Sec. 3.3 presents the system model. Sec. 3.4 is the performance analysis about S-ALOHA in ideal systems, i.e., without power control and fading. Sec. 3.5 takes into account imperfect power control under wide-band system. Sec. 3.6 analyze the S-ALOHA in narrow band system with imperfect power control. Sec. 3.7 proves the accuracy of proposed model by simulation and gives some deduced design guidelines. Sec. 3.8 concludes this chapter.

3.2 Related work

Lamaire et al. [85] derive the optimal transmit power distribution under three models: perfect capture model, signal-to-interference threshold with and without Rayleigh fading model. Altman et al. [86] propose to differentiate transmission priority by using different transmit power levels and convert it as a game problem. Both [85, 86] ignore the impact of power control error for the transmit power distribution. Yang et al. [87] analyze backoff algorithms for LTE Random Access Channel (RACH), which employ ALOHA-like protocol. Nielsen et al. [88] analyze the outage probability for LTE four-steps random access mechanism. Both [87, 88] use an analytical model adapted from Bianchi model [89]. Zozor et al. [90] study collision probability for the pure time-frequency ALOHA access via stochastic geometry approach and calculate the load capacity according to a maximal packet loss rate. Goursaud et al. [91] consider the carrier frequency uncertainty issue and study ALOHA protocol behavior. It should be noted that [87–91] have not taken into account the capture effect and diversity of transmit power. Bayrakdar et al. [92] evaluate the throughput performance of S-ALOHA based cognitive radio network under Rayleigh fading channels with capture effect, but with identical transmit power in each transmission.

As far as we know, few works about S-ALOHA protocol jointly consider the impact of capture effect, power control error, diversity of transmit power levels, and give a multi-criteria performance analysis for M2M environment. In this chapter, we propose an analytical model to study the steady-state performance of S-ALOHA including packet loss rate, throughput, energy-efficiency and average number of transmission under the following situations:

- Ideal system with perfect power control and without fading;

- Wide band systems with imperfect power control,
- Narrow band systems with imperfect power control.

In the proposed model, the basic idea is to numerically obtain cumulative distribution function (CDF) of the total interference from its characteristic function (CF). This allows calculating the capture probability and thus the transmission failure probability for a single trial. We then use a fixed point analysis to calculate the steady state packet loss rate, throughput, energy efficiency and average number of transmissions.

3.3 System Model

We consider a single Base Station (BS). Terminals served by this base station employ S-ALOHA protocol to transmit packets. The behavior of different terminals is independent. The time axis is divided into slots of fixed length T_{slot} equal to the transmission time of a single packet. The arrival of fresh packet is assumed to follow a stationary Poisson process with intensity λ. Thus, the average arrival rate of fresh packet in unit slot is λT_{slot}.

3.3.1 Retransmission Mechanism

In case of transmission failure, the retransmission is scheduled after a random number of slots. Each packet is allowed to be transmitted at most $N_{\max}$ times. Since retransmissions take place at random over long intervals following the collisions that give rise to them and according to Poisson's splitting property [93], the aggregate packets arrival process can be divided into $N_{\max}$ mutually independent Poisson arrivals processes. Each process with index $n \in \{1,...,N_{\max}\}$ (i.e., for the n^{th} transmission) has a intensity $\lambda T_{\text{slot}} P_n$, where P_n is the steady-state probability for a packet to make at least n transmissions. Let Q_n be the failure probability that the n^{th} transmission trial is failed. Thus, we have:

$$P_1 = 1;\ P_2 = P_1 Q_1;\ ...;\ P_{N\max} = P_{N\max-1} Q_{N\max-1} \tag{3.1}$$

3.3.2 Transmission Power Diversity Strategy

One objective of this work is to study system performance gain brought by the transmit power level diversity, instead of searching the optimal transmit power diversity strategy. The latter is planned as part of future work. To this end, we consider a simple and easy to be implemented method for low-cost M2M devices to adjust the transmit power levels: we assume that during the initial packet transmission, all M2M terminals set their respective

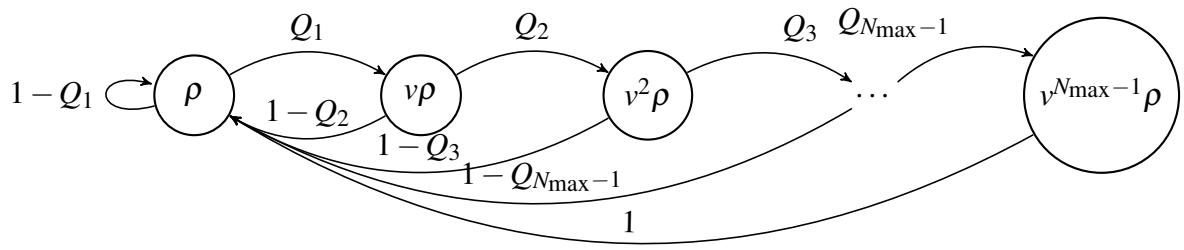

Fig. 3.1 The transition of transmission power level diversity

initial transmit powers so that the target received power ρ at the BS is identical. For each retransmission, the transmit power level is multiplied by a factor v. Thus, the target received power is also multiplied by v. In addition, we assume that one device has a valid transmit power level interval (i.e. there exist a minimum valid transmit power and a maximum transmit power constraint.). Therefore, according to the value of v, we define three strategies to be evaluated:

- Identical transmit power strategy with $v = 1$. Namely, the transmit power of all devices never changes and is the minimum valid power;
- Incremental transmit power strategy with $v > 1$. The initial transmit power is the minimum valid value. A concrete example is the power ramping technique used in LTE random access stage;
- Decremental transmit power strategy with $v < 1$. The initial transmit power should ensure that the last transmission trial (i.e., for the $N_{\max}$th transmission trial) use the minimum valid power level.

A schematic diagram for the device states (i.e. target received power level) in the transmission power diversity is shown in Fig. 3.1, in which each state represents one target received power.

3.3.3 Capture Effect

In terms of capture effect, Signal-to-Interference-and-Noise ratio (SINR) threshold model is applied. In such a model, the other simultaneous packet transmissions are interference sources for a given transmission. One packet transmission is failed if and only if its received SINR is less than a threshold[1] θ_T, which depends on the modulation coding and receiver characteristics [94].

[1]The term SINR threshold and capture ratio are interchangeably used in this chapter.

Due to capture effect and the fact that the background noise is negligible compared to interfering transmissions, the failure probability Q_n of a n^{th} retransmission is:

$$Q_n = \mathbf{P}\{p_n/I < \theta_T\}, \tag{3.2}$$

where p_n refers to the received power at BS side for the n^{th} transmission trial, I is the cumulative interference caused by all other simultaneous transmissions. Since I depends on all $N_{\max}$ Poisson process, each of which has an intensity $\lambda T_{\text{slot}} P_n$. Thus, Q_n is a function of probability vector $P_1, ..., P_{N_{\max}}$. We thus obtain a fixed point equation array between $P_1, ..., P_{N_{\max}}$ and $Q_1, ..., Q_{N_{\max}}$ from (3.2). Starting with initial vector $1, 0, 0, ..., 0$ for $P_1, ..., P_{N_{\max}}$, we iteratively obtain the probability vector $P_1, ..., P_{N_{\max}-1}, P_{N_{\max}}$. This is a general fixed point analysis framework for the rest sections.

3.3.4 Performance Metrics

It is straightforward to prove that $P_{N_{\max}+1}$ is the steady-state packet loss rate, where $N_{\max}$ is the maximum allowed transmission number. Therefore, the steady-state throughput of S-ALOHA is $\lambda T_{\text{slot}}(1 - P_{N_{\max}+1})$.

Apart from steady-state packet loss rate and throughput, the probability vector P_1, P_2, ..., $P_{N_{\max}}$ allows to analyze average normalized energy efficiency[2] $\overline{\text{EE}}$. The latter is defined as the ratio between number of delivered packets and the total energy consumed (including for dropped packets). For an ergodic stochastic process, statistical average of energy efficiency can be well approximated by its temporal average. Note that what we care about is the impact of transmit power diversity and power control error on energy efficiency. The attenuation caused by propagation distance is not considered without affecting the performance comparison result. The normalized average energy efficiency thus can be expressed in terms of received powers:

$$\overline{\text{EE}} = \frac{1 - P_{N_{\max}}}{\sum_{n=1}^{N_{\max}} P_n \overline{J_n}}, \tag{3.3}$$

where $\overline{J_n} = p_n T_{\text{slot}}$ is the average energy consumed by a packet on n^{th} transmission.

[2]The term average normalized energy efficiency is simpled called energy efficiency in this chapter.

The expected number of transmissions is denoted by $\overline{N_{Tx}}$. This metric gives an estimation of the average delay of S-ALOHA.

$$\overline{N_{Tx}} = \sum_{n=1}^{N_{\max}} P_n$$

In the following, we show how to numerically calculate probability vector of interest under different situations.

3.4 Ideal systems with perfect power control

In this section we assume the power control is perfect. Fading and shadowing effects are ignored. Recall that at the first transmission, all terminals transmit at a power such that the received power at the base station is ρ. Without loss of generality, let ρ be 1 for the simplicity of notation. At each retransmission, the power is multiplied by a factor v. Hence, at the n^{th} transmission the received power p_n is v^{n-1}.

In order to keep received power levels as integer, we assume that v can be expressed $v = a/b$ where a and b are integers, and compute power levels normalized by $1/b^{N\max-1}$. Hence, at the n^{th} transmission, the normalized received power is $p_n = a^{n-1}b^{N\max-n}$. Its corresponding normalized cumulative interference Y:

$$Y = \sum_{n=1}^{N_{\max}} Z_n = \sum_{n=1}^{N_{\max}} \sum_{j=1}^{N_n} a^{n-1}b^{N\max-n}, \tag{3.4}$$

where $Z_n = \sum_{j=1}^{N_n} a^{n-1}b^{N\max-n}$ refers to the normalized cumulative interference from n^{th} transmission Poisson process and N_n denotes the number of packets on n^{th} transmission following Poisson distribution with average arrival rate $\lambda T_{\text{slot}} P_n$.

The cumulative interference component Z_n is a compound random variable [95], whose definition is as follows:

Definition 3.4.1. The random variable $\sum_{i=1}^{N} X_i$, equal to the sum of a random number N of independent and identically distributed random variables X_i that are also independent of N, is called a compound random variable.

The Laplace transform of a compound random variable is detailed in Appendix A. Applying (A.1), we have:

$$\mathscr{L}\{Z_n\}(s) = \exp\left\{\lambda T_{\text{slot}} P_n \left(\exp(-sa^{n-1}b^{N\max-n}) - 1\right)\right\},$$

where $\mathscr{L}\{f(\cdot)\}(s)$ is the Laplace transform operator with complex variable s for function $f(\cdot)$.

Since the series of random variables $Z_n, n = 1,...,N_{\max}$ are independent, the Laplace transform of Y is:

$$\begin{aligned}\mathscr{L}\{Y\}(s) &= \prod_{n=1}^{N_{\max}} \mathscr{L}\{Z_n\}(s) \\ &= \exp\left\{\lambda T_{\text{slot}}\left(\sum_{n=1}^{N_{\max}} P_n \exp(-sa^{n-1}b^{N_{\max}-n}) - \sum_{n=1}^{N_{\max}} P_n\right)\right\}\end{aligned}$$

With a substitution $s = -i\omega$, we obtain the characteristic function $\phi_Y(\omega)$ of Y:

$$\phi_Y(\omega) = \exp\left\{\lambda T_{\text{slot}}\left(\sum_{n=1}^{N_{\max}} P_n \exp(i\omega a^{n-1}b^{N_{\max}-n}) - \sum_{n=1}^{N_{\max}} P_n\right)\right\}$$

Note that Y is a discrete random variable. Via a numerical integral method detailed in [96], the cumulative distribution function $F_Y(x)$ of Y can be derived from its characteristic function $\phi_Y(\omega)$.

$$F_Y(x) = \frac{1}{\pi}\int_0^{\pi} \frac{\sin[(x+1)\omega/2]}{\sin[\omega/2]} \Re\left\{\phi_Y(\omega)\, e^{-ix\omega/2}\right\} d\omega, \tag{3.5}$$

where $\Re\{\cdot\}$ is the operator taking real part of complex number.

Cumulative distribution function F_Y can be numerically and rapidly obtained by trapezoidal rule. Due to capture effect, the transmission failure probability Q_n of a packet on n^{th} transmission is thus:

$$Q_n = \mathbb{P}\left\{\frac{a^{n-1}b^{N_{\max}-n}}{Y} < \theta_T\right\} = 1 - F_Y\left(\lfloor\frac{a^{n-1}b^{N_{\max}-n}}{\theta_T}\rfloor\right), \tag{3.6}$$

where operator $\lfloor x \rfloor$ returns back the maximal integer not greater than x.

Substituting (3.5) and (3.6) into (3.1), we get a fixed point equation for probability vector $\langle P_1,...,P_{N_{\max}+1}\rangle$.

3.5 Wide band Systems with Imperfect Power Control

We consider that data packets are transmitted with a wide band signal (e.g. by use of a spread spectrum technique). Hence, there is no Rayleigh fading. The received power level of packet transmission is affected by imperfect power control. The effect of imperfect power control

in the literature can be assumed to be a multiplier ε following lognormal distribution [97]. Still let ρ be the received power for the initial transmission at the BS without power control error. Normalized by ρ, the received power p_n for the n^{th} transmission, for a given device with index i, can be written as follows:

$$p_{ni} = v^{n-1} e^{\beta \varepsilon_i}, \text{with } \beta = \frac{\ln(10)}{10}$$

The power control error factor ε_i is a zero-mean Gaussian random variable with a standard deviation of σ, namely $\varepsilon_i \sim N\left(0, \sigma^2\right)$.

The cumulative interference I, caused by those terminals simultaneously transmitting packet, during the n^{th} transmission is thus:

$$I = \sum_{n=1}^{N\max} v^{n-1} \sum_{j=1}^{N_n} e^{\beta \varepsilon_j},$$

where N_n refers to the number of packets on n^{th} transmission and follows Poisson distribution with arrival rate $\lambda T_{\text{slot}} P_n$.

Due to capture effect, a n^{th} transmission trial is failed under the condition that the ratio between received power p_n and cumulative interference I is less than a threshold θ_T, namely:

$$\sum_{m=1}^{N\max} v^{m-n} \sum_{j=1}^{N_m} e^{\beta\left(\varepsilon_j - \varepsilon_i\right)} > \frac{1}{\theta_T}$$

Let us focus the normalized cumulative interference Y_n corresponding to a packet on n^{th} transmission:

$$Y_n = \sum_{m=1}^{N\max} v^{m-n} \sum_{j=1}^{N_m} e^{\beta\left(\varepsilon_j - \varepsilon_i\right)} = \sum_{m=1}^{N\max} \sum_{j=1}^{N_m} e^{(m-n)\ln(v) + \beta\left(\varepsilon_j - \varepsilon_i\right)}$$

With substitution $\chi = (m-n)\ln(v) + \beta\left(\varepsilon_j - \varepsilon_i\right)$, we have:

$$Y_n = \sum_{m=1}^{N\max} Z_m = \sum_{m=1}^{N\max} \sum_{j=1}^{N_m} e^{\chi} \tag{3.7}$$

Since Z_m for $m = 1, \ldots, N_{\max}$ are mutually independent, thus, the Laplace transform of Y_n is:

$$\mathscr{L}\left\{Y_n\right\}(s) = \prod_{m=1}^{N\max} \mathscr{L}\left\{Z_m\right\}(s) = \prod_{m=1}^{N\max} \exp \lambda T_{\text{slot}} P_m \left(\mathscr{L}\left\{e^{\chi}\right\}(s) - 1\right) \tag{3.8}$$

We verify that χ follows a normal distribution with mean $(m-n)\ln(v)$ and variance $2\beta^2\sigma^2$. Namely $\chi \sim N\left((m-n)\ln(v), 2\beta^2\sigma^2\right)$.

A closed form expression of the Laplace transform of the lognormal distribution does not exist. Yet, according to reference [98], the Laplace transform of a lognormal random variable can be approximated as follows:

$$\mathscr{L}\{e^{\chi}\}(s) = \frac{\exp(-\frac{W(s\sigma_\chi^2 e^{\mu_\chi})^2 + 2W(s\sigma_\chi^2 e^{\mu_\chi})}{2\sigma_\chi^2})}{\sqrt{1+W(s\sigma_\chi^2 e^{\mu_\chi})}}, \tag{3.9}$$

where $W(\cdot)$ is the Lambert W function [99], which is defined as the solution in principal branch of the equation $W(x)e^{W(x)} = x$.

Combining (3.8) and (3.9)), with substitution $s = -i\omega$, we obtain the characteristic function of cumulative function $\phi_Y(w)$:

$$\mathscr{L}[Y_n] = \exp\left\{\lambda T_{\text{slot}}\left(\sum_{m=1}^{N_{\max}} \frac{P_m}{\sqrt{1+W(i\omega\sigma_\chi^2 e^{\mu_\chi})}} \exp(-\frac{W\left(i\omega\sigma_\chi^2 e^{\mu_\chi}\right)^2 + 2W\left(i\omega\sigma_\chi^2 e^{\mu_\chi}\right)}{2\sigma_\chi^2}) - \sum_{m=1}^{N_{\max}} P_m\right)\right\},$$

where i is the imaginary unit, $e^{\mu_\chi} = v^{(m-n)}, \sigma_\chi^2 = 2\beta^2\sigma^2$.

As a continuous random variable, the cumulative distribution function $F_{Y_n}(x)$ of Y_n can be directly derived from its characteristic function $\phi_{Y_n}(w)$, for example by use of Gil-Pelaez Theorem [100], which is stated as follows:

Theorem 3.5.1. *Gil-Pelaez theorem: Let $F_X(x)$, $\phi_X(\omega)$ respectively be the distribution function and characteristic function of random variable X. The relationship between $F_X(x)$ and $\phi_X(\omega)$ is as follows:*

$$F_X(x) = \frac{1}{2} - \int_{-\infty}^{+\infty} \text{Im}\left(\frac{\phi_X(\omega)\exp(-i\omega x)}{2\pi\omega}\right) d\omega$$

However, directly using Gil-Pelaez Theorem needs long time. Applying mathematical techniques used in finance domain [101], we seek to calculate the Fourier transform of $e^{-\eta x}F_{Y_n}(x)$ where term $e^{-\eta x}$ is a damping function with $\eta > 0$.

$$\int_{-\infty}^{+\infty} e^{iwx}e^{-\eta x}F_{Y_n}(x)\,dx = \frac{1}{\eta - iw}\phi_{Y_n}(\omega + i\eta) \tag{3.10}$$

Applying Fourier inversion for (3.10), we obtain the expression for $F_{Y_n}(x)$ as follows:

$$\begin{aligned} F_{Y_n}(x) &= \frac{e^{\eta x}}{2\pi}\int_{-\infty}^{+\infty} e^{-i\omega x}\frac{1}{\eta - i\omega}\phi_{Y_n}(\omega + i\eta)\,d\omega \\ &= \frac{e^{\eta x}}{\pi}\Re\left\{\int_{0}^{+\infty} e^{-i\omega x}\frac{1}{\eta - i\omega}\phi_{Y_n}(\omega + i\eta)\,d\omega\right\}, \end{aligned} \tag{3.11}$$

The cumulative distribution function $F_{Y_n}(x)$ now can be derived directly from (3.11) using a single numerical integration.

The transmission failure probability for the n^{th} transmission Q_n is:

$$Q_n = 1 - F_{Y_n}\left(\frac{1}{\theta_T}\right) \tag{3.12}$$

Similar with what we analyze in Sec. 3.4, combining (3.1), (3.11) and (3.12), we can use fixed point method to get the solution for probability vector $P_1, \ldots, P_{N_{\max}}$.

3.6 Narrow band Systems with Imperfect Power Control

In this section, we consider narrow band LPWAN networks. The packet transmission suffers Rayleigh fading and its power control is not perfect. An example of the narrow band system that suffers from fading and imperfect power control is LoRaWAN. Although LoRaWAN applies spectrum spreading technology, it can still be assumed to suffer Rayleigh fading in literature [102]. As discussed in Section 3.5, imperfect power control is still characterized by a lognormal random variable (RV) and can be written as $e^{\beta\varepsilon}$ with $\beta = \frac{\ln(10)}{10}$, where ε is a Gaussian RV with zero mean and variance σ_ε. The fading effect can be characterized by a multiplier H of exponential RV with unit mean. For a device with index i attempting kth retransmission, the received power p_{ni} can be expressed as:

$$p_{ni} = v^{n-1} \cdot e^{\beta\varepsilon_i} \cdot H_i,$$

where v refers to power increment factor.

Let I denote the its suffered cumulative interference, namely $I = \sum_{m=1}^{N_{\max}} \sum_{j=1}^{N_m} p_{mj}$. Let Θ denote the SINR (in decimal) for the considered device i. Recall that a transmission is regarded as successful if its SINR is not less than a predefined threshold θ_T. The transmission failure probability Q_n of a packet on n^{th} transmission is as follows:

$$Q_n = 1 - \mathbb{P}(\Theta \geq \theta_T) = 1 - \mathbb{P}(p_n \geq I\theta_T) = 1 - \mathbb{P}\left(H_i \geq \frac{I}{v^{n-1}e^{\beta\varepsilon_i}}\theta_T\right)$$

With substitution $U_n = \frac{I}{\nu^{n-1}e^{\beta\varepsilon_i}}$, and let $f_{U_n}(u)$ denote probability density function (PDF) of U_n. Note that H_i follows exponential distribution with unit mean.

$$\mathbb{P}(\Theta \geq \theta_T) = \int_0^\infty f_{U_k}(u)e^{-u\theta_T}du = \mathscr{L}\{U_k\}(\theta_T),$$

which is the Laplace Transform value for random variable U_n at point θ_T. Now the problem is down to calculate the Laplace Transform of U_n. Let regard the random variable U_n:

$$\begin{aligned} U_n &= \frac{I}{\nu^{n-1}e^{\beta\varepsilon_i}} \\ &= \frac{\sum_{m=1}^{N\max}\nu^{m-1}\cdot\sum_{j=1}^{N_m}e^{\beta\varepsilon_j}\cdot H_j}{\nu^{n-1}e^{\beta\varepsilon_i}} \\ &= \sum_{m=1}^{N\max}\nu^{m-n}\sum_{j=1}^{N_m}H_j e^{\beta(\varepsilon_j-\varepsilon_i)} \\ &= \sum_{m=1}^{N\max}\nu^{m-n}Z_m, \end{aligned}$$

where $Z_m = \sum_{j=1}^{N_m} Z_{m,j}, Z_{m,j} = H_j e^{\beta(\varepsilon_j-\varepsilon_i)}$.

Since the series of RV Z_m for $m = 1,\ldots,N_{\max}$ are mutually independent, we have:

$$\mathscr{L}\{U_n\}(s) = \prod_{m=1}^{N\max}\mathscr{L}\{U_n\}\left(\nu^{m-n}s\right),$$

where s is a complex number.

The term $Z_m = \sum_{j=1}^{N_m} Z_{m,j}$ is a compound random variable, where N_m follows Poisson distribution with arrival rate $\lambda T_{\text{slot}} P_m$. The Laplace transform of Z_m can be obtained by using the formula (A.1) shown in Annexe A.

$$\mathscr{L}\{Z_m\}(s) = \exp\left\{\lambda T_{\text{slot}}P_m\left(\mathscr{L}\left\{Z_{m,j}\right\}(s)-1\right)\right\}$$

$$\mathscr{L}\{U_n\}(s) = \exp\left\{\lambda T_{\text{slot}}\left(\sum_{m=1}^{N\max}P_m\mathscr{L}\left\{Z_{m,j}\right\}\left(\nu^{m-n}s\right) - \sum_{m=1}^{N\max}P_m\right)\right\} \tag{3.13}$$

The random variable $Z_{m,j}$ is the product of a lognormal type RV and an exponential type RV. Its Laplace transform is as follows. More analysis details are given in Annexe A.

$$\mathscr{L}\left\{Z_{m,j}\right\}(s) \approx \frac{1}{1+s^{\left(1+\frac{\pi\sigma^2}{8}\right)^{-\frac{1}{2}}}}, \tag{3.14}$$

where $\sigma^2 = 2\beta^2\sigma_\varepsilon^2$.

Combining (3.14) and (3.13) and letting $s = \theta_T$, we obtain:

$$\begin{aligned} Q_n &= 1 - \mathscr{L}\left\{U_n\right\}\left(e^{\beta\varepsilon_i}\right) \\ &= 1 - \exp\left\{\lambda T_{\text{slot}}\left(\sum_{m=1}^{N_{\max}} \frac{P_m}{1+\left(v^{m-n}\theta_T\right)^{\left(1+\frac{\pi\sigma^2}{8}\right)^{-\frac{1}{2}}}} - \sum_{m=1}^{N_{\max}} P_m\right)\right\} \end{aligned} \tag{3.15}$$

With (3.15), we form a fixed point equation to solve probability vector $P_1, ..., P_{N_{\max}}$.

3.7 Simulation results and discussion

3.7.1 Accuracy of proposed models

To verify the accuracy of proposed analytical model, we develop a Python-based simulator. In the simulation, we define N M2M devices. Each device generates a fresh packet with probability of $\lambda T_{\text{slot}}/N$ in each slot. The total number of packets generated by all devices during T_{slot} approximately follows a Poisson distribution with intensity λT_{slot} if $\lambda T_{\text{slot}}/N$ is enough small (e.g. less than 0.01). In case of transmission failure, a retransmission is scheduled after a random number of slots following exponential distribution with mean of 50 slots. To calculate 95% confidence interval, simulation is repeated 40 times for each fresh arrival intensity.

For the diversity of transmit power, we consider three strategies: 1) identical transmit power level with $v = 1$; 2) incremented transmit power level with $v = 2$; 3) decremented transmit power level with $v = 0.5$. The maximum allowed transmission number $N_{\max}$ is set as 5. In terms of capture effect, we confirm our analytical model under three SINR threshold: 3 dB, 0 dB, -3 dB. To confirm the accuracy of proposed analytical model, we compare the results obtained from analytical and simulation results in terms of packet loss rate, throughput, energy efficiency and expected number of transmissions. We just show the packet loss rate results (95% confidence interval).

Table 3.1 Packet loss rate ratio between simulation and analytical results. Capture ratio: 3 dB. P_{sim}:packet loss rate by simulation. P_{ana}: packet loss rate from analytical model

$\nu = 2.0$		$\nu = 1.0$		$\nu = 0.5$	
load	$10\log_{10}(\frac{P_{sim}}{P_{ana}})$	load	$10\log_{10}(\frac{P_{sim}}{P_{ana}})$	load	$10\log_{10}(\frac{P_{sim}}{P_{ana}})$
0.44	2.910	0.30	1.157	0.40	-0.061
0.46	3.052	0.32	0.788	0.42	-0.115
0.48	1.591	0.34	0.648	0.44	-0.032
0.50	1.590	0.36	0.337	0.46	-0.126
0.52	0.785	0.38	0.117	0.48	-0.202
0.54	0.641	0.40	0.154	0.50	-0.044
0.56	-0.064	0.42	-0.188	0.52	0.046
0.58	-0.365	0.44	-0.268	0.54	-0.067
0.60	-0.468	0.46	-0.518	0.56	-0.004
0.62	-0.620	0.48	-0.454	0.58	-0.118
0.64	-0.361	0.50	-0.291	0.60	-0.155

The performance of packet loss rate in an ideal S-ALOHA based system in shown in Fig. 3.2. The case of wide-band system affected by imperfect power control is shown in Fig. 3.3. The packet loss rate performance for a system that suffers Rayleigh fading and imperfect power control is illustrated in Fig. 3.4. The power control error standard deviations in Fig. 3.3 and Fig. 3.4 are 1 dB. In addition, to well reflect the accuracy of our analytical models, we calculate the ratio between packet loss rates obtained by simulation and analytical results (i.e. $10\log_{10}(\frac{P_{sim}}{P_{ana}})$). We resume the obtained ratio for the case of 3 dB in a wide band system with imperfect power control of 1 dB (corresponding to leftmost subfigure of Fig. 3.3) into Tab. 3.1. In these three figures and Tab. 3.1, we observe that, the proposed analytical results coincide with that of simulation in most cases. There exists a difference between analytical and simulation result in Fig. 3.3(c), when fresh packet arrival rate λT_{slot} is between 1.08 and 1.1. For regime of interest, from 10^{-3} to 10^{-1}, the proposed model still gives an accurate estimation of packet loss rate.

For a given arrival rate λT_{slot}, with our proposed analytical models, the performance metrics can be obtained by less than 30 iterations, within several seconds. This means that the proposed model can be integrated into M2M network dimensioning tools box.

3.7.2 Evaluation for wide band systems with imperfect power control

The performance of S-ALOHA based M2M networks is evaluated in terms of packet loss rate, throughput, energy efficiency, expected number of transmissions. About the capture

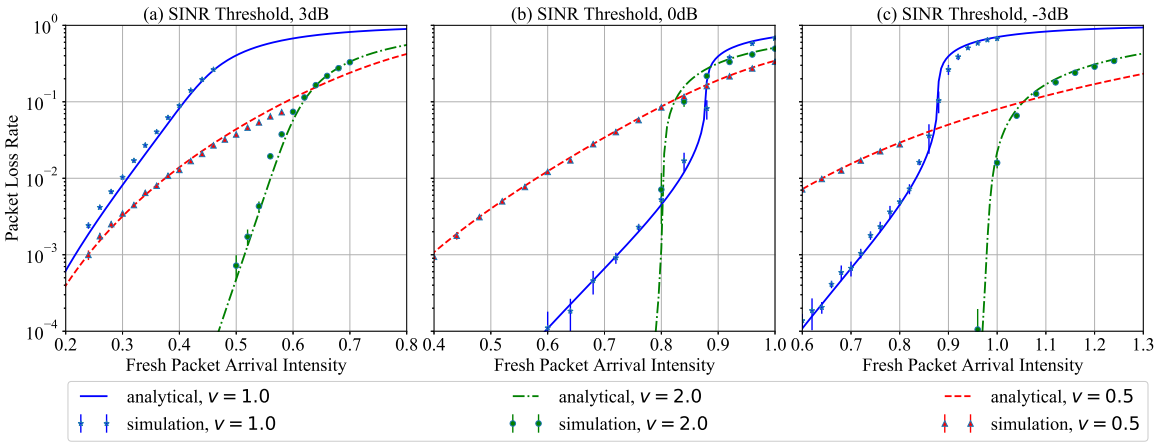

Fig. 3.2 Packet loss rate with different transmit power diversity strategies and capture ratios in S-ALOHA based ideal systems

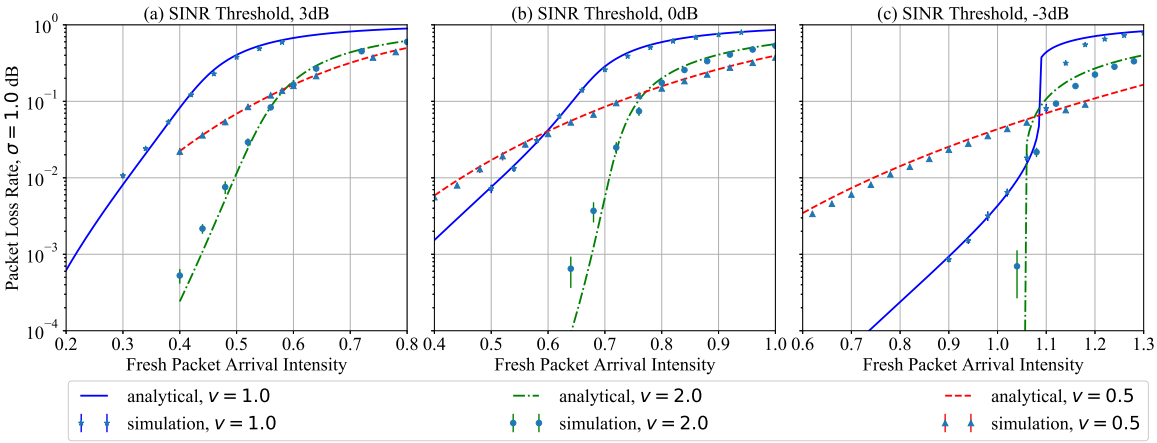

Fig. 3.3 Packet loss rate with different transmit power diversity strategies and capture ratios in S-ALOHA wide-band systems

effect, SINR thresholds of 3 dB, 0 dB, -3 dB are considered. The case of in ideal S-ALOHA based system (i.e. with perfect power control) serves as comparison reference.

Fig. 3.5 shows the performance with SINR threshold 3dB. Each sub-figure of Fig. 3.5 shows the comparison under two different power control error standard deviations $\sigma = 0, 3$ dB. Note that $\sigma = 0.0$ dB refers to the perfect power control case. Some remarks obtained from Fig. 3.5 are listed as follows:

- We observe that within a network applying identical transmit power strategy (the power incrementation factor $v = 1$), when power control error standard variance is 3dB, the S-ALOHA performance gets improved in terms of all metrics. This means that in the case, the degradation of power control precision (σ varies from 0 dB to 3 dB) has a

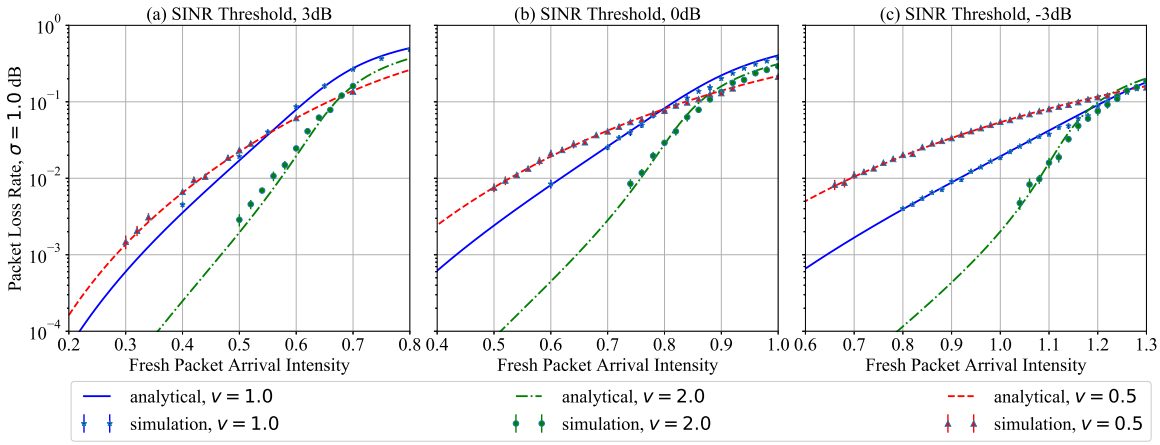

Fig. 3.4 Packet loss rate with different transmit power diversity strategies and capture ratios in S-ALOHA networks that suffer from fading and imperfect power control

positive impact to systems. The reason is that power control error serves as a way to make transmit power levels more diverse and the presence of capture effect leverages such a received power level diversity. However, imperfect power control has a negative impact for incremental or decremental strategies, because power control error reduces the transmit powers diversity introduced by factor v.

- The comparison between different transmit power levels strategies with the same power control precision indicates that incremental or decremental strategies outperform the identical strategy except in term of energy efficiency. For example, in Fig. 3.5(c), S-ALOHA using identical transmit power outperforms than other strategies in terms of energy efficiency. The reason is that these two strategies gain a high level transmit power diversity at the cost of more energy consumption. The energy efficiency of decremental power strategy is always at low level, since this strategy requires to start with high power levels then decreases for the future retransmission.

Fig. 3.6 shows the comparison result under capture ratio 0 dB. Each sub-figure shows the comparison under two different power control error standard deviation $\sigma = 0, 3$dB. Compared with Fig. 3.5, the remarks that we get are as follows:

- In this case, power control error brings a negative impact to the performance of S-ALOHA, no matter which transmit power strategy is employed. That means that for networks with spreading factors to achieve capture ratio 0 dB, it is important to keep the power control more precise. Otherwise, the performance gain will be neutralized due to power control precision.
- In this case, identical transmit power strategy has the best performance in terms of all metrics.

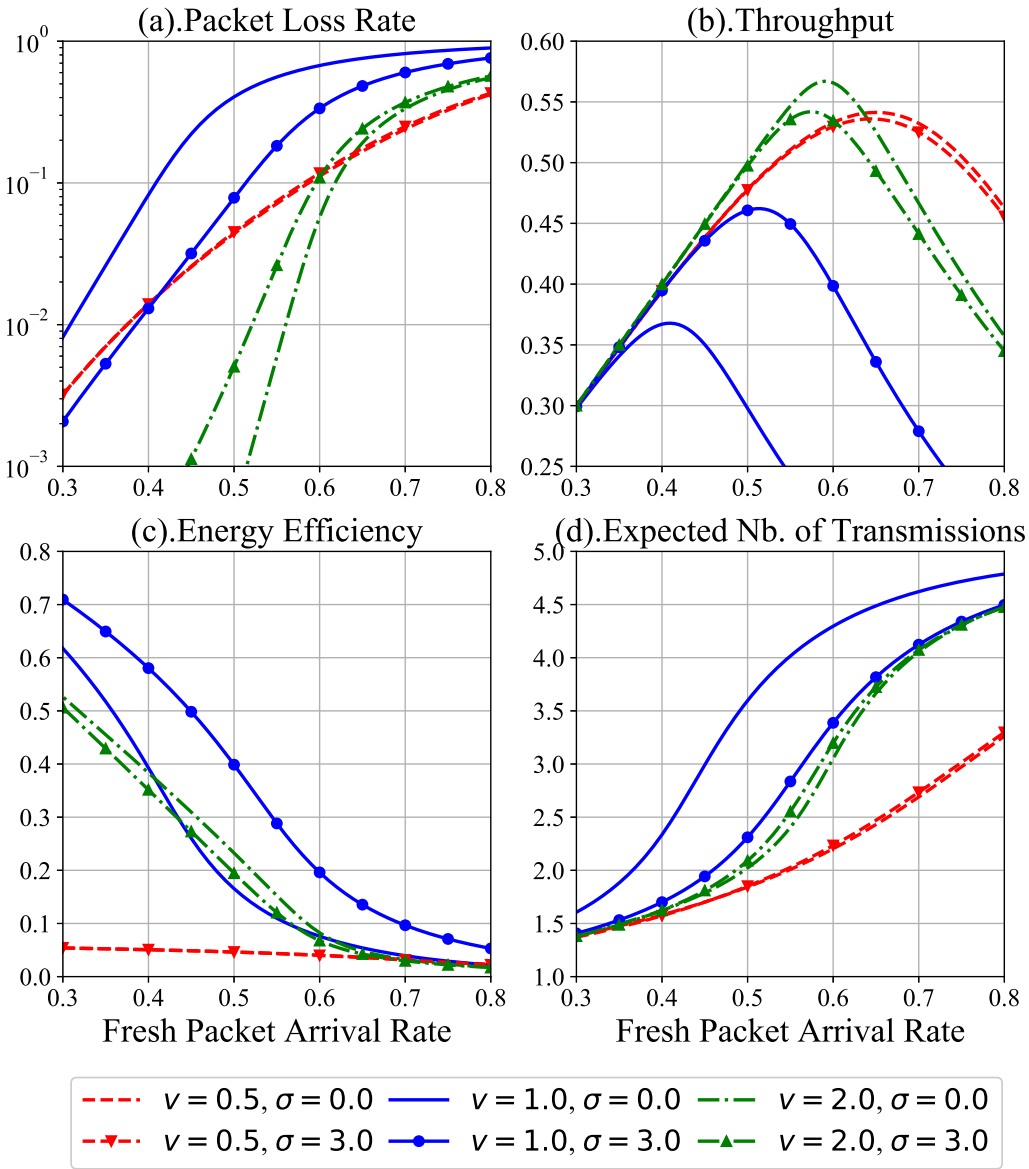

Fig. 3.5 Performance comparison with different transmit power diversities and power control precisions in wide band systems. SINR threshold 3 dB

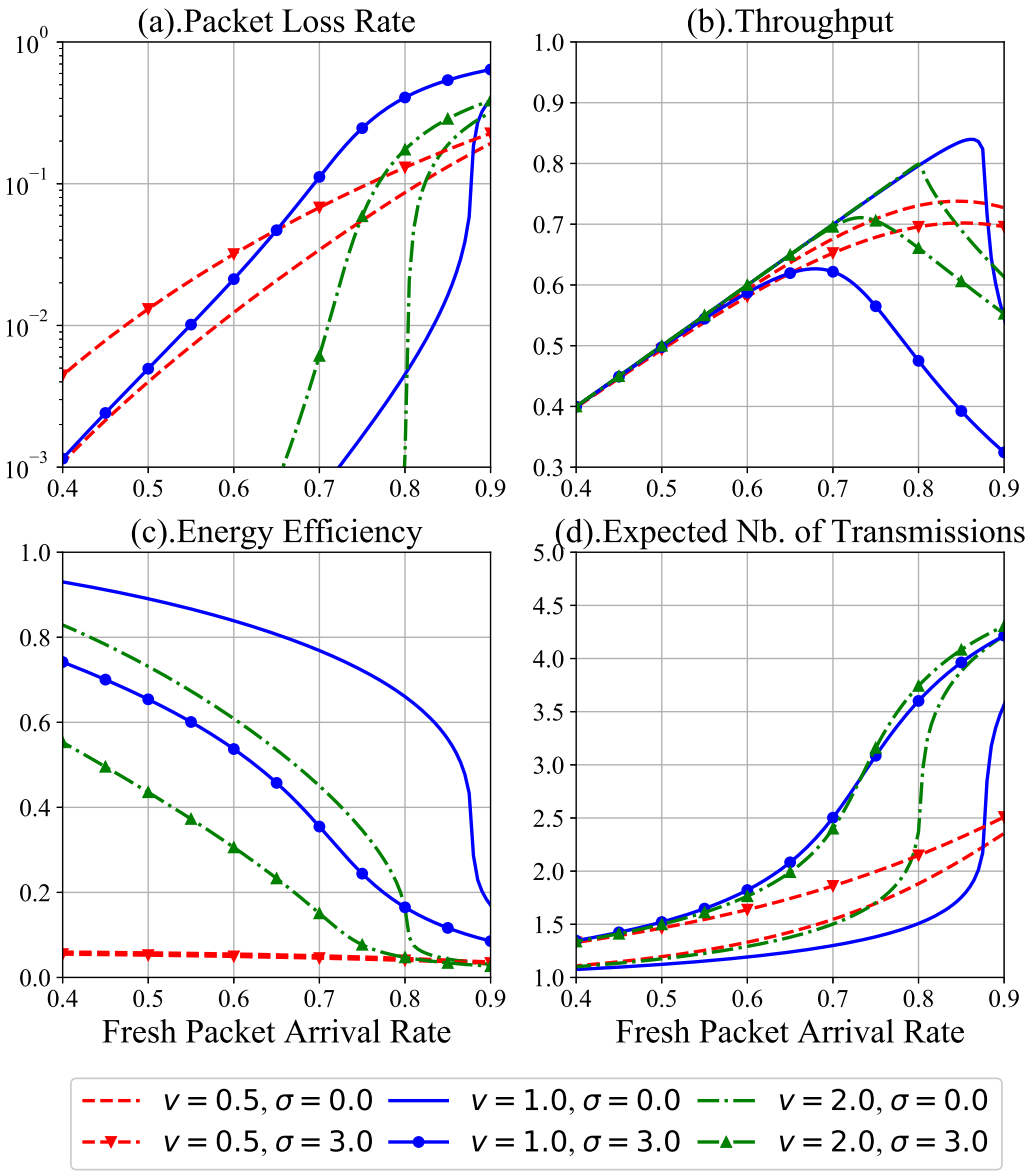

Fig. 3.6 Performance comparison with different transmit power diversities and power control precisions in wide band systems. SINR threshold 0 dB

Now we consider a M2M network with -3 dB as capture ratio. The observations and remarks obtained are:

- When wide-band systems have -3 dB capture ratio, for identical transmit power diversity strategies, there exists a critical point about fresh arrival intensity. Beyond this critical point, the imperfect power control has a positive impact to system performance. For incremental and decremental strategy, the impact of imperfect power control is always positive.

- In this case, the best transmit power strategy depends on the network requirements and system load. In fresh arrival intensity interval $[0, 0.8]$, identical transmit power diversity is the most suitable one. However, when arrival intensity is beyond 0.8 and the network has low latency requirement, the incremental strategy is more better than others. However, if arrival intensity is beyond 0.8 and the network has energy efficiency requirement, the identical transmit power diversity strategy with imperfect power control is recommended.

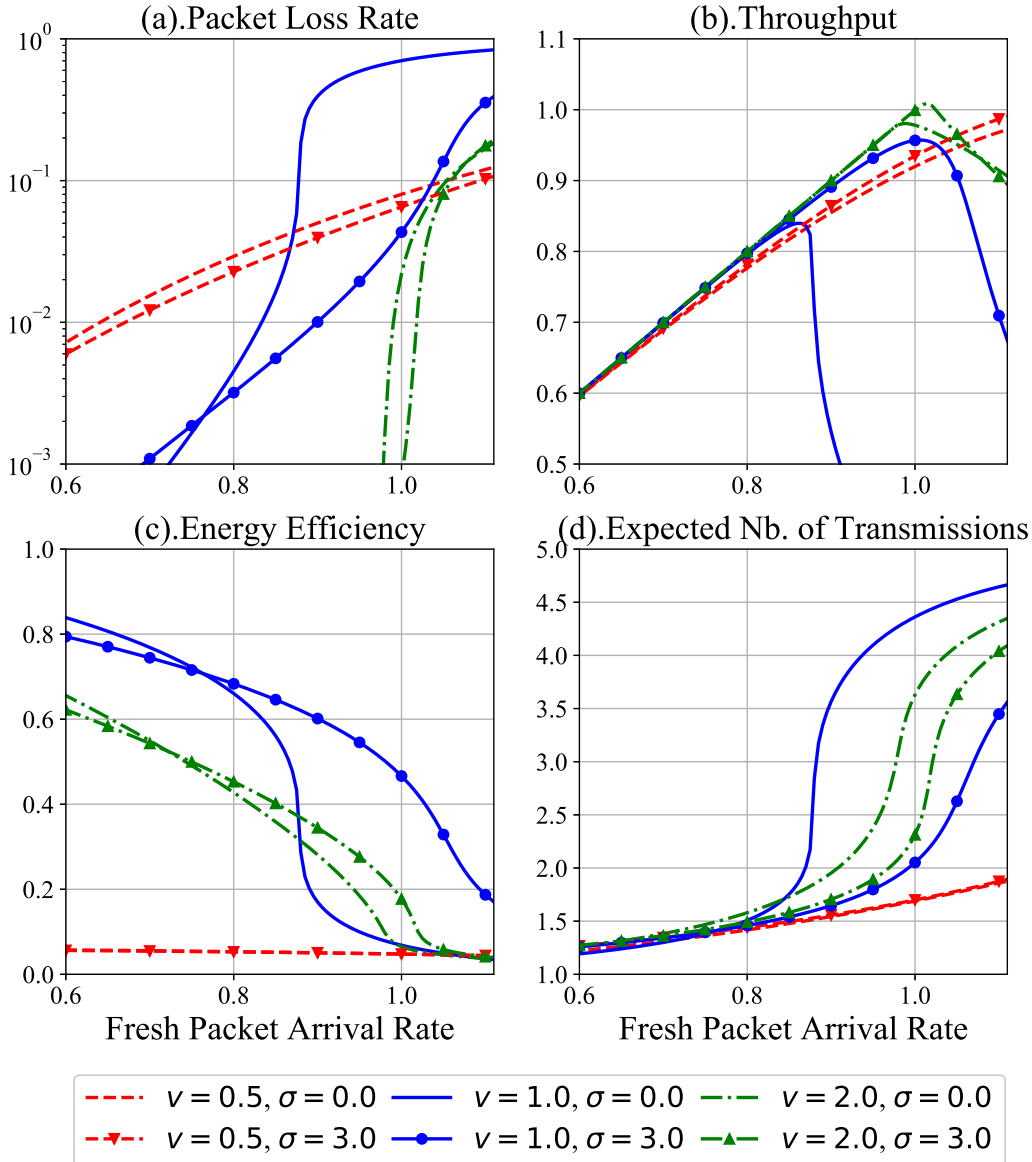

Fig. 3.7 Performance comparison with different transmit power diversities and power control precisions in wide band systems. SINR threshold -3 dB

3.7.3 Evaluation for narrow band systems with imperfect power control

In this section, we conduct performance comparison with different transmit power diversity strategies in narrow band system with imperfect power control. The power control error is 3 dB. The considered capture ratios are: $3, 0, -3$ dB. The case of in ideal S-ALOHA narrow based system (i.e. with perfect power control Rayleigh fading) serves as comparison reference.

Fig. 3.8 shows the case of capture ratio 3 dB. The remarks that we derive from both figures are as follows:

- The performance of all three diversity strategies are slightly improved by imperfect power control improves system performance.
- For systems that requires energy efficiency, the identical transmit power diversity is the best choice, and for system with latency requirement, the decremental strategy is better. However, identical transmit power diversity is the recommended since it has a good comprise between all metrics, especially in interval $[0.4, 0.6]$.

Fig. 3.9 shows the case of capture ratio 0 dB. From this figure, we observe that the precision of power control almost has no impact to system performance except for packet loss rate.

Fig. 3.10 shows the case of capture ratio -3 dB. In this case, the imperfect power control has negative impact to the system, and the identical strategy is still the best one.

From above three figures, Fig. 3.8, Fig. 3.9 and Fig. 3.10, we observe that the impact of imperfect power control to narrow band systems is partially neutralized by fading effect. Whether the impact is positive depends on the capture ratio. The identical transmit power diversity is the best choice for all above three cases.

3.8 Summary

In this chapter, we presented an accurate analytical model to evaluate the performance of S-ALOHA based LPWAN networks. By the proposed analytical model, we can estimate steady-state performances such as packet loss rate, throughput, energy efficiency and average number of transmissions. The model takes into accounts various performance-affecting factors, such as capture effect, diversity of transmit power levels, power control error, which have not been jointly considered in previous researches and can not be handled by widely used Bianchi's model.

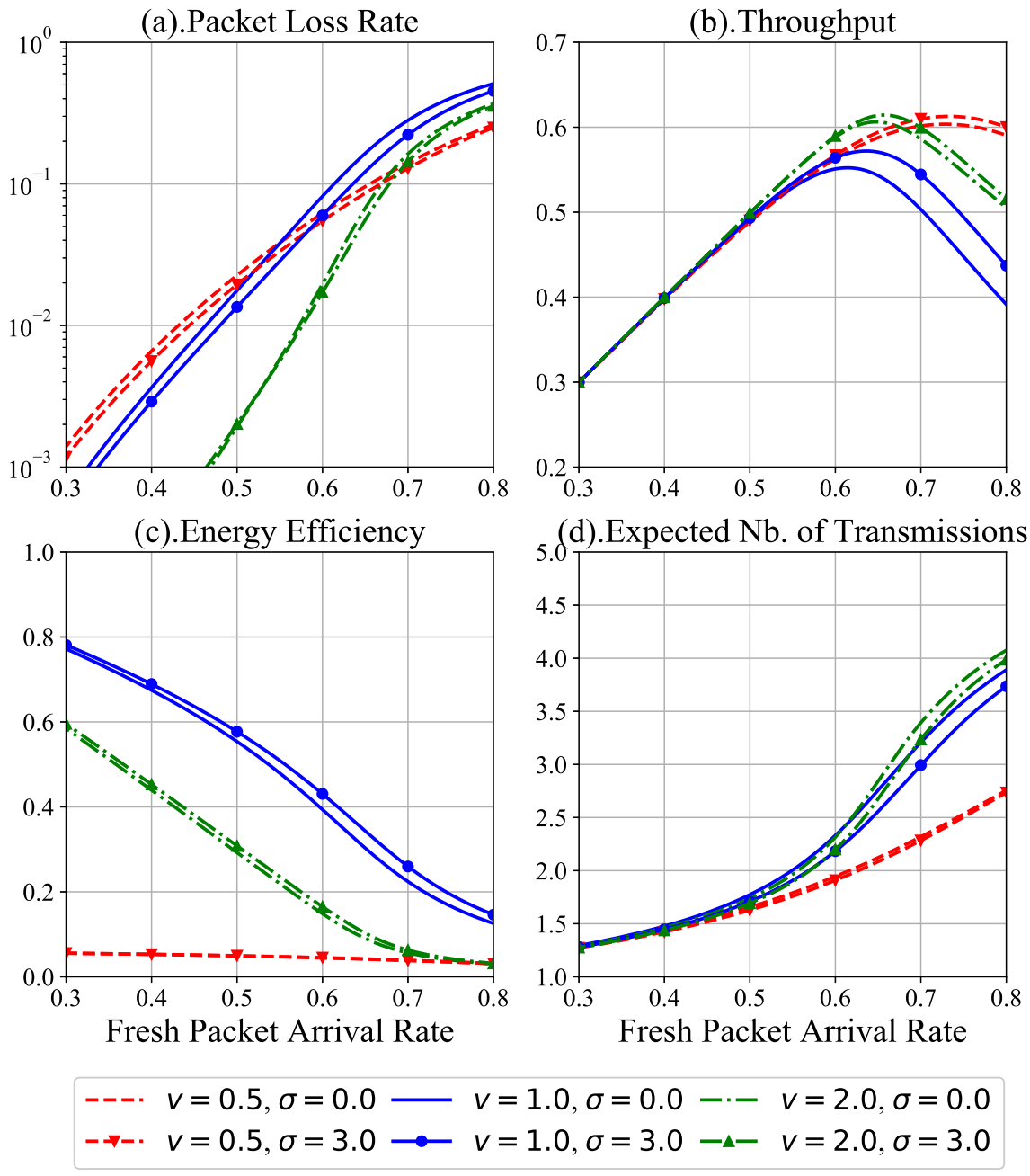

Fig. 3.8 Performance comparison with different transmit power diversities and power control precisions in narrow band systems. SINR threshold 3 dB

We employ numerical integration method to calculate cumulative distribution function (CDF) of total interference from its corresponding characteristic function and fixed point analysis to solve the problem. The computational complexity for wide band system analysis is reduced by combining the recent research effort about lognormal sum (LNS) approxima-

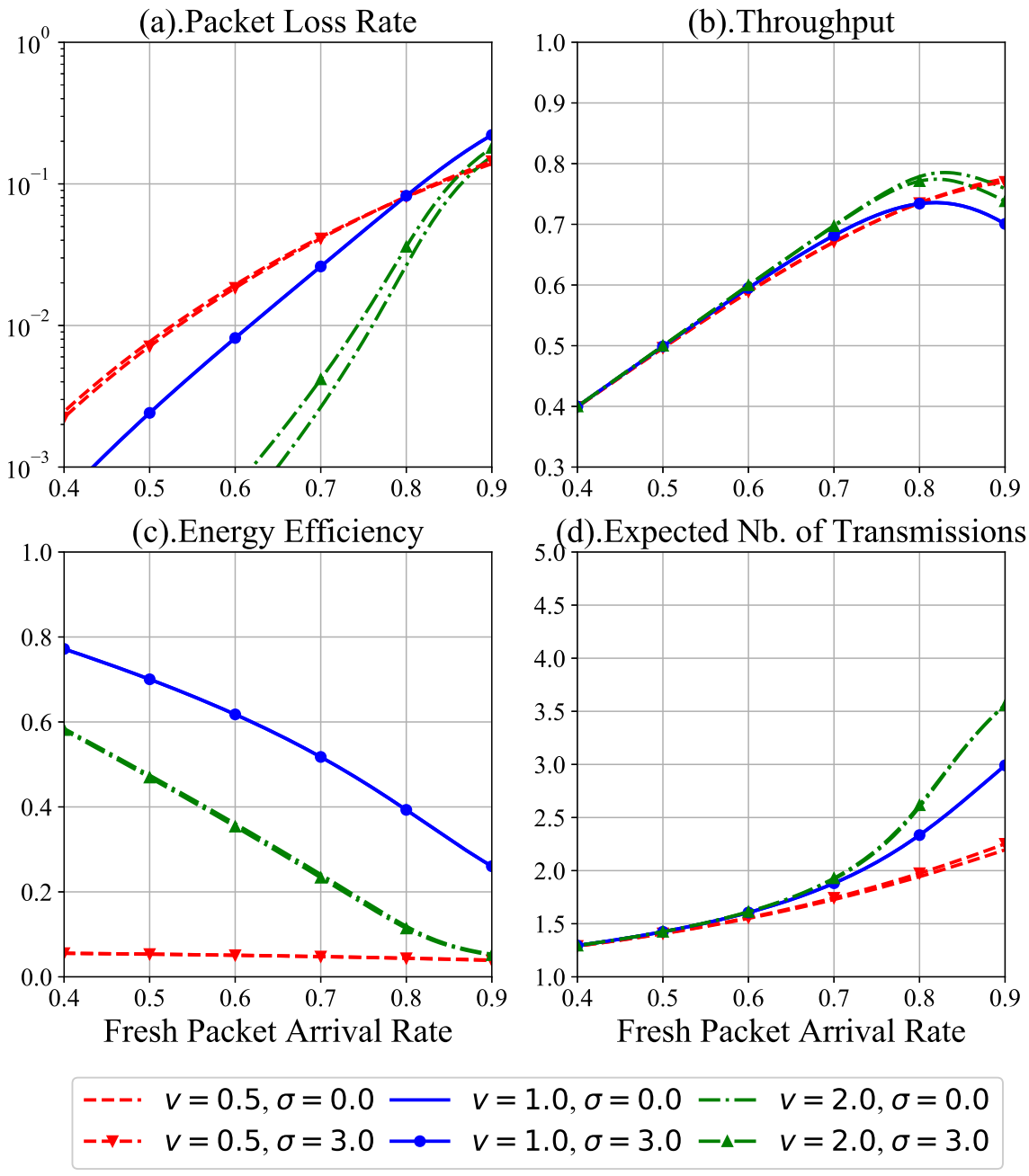

Fig. 3.9 Performance comparison with different transmit power diversities and power control precisions in narrow band systems. SINR threshold 0 dB

tion problem and mathematical skills used in finance domain. The accuracy of the proposed model is confirmed by simulation. Due to its low complexity, our model can be used as a dimensioning tool to accurately and rapidly estimate the steady-state system outage capacity and throughput of S-ALOHA-based LPWAN networks.

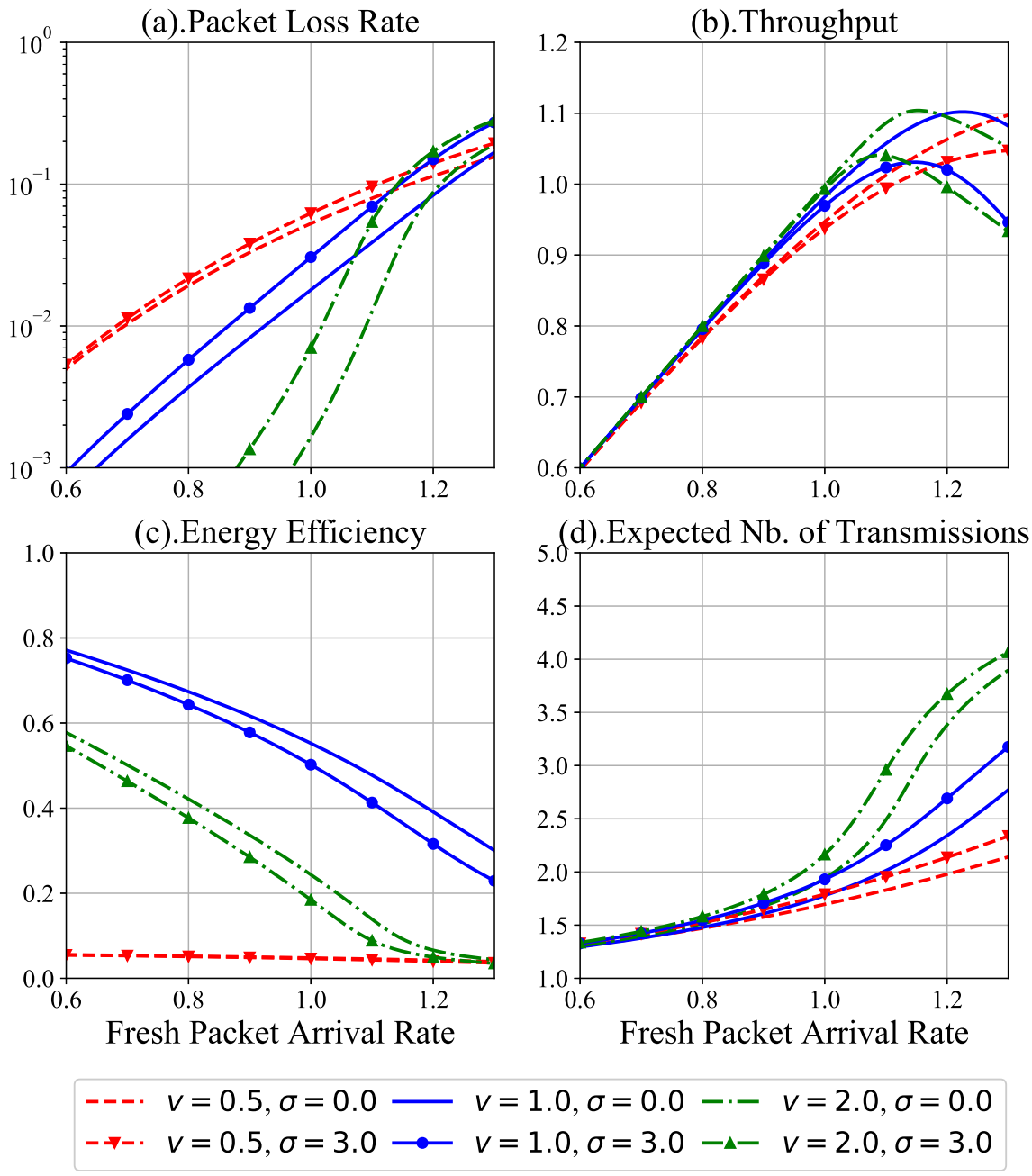

Fig. 3.10 Performance comparison with different transmit power diversities and power control precisions in narrow band systems. SINR threshold -3 dB

By exploiting the proposed models, we also obtain some design guidelines for S-ALOHA. For example, in a wide band LPWAN system that suffers from imperfect power control, if the deployed devices use identical transmit power strategy and capture ratio is 3 dB, the imprecision of power control can be leveraged to improve the system performance. The

decremental strategy is a choice for systems that has latency requirement and has no energy efficiency constraint.

In this work, the impact of the location of deployed MTC devices are not considered. Thus, we will also take into account the impact of device's spatial distribution and multiple base stations in the future work.

Chapter 4

Performance Evaluation of macro reception diversity in large-scale ALOHA networks

4.1 Introduction

In Chapter. 3, we discussed the performance of S-ALOHA in the context of a single Base Station (BS). However, a realistic LPWAN is composed by a group of BS, and pure ALOHA is used by some types of LPWAN, for example, Sigfox. In this chapter, we evaluate the performance of ALOHA, including slotted and pure ALOHA, in the context of multiple BS.

In cellular networks, the packet is sent in unicast mode: the destination Base Station (BS) is indicated by the terminal. However, it also could be sent in broadcast mode, and benefit from macro reception diversity, which is defined as the capacity of several BS to receive the same packet. The combining techniques can be combined with macro reception diversity to improve performance of LPWAN.

In the simplest diversity scheme, each BS autonomously and independently decodes the packets and then sends the decoded packets to the core network. That is to say, each BS is equipped with a packet decode function, and the backhaul link between BS and core network transmits only when a packet is received at the BS. The core network is in charge of duplicate received packets removal (e.g., by comparing the identity and message content conveyed in packets). A packet is successfully delivered if at least one BS decodes the packets. This scheme is referred to as *selection-combination-based macro diversity*, simply written as *SC macro diversity*. It is currently used by Sigfox and LoRaWAN [24].

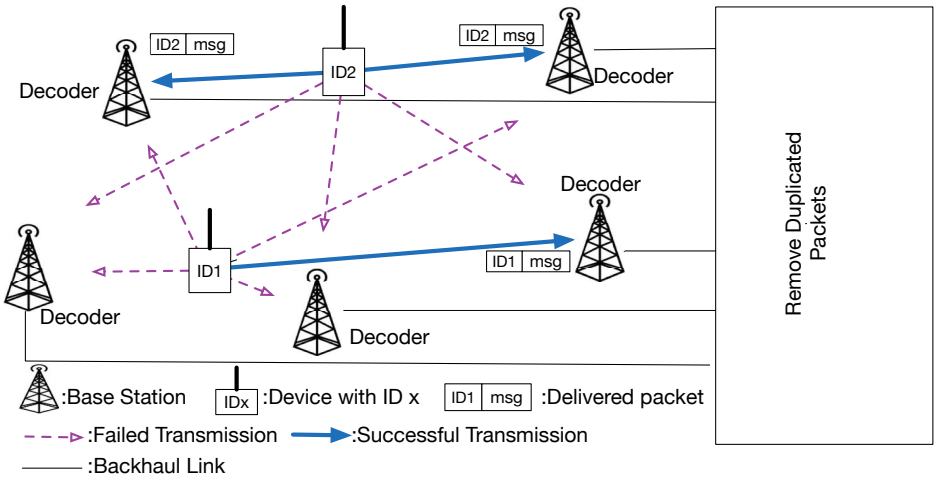

Fig. 4.1 Selective Combining (SC) Macro Reception Diversity Scheme Illustration. Each BS is equipped with a packet decode function. The decoded packet is sent to the core network and the latter is in charge of duplicated packets

Another network architecture that implements macro reception diversity is possible as illustrated in Fig. 4.1. Its principle is similar to the centralized RAN of cellular networks: a radio unit is installed at each site. The radio unit converts the received radio signal into base band signal, digitalizes it and transmits it to the central unit via a fronthaul link. The central unit is responsible for the demodulation and decoding process. Thus, it is possible to linearly combine the signals from different radio units and use maximum ratio combining (MRC) techniques to decode the packet. A series of MRC function blocks are installed within the central unit so that several transmitted packets in the radio network can be simultaneously decoded. This scheme is referred to as *maximum-ratio-combining-based macro diversity*, simply written as *MRC macro diversity*.

Not surprisingly, macro reception diversity outperforms the traditional unicast mode in terms of one-shot random access packet loss rate, which means higher system capacity constrained by packet loss rate. The capacity of each mode, which is the maximum supported load for a given packet loss rate target is derived. The ratio between the two capacity values is called the *macro diversity gain*. In this chapter, we want to answer the following questions: what's the performance of ALOHA based networks supporting macro reception diversity? what's the macro diversity gain? Does the retransmission mechanism have impact to the comparison between macro diversity and traditional BS attach method?

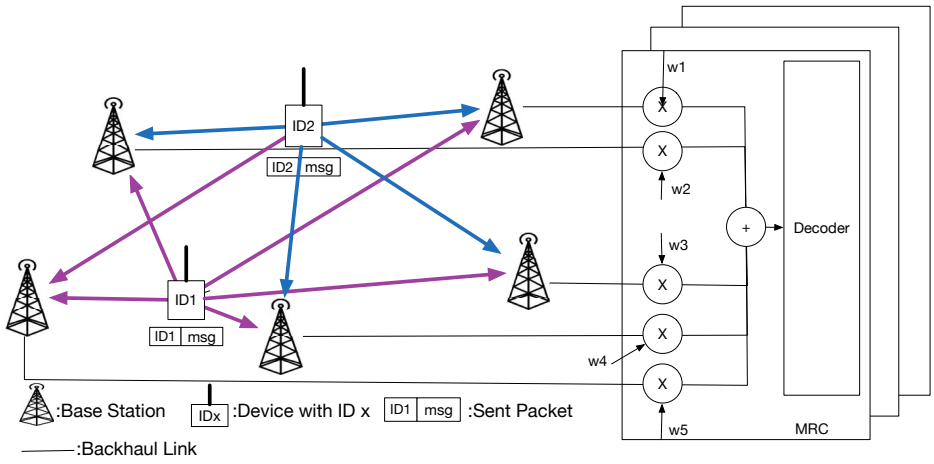

Fig. 4.2 Maximum Ratio Combining (MRC) Macro Reception Diversity Scheme Illustration

4.2 State of the Art

Stochastic geometry is a powerful mathematical tool that deals with the geometry problems using mathematical tools of stochastic process and probability theory. It is applied in many fields, including image object cognition, biochemistry cell analysis, geographic survey, communication models and so on. This mathematical tool has been applied to wireless networks for more than two decades, in particular to model and analyze systems with random channel access (e.g., ALOHA and carrier sensing multiple access (CSMA)).

In this chapter, we leverage stochastic geometry to give a comprehensive study about macro reception diversity, due to the intrinsic spatial randomness that LPWAN networks exhibit. As the first step, we give a brief introduction about a set of basic concepts and notations of stochastic geometry and Poisson point process in Sec 4.2.1. More details and discussions are available in [103–109]. We then give a state of the art about research efforts based on stochastic geometry for wireless networks in Sec. 4.2.2.

4.2.1 Fundamental Concepts and Theorems of Stochastic Geometry

4.2.1.1 Point process and Poisson point process

In stochastic geometry analysis, the network is abstracted to a convenient point process (PP) which captures the network properties. Point process is a basic stochastic process representing a certain point pattern $\Phi = \{x_1, x_2, ...\}$. It provides the mathematical models for various patterns of points, and helps constructing other complex processes. The theory of point process is on the basis of measure theory and modern probability theory.

Definition 4.2.1. A point process is a countable random collection of points that reside in some measure space, usually the Euclidean space $\mathbb{R}^d$.

Since we modelize a LPWAN system on an infinite two-dimension plane in this thesis, in the following definitions, we let $d = 2$. A point process is characterized by counting the number of points falling in sets $A \subset \mathbb{R}^2$, i.e., $\Phi(A)$. Hence $\Phi(A)$ is a random variable that assumes that non-negative integer values. $\Phi(\cdot)$ is called random counting measure.

An essential characteristic of point process is void probability. Its definition is as follows:

Definition 4.2.2. Void probability: Let Φ be a point process. Its void probabilities over all bounded set A are defined as $\mathbb{P}(\Phi(A) = 0)$ for $A \subset \mathbb{R}^2$.

The void probability can be used to verify the equivalence of point processes: two simple point processes are equivalent if they have the same void probability distributions for all bounded sets.

Definition 4.2.3. Stationarity: Let a point process $\Phi = x_n$. Φ is said to be stationary if the translated point process $\Phi_x = \{x_n + x\}$ has the same distribution as Φ for every $x \in \mathbb{R}^2$.

Definition 4.2.4. Density measure: for a given point process Φ, its density is defined as follows:

$$\lambda = \frac{\mathbb{E}\{\Phi(A)\}}{|A|}, \text{ for every } A \subset \mathbb{R}^2,$$

where $|A|$ denotes the area of A.

Definition 4.2.5. A point process is a stationary Poisson point process (PPP) if the following two conditions are satisfied:

- The number of points in any bounded set $A \subset \mathbb{R}^2$ has a Poisson distribution with mean $\lambda |A|$, i.e.

$$\mathbb{P}(\Phi(A) = k) = \frac{(\lambda |A|)^k}{k!} \exp(-\lambda |A|)$$

- The number of points in disjoint sets are independent, i.e., for every $A \subset \mathbb{R}^2$ and $B \subset \mathbb{R}^2$ with $A \cap B = \varnothing$, $\Phi(A)$ and $\Phi(B)$ are independent.

A homogeneous PPP is completely characterized by a single parameter λ. A realization of PPP is illustrated in Fig. 4.3.

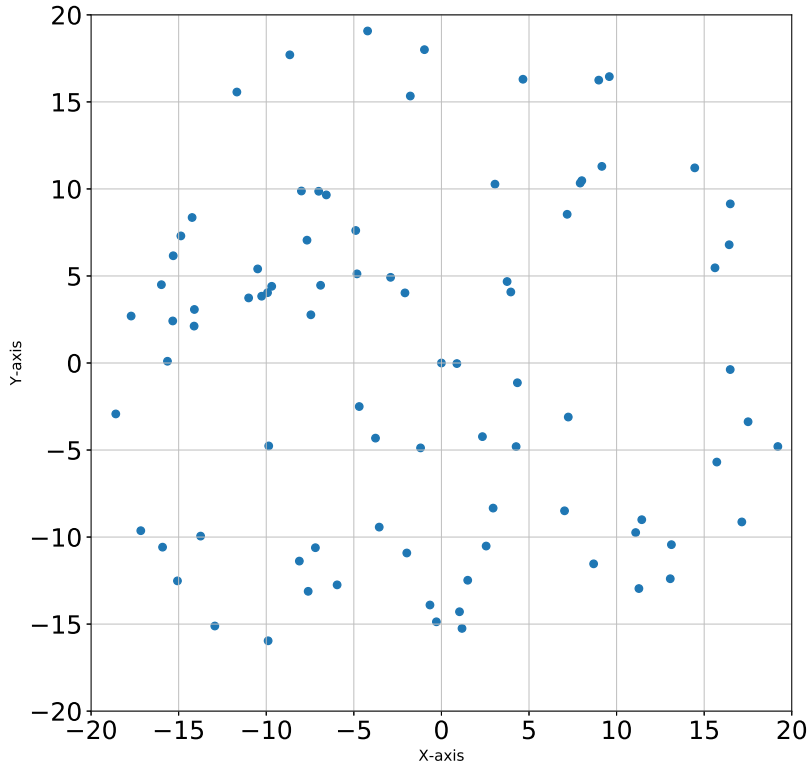

Fig. 4.3 A realization of Poisson point process

4.2.1.2 Useful theorems

Theorem 4.2.6. *Slivnyak's theorem: Let* Φ *be any homogeneous PPP. Then conditioned on* $x \in \Phi$, $\mathbb{P}(f(\Phi)|x \in \Phi) = \mathbb{P}(f(\Phi \cup \{x\}))$ *for any function* f.

Slivnyak's theorem is an important result that allows us to compute probabilities of events conditioned on the event that there is a point of Φ at location x, which is a zero probability event. It essentially says that conditioned on the event that there is a point of Φ at location x, the distribution is equivalent to a new process that is a union of Φ and an extra point at x.

Theorem 4.2.7. *Campbell's theorem: For any measurable function* $f : \mathbb{R}^d \to \mathbb{R}$ *and for a homogeneous PPP with density* λ*:*

$$\mathbb{E}\left\{\sum_{n:x_n \in \Phi} f(x_n)\right\} = \int_{R^d} f(x)dx$$

Definition 4.2.8. Let G be the family of all non-negative, bounded measurable functions $g : \mathbb{R}^d \to \mathbb{R}$ on $\mathbb{R}^d$ whose support $\left\{x \in \mathbb{R}^d : g(x) > 0\right\}$ is bounded. Let F be the family of

all functions $f = 1 - g$, for $g \in G$, $0 \leq g \leq 1$. Then the probability-generating functional (PGFL) for a point process $\Phi = \{x_n\}$ is defined as:

$$PGFL(f) = \mathbb{E}\left\{\prod_{x_n \in \Phi} f(x_n)\right\}$$

Theorem 4.2.9. *For a homogenous PPP Φ with density λ, the PGFL is given by:*

$$PGFL(f) = \exp(-\int (1 - f(x)\lambda dx))$$

Theorem 4.2.9 is very useful for deriving the packet loss rate in a PPP-distributed wireless network by allowing us to compute the expectation of a product of functions over the entire PPP. We will make use of Theorem 4.2.9 quite frequently in Chapter 4 of thesis.

Theorem 4.2.10. *Split Property of Poisson process: Suppose a system has Poisson arrivals at rate λ, and each arrival is independently labeled $\mathscr{L}$ with probability p. Then the arrivals that are label $\mathscr{L}$ are Poisson arrivals, with rate $p\lambda$.*

Theorem 4.2.11. *Additive Property of Poisson process: Suppose a system has two independent streams of Poisson arrivals, with rates λ_1 and λ_2. Then they combine to give Poisson arrivals with rate $\lambda_1 + \lambda_2$.*

4.2.2 Use of stochastic geometry for the performance analysis of wireless networks

Stochastic geometry has been used in wireless networks modeling and performance analysis for the first time by François Baccelli in 1996 [110, 111]. Up to present, there are plenty of research efforts based on stochastic geometry in the literature. To name a few, Baccelli et al. [112] use Laplace transform for interference analysis for slotted ALOHA. Novlan et al. [113] study the performance of uplink channel in cellular networks by taking into account per-mobile power control. Gharbieh et al. [114] study the random access performance of LTE networks in IoT environment. Haenggi et al. [115] extensively study the outage probability in SINR-based capture model for slotted ALOHA. Błaszczyszyn et al. [116] open the door to study pure ALOHA with stochastic geometry and give the close-from expressions. The spatial and temporal correlation of the interference have been discussed in [117]. Vu et al. [118] analyze the performance of best BS attach using methods different from that we use in this thesis. Vu et al. [119] evaluate the outage probability and the handover probabilities by taking into account the effect of path loss, shadowing, Rayleigh fast fading,

frequency factor reuse and conventional beam-forming. In addition, a few of survey papers, such as [108, 107, 120], are available by which one can get an overview about application of stochastic geometry in wireless network. After the state-of-the-art work, to our best knowledge, we find that macro reception diversity for ALOHA systems has not been studied in literature.

4.3 System model

4.3.1 Distribution of Nodes and Traffic Model

We consider a large wireless network over a two-dimension infinite plane. The locations of terminals form a stationary Poisson point process (PPP) $\Phi_m = \{x_i\}$ on the plane $\mathbb{R}^2$, where x_i refers to the coordinates of device with label i. The spatial density of Φ_m is λ_m. Similarly, the locations of base stations also form a stationary PPP $\Phi_b = \{y_j\}$ with spatial density λ_b. All the packets transmitted by devices have the same duration T_{slot}.

4.3.2 Slotted ALOHA and Pure ALOHA

For a comparison between macro reception diversity and traditional BS attach method, we consider three types of ALOHA-based network. As a comparison reference, we consider a traditional cellular network which employs slotted ALOHA. The devices in such a network attach to its best BS for which the received power averaged over all fading realizations is the strongest. For macro reception diversity, it is assumed to run in pure slotted ALOHA. Furthermore, this networks with macro reception diversity can be divided into two categories: with downlink for acknowledgment (e.g. LoRaWAN) and without downlink for acknowledgment (note that Sigfox has downlink support but does not use it for acknowledgment). Note that whether acknowledgment is supported has an impact on retransmission mechanism.

For slotted ALOHA, the time domain is equally divided into slots with duration T_{slot}. In each slot, each device independently decides to transmit a packet with probability p. The propagation delay is assumed to be much smaller than T_{slot}. Hence, there is a global slot synchronization over the whole network.

In pure ALOHA, devices send packets without synchronization, but we still use parameter p. The packet generation process can be seen as an internal slotted system in each device with p the probability to transmit in a slot of duration T_{slot}.

At a given time, the locations of terminals that are transmitting a packet form a thinned PPP with spatial density $p\lambda_m$. For slotted and pure ALOHA, we define the normalized load

(per BS) as $L = p\lambda_m/\lambda_b$. In addition, we first consider one-shot random access, then extend to the case with retransmission mechanism.

4.3.3 Random Channel and Capture Effect

We assume that M2M devices transmit with the same power. M2M-dedicated networks are usually narrow band and thus can be assumed to suffer from Rayleigh fading. As a proof, NB-IoT use 180 kHz bandwidth [121] and Sigfox's bandwidth is 100 Hz [122]. The bandwidth of LoRaWAN varies from 125 kHz to 500 kHz according to different spread-spectrum sequence. Although LoRaWAN applies spectrum spreading technology, it can still be assumed to suffer Rayleigh fading in literature [102]. Thus, the received power $P_{r'}$ of a packet at the base station side depends on path-loss attenuation $K{r_g}^{-\gamma}$, Rayleigh fading H and shadowing effect $\exp(\chi)$:

$$P_r = P_t K {r_g}^{-\gamma} H \exp(\chi), \tag{4.1}$$

where K is a constant which depends on the antenna characteristics and the average channel attenuation, r_g refers to the distance between the transmitter and the receiver, γ is the path-loss exponent[1], H is an exponentially distributed random variable (r.v.) with unit mean, χ is a zero-mean Gaussian r.v. with variance σ^2. Log-normal shadowing is usually characterized in terms of its dB-spread with standard deviation $\sigma_{dB} = \frac{10}{\ln(10)}\sigma$. We assume that H and χ are both constant during a packet transmission, and mutually independent for different links.

Capture effect refers to the fact that signals in collision can still be demodulated if their received SINR are greater than or equal to a certain threshold θ_T. Capture effect is taken into account in the proposed model. Thus, the transmission success probability p_s for a transmit-receiver pair is defined as follows:

$$p_s = \mathbb{P}\left\{\text{SINR} = \frac{P_r}{I+\sigma_n^2} \geq \theta_T\right\}, \tag{4.2}$$

where I refers to the suffered cumulative interference during packet transmission, σ_n^2 is the background noise power. It is worthwhile to mention that in some cases the background noise is rationally negligible for the sake of tractability.

[1]The path loss exponent strongly depends on the local terrain characteristics as well as the BS coverage area. Typical values for path-loss exponent are $2 \leq \gamma \leq 8$.

4.3.4 Association Policy and Displacement Theorem

For traditional BS attach method, we assume that each device attaches to the BS that provides the highest long-term biased received power. The inclusion of shadowing allows to rewrite (4.1) as follows:

$$P_r = H\left[\exp(-\chi/\gamma)r_g\right]^{-\gamma}, \tag{4.3}$$

where shadowing can be interpreted as a random displacement of the BS original location. Concretely, for a considered device, the distance to nearest BS changes from r_g to $\exp^{-1/\gamma}(\chi)r_g$. This fact can be leveraged by using displacement theorem. The latter is given in form of lemma by [123, lemma 1]. Detailed proof is given in [124, Corollary 3].

Lemma 4.3.1. *For a homogeneous PPP $\Phi \subset \mathbb{R}^2$ with spatial density λ_b, if each point $r_g \in \Phi$ is transformed to $r \in R^2$ such that $r = X^{-\frac{1}{\gamma}} r_g$, where $\{X\}$ are i.i.d., such that $\mathbb{E}\left[X^{-\frac{2}{\gamma}}\right] < +\infty$, the new point process $\Phi' \subset \mathbb{R}^2$ defined by the transformed points r is also a homogeneous PPP with density $\lambda_b' = \lambda_b \mathbb{E}\left[X^{-\frac{2}{\gamma}}\right]$.*

Lemma 4.3.1 indicates that attaching to the best BS in a PPP of intensity λ_b with shadowing is equivalent to attaching the geographically nearest one in a transformed PPP of intensity $\lambda_b' = \lambda_b \mathbb{E}\left[e^{-\frac{2}{\gamma}\chi}\right] = \lambda_b e^{\frac{2\sigma^2}{\gamma^2}}$ without shadowing.

In the transformed PPP, let r be the distance between a given device and its nearest BS. Proved in [125], the probability density function of r is given as follows:

$$\begin{aligned} f_r(r) &= \frac{dF_r(r)}{dr} \\ &= 2\pi\lambda_b e^{\frac{2\sigma^2}{\gamma^2}} \exp(-\lambda_b e^{\frac{2\sigma^2}{\gamma^2}} \pi r^2) r, r \in [0, +\infty], \end{aligned} \tag{4.4}$$

where $F_r(r)$ is the cumulative distribution function of r. Similarly, we can obtain the PDF of r_g.

4.4 Link-level Transmission Success Probability

We first study the transmission success probability $p_s(r)$ for a given uplink between a device with label x_0 and a device with label y_0. The distance[2] between x_0 and y_0 is denoted by r.

[2]Recall that r is the distance to the nearest BS in the transformed PPP, r_g is distance to the geographical nearest BS in the initial PPP. The probability $p_s(r_g)$ will be discussed in Sec. 4.5.2.

For the considered device x_0, all the other interfering devices constitute a PPP $\Phi_m \backslash \{x_0\}$. Combining (4.1) and (4.2), we have:

$$p_s(r) = \mathbb{P}\left\{ \frac{P_t K H r^{-\gamma}}{\sum_{x_j \in \Phi_m \backslash \{x_0\}} P_t K H_{x_j} r_{x_j}^{-\gamma} + \sigma_n^2} \geq \theta_T \right\}, \tag{4.5}$$

Using Slivnyak's theorem 4.2.6, (4.5) can be further simplified:

$$p_s(r) = \mathbb{P}\left\{ \frac{P_t K H r^{-\gamma}}{\sum_{x_j \in \Phi_m} P_t K H_{x_j} r_{x_j}^{-\gamma} + \sigma_n^2} \geq \theta_T \right\}. \tag{4.6}$$

Let $I = \sum_{x_j \in \Phi_m} P_t K H_{x_j} r_{x_j}^{-\gamma}$, which is the cumulative interference suffered by x_0. As shown in [115], $p_s(r)$ can be expressed in terms of Laplace transform of cumulative interference $\mathscr{L}_I(s)$ at point $\theta_T r^\gamma$:

$$\begin{aligned} p_s(r) &= \mathbb{P}\left\{ H \geq (I + \frac{\sigma_n^2}{P_t K}) \theta_T r^\gamma \right\} \\ &= \exp(-\frac{\sigma_n^2 \theta_T}{P_t K} r^\gamma) \left[\int_0^{+\infty} \exp(-y \theta_T r^\gamma) f_I(y) dy \right] \\ &= \exp(-\frac{\sigma_n^2 \theta_T}{P_t K} r^\gamma) \mathscr{L}_I\{\theta_T r^\gamma\}, \end{aligned} \tag{4.7}$$

where $f_X(x)$ is the probability density function (PDF) of random variable X. Now the problem is down to calculate the Laplace transform of cumulative interference suffered by the BS at the origin.

4.4.1 Slotted ALOHA

In slotted ALOHA, the cumulative interference is constant during each slot. The geometry-aware interference analysis for slotted ALOHA is well investigated. Reference [115] gives a closed-form expression about the Laplace transform of cumulative interference. With independent Rayleigh fading and log-normal shadowing, we have:

$$\mathscr{L}_I(s) = \exp\left\{ -p \lambda_m \pi A \exp\left(2\sigma^2/\gamma^2\right) s^{2/\gamma} \right\}, \tag{4.8}$$

where $A = \Gamma(1 - \frac{2}{\gamma})\Gamma(1 + \frac{2}{\gamma})$ and $\Gamma(z) = \int_0^{+\infty} x^{z-1} e^{-x} dx$.

4.4.2 Pure ALOHA, average interference

In pure ALOHA, the cumulative interference $I(t)$ suffered by a given packet transmitted in interval $[T, T+T_{\text{slot}}]$ is variable during the packet transmission. When advanced transmission techniques (e.g., interleaving, robust channel coding, etc.) are used, $p_s(r)$ is a function of the average interference[3] $I^{\text{mean}} = \frac{1}{T_{\text{slot}}} \int_T^{T+T_{\text{slot}}} I(t)dt$, which replaces I in (4.2).

Błaszczyszyn et al. propose a Poisson-rain model [126, Sec.2.4] that approximates well this case and allows to compute the cumulative interference. They prove that formula (4.8) can be reused by letting $A = \frac{2\gamma}{\gamma+2}\Gamma(1-\frac{2}{\gamma})\Gamma(1+\frac{2}{\gamma})$.

4.4.3 Pure ALOHA, maximum interference

Another case of pure ALOHA is assumed to have no error correction neither interleaving techniques for the purpose of reducing the device-side cost. In this case, the packet is delivered if and only if each bit is correctly received. Hence, the SINR should be larger than or equal to θ_T during T_{slot}. Hence, p_s is a function of maximum interference[4] $I^{\max} = \max_{t\in[T,T+T_{\text{slot}}]} I(t)$. According to [126, Sec.2.4], there is no closed-form for $I^{\max}$, and the authors use a simulation approach to study. Next, we propose a simple upper bound to estimate $I^{\max}$. Section 4.5.5 shows that the bias is at an acceptable level.

Consider a packet transmitted in interval $[T, T+T_{\text{slot}}]$. Any device generating its interference at T terminates packet transmission before $T+T_{\text{slot}}$. The interfering packets at $T+T_{\text{slot}}$ do not exist at T, because the packet transmission duration is T_{slot}. Hence, cumulative interference $I(T)$ and $I(T+T_{\text{slot}})$ are two independent and identically distributed random variables. Furthermore, any device generating interference on the packet is either active at T or at $T+T_{\text{slot}}$. The maximum interference is thus upper bounded by $I(T)+I(T+T_{\text{slot}})$. Therefore, the Laplace transform of maximum cumulative interference upper bound $\mathscr{L}_{I^{\text{upper}}}(s)$ during interval $[T, T+T_{\text{slot}}]$ is equal to $\mathscr{L}_{I(T)+I(T+T_{\text{slot}})}(s) = \left[\mathscr{L}_{I(T)}(s)\right]^2$.

We can reuse (4.8) to calculate $\mathscr{L}_{I(T)}(s)$. Thus, Laplace transform of I^{upper} can be unified into (4.8) by letting $A = 2\Gamma(1-\frac{2}{\gamma})\Gamma(1+\frac{2}{\gamma})$.

4.4.4 Generalized model

Based on interference analysis in Sec. 4.4.1 and 4.4.2, the generalized Laplace transform for cumulative interference, which covers pure and slotted ALOHA systems, is given as

[3] In the rest of this chapter, average interference refers to the average interference level during the considered packet transmission.

[4] In the rest of this chapter, maximum interference refers to the maximum interference level during the considered packet transmission.

follows:

$$\mathscr{L}_I(s) = \exp\left\{-p\lambda_m \pi A \exp\left(2\sigma^2/\gamma^2\right) s^{2/\gamma}\right\}, \tag{4.9}$$

where $\sigma = \frac{\ln(10)}{10}\sigma_{dB}$ and:

$$A = \begin{cases} \Gamma\left(1-\frac{2}{\gamma}\right)\Gamma\left(1+\frac{2}{\gamma}\right), & \text{for slotted ALOHA} \\ \frac{2\gamma}{\gamma+2}\Gamma\left(1-\frac{2}{\gamma}\right)\Gamma\left(1+\frac{2}{\gamma}\right), & \text{for pure ALOHA, average interference} \\ 2\Gamma\left(1-\frac{2}{\gamma}\right)\Gamma\left(1+\frac{2}{\gamma}\right), & \text{for pure ALOHA, maximum interference} \end{cases}$$

By combining (4.7) and (4.9), we can generalize the link-level success transmission probability $p_s(r)$ for all ALOHA cases (slotted and pure ALOHA) :

$$\begin{aligned} p_s(r) &= \exp(-\frac{\sigma_n^2\theta_T}{P_t K} r^\gamma)\exp(-p\lambda_m \pi A \theta_T^{\frac{2}{\gamma}} e^{\frac{2\sigma^2}{\gamma^2}} r^2), \\ &= \exp\left(-\eta_T r^\gamma\right)\exp\left(-\varepsilon_T r^2\right) \end{aligned} \tag{4.10}$$

where σ_n^2 is the background noise power, θ_T is the capture ratio, P_t refers to the device transmit power, K is a positive constant related to propagation model and constant A is defined in (4.9). For the simplicity of notation, let $\eta_T = \frac{\sigma_n^2\theta_T}{P_t K}$, $\varepsilon_T = p\lambda_m \pi A \theta_T^{\frac{2}{\gamma}} e^{\frac{2\sigma^2}{\gamma^2}}$.

From (4.10), we observe that the impact of the background noise to the system performance is reflected by term $\exp(-\frac{\sigma_n^2\theta_T}{P_t K} r^\gamma)$. This term can be neglected without materially changing the analysis results, especially in interference limited systems. For cases where the background noise is considered, path loss exponent γ is set as 4 for the sake of tractability.

4.5 Network Level Performance Without Retransmission

The analysis about link-level transmission success probability $p_s(r)$ paves the way to analyze the network level packet loss rate P_f, which is the base to calculate:1) the maximum normalized load $L_{\max}$ under packet loss rate constraint $P_{f,\max}$; 2) the normalized spatial throughput (per BS) $S = (1-P_f)p\lambda_m/\lambda_b$. We first consider two standard ALOHA transmission approaches in unicast mode (best and nearest BS attach) and then analyze the macro diversity case. For macro diversity case, we also consider two cases: selective ratio and maximum ratio combing.

4.5.1 Best BS attach method

In this subsection, we assume that the device attaches to the BS for which the received power averaged over all fading realizations is the strongest (i.e. the BS that maximizes ${r_g}^{-\gamma}\exp(\chi)$). Let $P_{f,b}$ be packet loss rate for this case, where the subscript b refers to the best BS attach. To calculate the network level packet loss rate, it just needs to calculate the expectation of $1-p_s(r)$ over random variable r. The PDF of r is give in (4.4).

4.5.1.1 With background noise and γ=4

When background noise is taken into account, only and only if path loss component $\gamma = 4$, we obtain the closed-form expression.

$$\begin{aligned} P_{f,b} &= \mathbb{E}_r\left[1-p_s\left(r\right)\right] \\ &= 1-\int_0^{+\infty} p_s(r)2\pi\lambda_b e^{\frac{2\sigma^2}{\gamma^2}}dr \\ &= 1-\int_0^{+\infty} \exp(-\eta_T r^4)\exp(-\varepsilon_T r^2)2\pi\lambda_b e^{\frac{2\sigma^2}{\gamma^2}}\exp(-\lambda_b e^{\frac{2\sigma^2}{\gamma^2}}\pi r^2)rdr \\ &= 1-\pi\lambda_b e^{\frac{2\sigma^2}{\gamma^2}}\int_0^{+\infty}\exp(-\eta_T r^4-(\varepsilon_T+\lambda_b\pi e^{\frac{2\sigma^2}{\gamma^2}})r^2)dr^2 \end{aligned} \tag{4.11}$$

Integral (4.11) is finally simplified as follows. The detailed steps are shown in Appendix A:

$$P_{f,b} = 1-\pi\lambda_b e^{\frac{2\sigma^2}{\gamma^2}}\frac{\sqrt{\pi}}{2}\sqrt{\frac{1}{\eta_T}}\exp(\frac{V^2}{4\eta_T})\left[1-\mathrm{erf}(\frac{V}{2\sqrt{\eta_T}})\right], \tag{4.12}$$

where $\eta_T = \frac{\sigma_n^2\theta_T}{P_t K}$, $V = \varepsilon_T + \pi\lambda_b \exp\left(\frac{2\sigma^2}{\gamma^2}\right)$

4.5.1.2 Without Background Noise

With ignorance of background noise, the link level transmission success probability $p_s(r)$, given in (4.10), is simplified as follows:

$$p_s(r) = \exp(-p\lambda_m\pi A e^{\frac{2\sigma^2}{\gamma^2}}\theta_T^{\frac{2}{\gamma}}r^2). \tag{4.13}$$

Similar to Sec 4.5.1.1, we have:

$$\begin{aligned} P_{f,b} &= \mathbb{E}_r\left[1 - p_s\left(r\right)\right] \\ &= 1 - \int_0^{+\infty} \exp(-p\lambda_m \pi A \theta_T^{\frac{2}{\gamma}} e^{\frac{2\sigma^2}{\gamma^2}} r^2) 2\pi\lambda_b e^{\frac{2\sigma^2}{\gamma^2}} \exp(-\lambda_b e^{\frac{2\sigma^2}{\gamma^2}} \pi r^2) r dr \\ &= 1 - \frac{1}{1 + A\theta_T^{\frac{2}{\gamma}} L}. \end{aligned} \tag{4.14}$$

By inverting (4.14), the maximum supported normalized load $L_{\max,b}$ (subscript b refers to the best BS attach method) is as follows:

$$L_{\max,b} = \frac{1}{A\theta_T^{\frac{2}{\gamma}}} \frac{P_{f,\max}}{1 - P_{f,\max}}. \tag{4.15}$$

The normalized spatial throughput S_b is as follows:

$$S_b = \frac{L}{1 + A\theta_T^{\frac{2}{\gamma}} L}. \tag{4.16}$$

From (4.16), it is not difficult to prove that, as L increases, the spatial throughput approaches its limit value $\frac{1}{A\theta_T^{\frac{2}{\gamma}}}$.

4.5.2 Nearest BS attach method

As a complementary analysis, in this subsection, we assume that the device attaches to the geographically nearest BS then transmits packets. Due to the measurement error, one considered device cannot always surely attach to the best BS each time. Thus, we analyze the case in which the device attaches to the geographical nearest BS. The performance of such an association policy is worse than that of best BS attach method. Thus, the performance of a realistic LPWAN network is bounded by that of best BS attach and nearest BS attach method. That's the motivation of conducting such an analysis.

To this end, we need to study the transmission success probability $p_s(r_g)$, where r_g is the distance to the geographical nearest BS. Similar to (4.6), we have:

$$p_s\left(r_g\right) = \mathbb{P}\left\{ \frac{P_t K H \exp(\chi) {r_g}^{-\gamma}}{\sum_{x_j \in \Phi_m} P_t K H_{x_j} \exp(\chi_{x_j}) r_{g,x_j}^{-\gamma} + \sigma_n^2} \geq \theta_T \right\}.$$

Let cumulative interference $I = \sum_{x_j \in \Phi_m} P_t K H_{x_j} \exp(\chi_{x_j}) r_{g,x_j}^{-\gamma}$. Similar to (4.7), $p_s(r_g)$ can be expressed in terms of Laplace transform of cumulative interference $\mathscr{L}_I(s)$ at point $\theta_T e^{-\chi} r_g^{\gamma}$:

$$\begin{aligned} p_s(r_g) &= \mathbb{P}\left\{ H \geq (I + \frac{\sigma_n^2}{P_t K}) \theta_T e^{-\chi} (r_g)^{\gamma} \right\} \\ &= \int_{-\infty}^{+\infty} \exp(-\frac{\sigma_n^2 \theta_T}{P_t K} e^{-x} (r_g)^{\gamma}) \left[\int_0^{+\infty} \exp(-y \theta_T e^{-x} (r_g)^{\gamma}) f_I(y) dy \right] f_{\chi}(x) dx \\ &= \mathbb{E}_{\chi} \left[\exp(-\eta_T e^{-\chi} (r_g)^{\gamma}) \mathscr{L}_I \left\{ \theta_T e^{-\chi} (r_g)^{\gamma} \right\} \right], \end{aligned} \tag{4.17}$$

where $\eta_T = \frac{\sigma_n^2 \theta_T}{P_t K}$, $f_X(x)$ is PDF of random variable X, $\mathbb{E}_X[\cdot]$ is the expectation operator with respect to X. Since the closed-form expression of (4.17) does not exist. To keep the tractability, the background noise is ignored. Thus, (4.17) is further simplified as follows:

$$p_s(r_g) = \mathbb{E}_{\chi} \left[\mathscr{L}_I \left\{ \theta_T e^{-\chi} (r_g)^{\gamma} \right\} \right], \tag{4.18}$$

The network packet loss rate $P_{f,n}$ (index n means nearest) is the expectation of $p_s(r_g)$ with respect to the distance to the nearest base station r_g . The PDF of r_g for a PPP is as follows:

$$f(r_g) = 2\pi \lambda_b r_g \exp(-\lambda_b \pi (r_g)^2), r_g \in [0, +\infty]. \tag{4.19}$$

Thus:

$$\begin{aligned} P_{f,n} &= \mathbb{E}_d [1 - p_s(r_g)] \\ &= 1 - \int_0^{+\infty} \mathbb{E}_{\chi} \left[\exp(-p \lambda_m \pi A \theta_T^{\frac{2}{\gamma}} e^{\frac{2\sigma^2}{\gamma^2}} (r_g)^2 e^{-\frac{2}{\gamma}\chi}) \right] 2\pi \lambda_b r_g e^{-\lambda_b \pi (r_g)^2} d[r_g] \\ &= 1 - \pi \lambda_b \mathbb{E}_{\chi} \left[\int_0^{+\infty} \exp(-p \lambda_m \pi A \theta_T^{\frac{2}{\gamma}} e^{\frac{2\sigma^2}{\gamma^2}} (r_g)^2 e^{-\frac{2}{\gamma}\chi} - \lambda_b \pi (r_g)^2) \right] d[(r_g)^2] \\ &= 1 - \mathbb{E}_{\chi} \left[\left(A \theta_T^{\frac{2}{\gamma}} e^{\frac{2\sigma^2}{\gamma^2}} L e^{-\frac{2}{\gamma}\chi} + 1 \right)^{-1} \right] \\ &= 1 - \int_{-\infty}^{+\infty} \frac{\gamma}{2\sqrt{2\pi}(e^t + 1)\sigma} \exp\left\{ -\frac{\gamma^2}{8\sigma^2} \left(t - \ln(AL\theta_T^{\frac{2}{\gamma}} e^{\frac{2\sigma^2}{\gamma^2}}) \right)^2 \right\} dt. \end{aligned} \tag{4.20}$$

Integral in (4.20) can be accurately approximated by a logistic function [127]. Thus,

$$\begin{aligned} P_{f,n} &\approx 1 - \frac{1}{1+\exp\left\{\left(1+\pi\sigma^2/(2\gamma^2)\right)^{-1/2}\ln(A\theta_T^{\frac{2}{\gamma}}e^{\frac{2\sigma^2}{\gamma^2}}L)\right\}} \\ &\approx 1 - \frac{1}{1+\left(A\theta_T^{\frac{2}{\gamma}}e^{\frac{2\sigma^2}{\gamma^2}}L\right)^C} \end{aligned} \tag{4.21}$$

where A is defined in (4.10), $L = p\lambda_m/\lambda_b$, $C = \left[1+\pi\sigma^2/(2\gamma^2)\right]^{-1/2}$. We conducted a Monte-Carlo simulation and found that the maximum difference between (4.20) and (4.21) is 2.46% in normalized load interval $[0.021, 0.3]$, which proves the accuracy of the proposed approximation formula (4.21) .

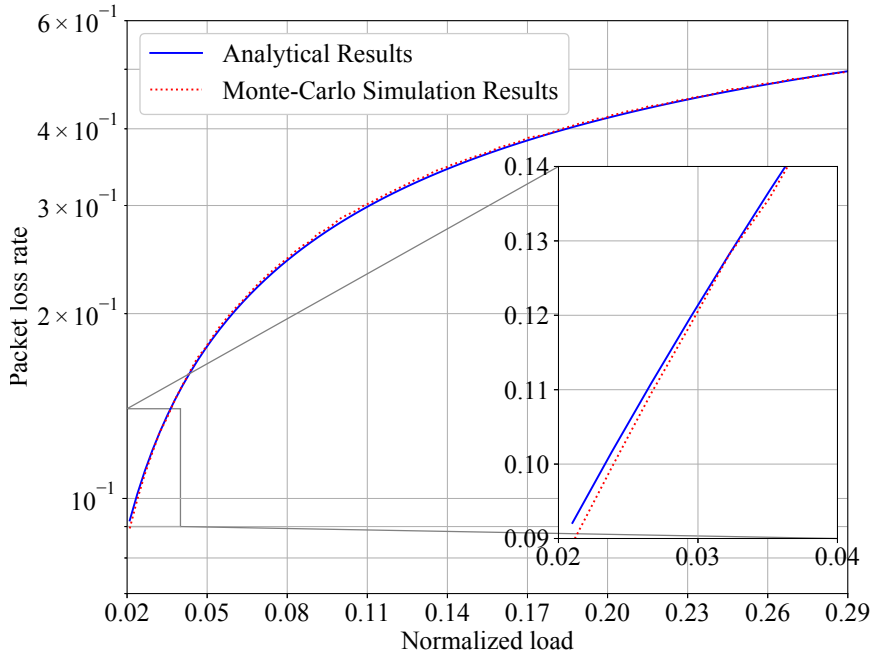

Fig. 4.4 Comparison between approximation formula (4.21) and Monte-Carlo simulation result.

From (4.21), the maximum supported normalized load $L_{\max,n}$ and normalized spatial throughput (index n refers to the nearest BS attach method) is obtained:

$$L_{\max,n} \approx \frac{1}{A\theta_T^{\frac{2}{\gamma}} e^{\frac{2\sigma^2}{\gamma^2}}} \left(\frac{P_{f,\max}}{1-P_{f,\max}} \right)^{\frac{1}{C}}, \tag{4.22}$$

$$S_n \approx \frac{L}{1+\left(A\theta_T^{\frac{2}{\gamma}} e^{\frac{2\sigma^2}{\gamma^2}} L \right)^C}. \tag{4.23}$$

It should be noted that according to approximation error, (4.23) is not valid when normalized load L is very high. A concise explication is as follows: let $\hat{P_{f,n}}$ and $o(L)$ respectively be the real packet loss rate value and approximation error, thus $\hat{P_{f,n}} = P_{f,n} + o(L)$. Thus, the approximation error between real spatial throughput $\hat{S_n}$ and (4.23) is thus $o(L)L$, which is not neglected as increase of L.

4.5.3 Selective Combining Macro Diversity

Since a transmitted packet is received by all surrounding BS, the transmission of this packet fails if and only if the received SINR at each BS is less than the capture ratio. In other words, if the maximum SINR is still less than the capture ratio, the packet transmission is failed. This is why such a scheme is called selective combining (SC) like macro reception diversity. In this section, we evaluate SC-like macro diversity in one-shot random access case.

Strictly speaking, the cumulative interferences at two different BS are correlated: when a device is transmitting, it generates some non-negligible interference on base stations that are not very far. However, it is still rational to assume that the interferences received by different BS are mutually independent. The reasons are in twofold:1) the interference correlation coefficient is shown to be close to 0 if locations of two BS are different with path-loss model $r^{-\gamma}$ [115, lemma 3.5]; 2) Each contribution to the cumulative interference is affected by fading and shadowing, which are i.i.d. random variable for different BS. Thus, the packet loss rate $P_{f,sc}$ (index m refers to macro reception diversity) is the expectation of the product of failure probabilities to each BS:

$$P_{f,sc} = \mathbb{E}\left[\prod_{y_i \in \Phi_b} (1 - p_s(r_{y_i})) \right], \text{with } r_{y_i} \in [0, +\infty], \tag{4.24}$$

where r_{y_i} is the distance between the considered device and BS with coordinates y_i. Formula (4.24) is actually the Probability Generating FunctionaL (PGFL) of PPP Φ_b for BS, which

states for some function $f(x)$ that $\mathbb{E}[\prod_{x\in\Phi} f(x)] = \exp(-\lambda(\int_{\mathbb{R}^2}(1-f(x))dx))$. Thus, term in $\mathbb{E}\left[\prod_{y_i\in\Phi_b}(1-p_s(r_{y_i}))\right]$ in (4.55) can be expressed as follows:

$$P_{f,sc} = \exp\left\{-2\pi\lambda_b e^{\frac{2\sigma^2}{\gamma^2}} \int_0^{+\infty} p_s(r) r dr\right\}, \tag{4.25}$$

Recall that $p_s(r)$ is given in (4.10). For the sake of readability, $p_s(r)$ is listed as follows:

$$p_s(r) = \exp\left(-\eta_T r^4\right) \exp\left(-\varepsilon_T r^2\right), \tag{4.26}$$

in which $\eta_T = \frac{\sigma_n^2 \theta_T}{P_t K}, \varepsilon_T = p\lambda_m \pi A \theta_T^{\frac{2}{\gamma}} \exp(\frac{2\sigma^2}{\gamma^2})$.

4.5.3.1 With Background Noise and $\gamma = 4$

When the background noise is taken into account, let $\gamma = 4$ for the sake of tractability. With mathematical operations shown in Appendix (A), (4.25) is finally simplified as follows:

$$\begin{aligned} P_{f,sc} &= \exp\left\{-2\pi\lambda_b e^{\frac{2\sigma^2}{\gamma^2}} \int_0^{+\infty} \exp(-\eta_T r^4)\exp(-\varepsilon_T r^2) r dr\right\} \\ &= \exp\left\{-\pi\lambda_b e^{\frac{2\sigma^2}{\gamma^2}} \int_0^{+\infty} \exp(-\eta_T r^2 - \varepsilon_T r) dr\right\} \\ &= \exp\left\{-\pi\lambda_b e^{\frac{2\sigma^2}{\gamma^2}} \frac{\sqrt{\pi}}{2}\sqrt{\frac{1}{\eta_T}} \exp(\frac{\varepsilon_T^2}{4\eta_T}) \left[1 - \operatorname{erf}(\frac{\varepsilon_T}{2\sqrt{\eta_T}})\right]\right\}, \end{aligned} \tag{4.27}$$

where $\eta_T = \frac{\sigma_n^2 \theta_T}{P_t K}, \varepsilon_T = p\lambda_m \pi A \theta_T^{\frac{2}{\gamma}} \exp(\frac{2\sigma^2}{\gamma^2})$.

4.5.3.2 Without Background Noise

In case of background noise is neglected, combining with (4.13) and changing integration order, (4.25) can be directly simplified:

$$P_{f,sc} = \exp\left\{-\frac{1}{A\theta_T^{\frac{2}{\gamma}} L}\right\}, \tag{4.28}$$

where A is defined in (4.10). From (4.28), we can easily find the maximum load and throughput:

$$L_{\max,sc} = -\frac{1}{A\theta_T^{2/\gamma}} \frac{1}{\ln(P_{f,\max})} \tag{4.29}$$

$$S_{sc} = L\left(1 - \exp\left\{-\frac{1}{A\theta_T^{\frac{2}{\gamma}} L}\right\}\right) \tag{4.30}$$

The macro diversity gain against the best BS attach mode $G_{\text{diversity},b}$ is obtained by the ratio (4.29) and (4.15):

$$G_{\text{diversity},b} = (1 - P_{f,\max}) / \left(P_{f,\max} \ln(1/P_{f,\max})\right). \tag{4.31}$$

From (4.30), it is not difficult to prove that, as L increases, the spatial throughput approaches its limit value $\frac{1}{A\theta_T^{\frac{2}{\gamma}}}$.

4.5.4 Maximum Ratio Combining Macro diversity

Due to the fact that a transmitted packet theoretically can be simultaneously received by all BS (ignorance of background noise), linear combining of signals at each BS can be leveraged so that the output SINR is maximized. Such a scheme is called Maximum Ratio Combining (MRC) based macro diversity In this section, the performance of MRC-based macro diversity in case of one-shot random access is evaluated. The background noise is neglected for the sake of tractability.

Consider a typical device x_0 at origin, it has been proved that if the weigh factors involved in MRC context is well designed (see Fig. 4.2), the output SINR Θ of best combiner is expressed as follows [128]:

$$\Theta = \sum_{y_j \in \Phi_b} \theta_{y_j} = \sum_{y_j \in \Phi_b} \frac{H_{y_j} \exp(\chi_{y_j}) r_{y_j}^{-\gamma}}{I_{y_j}} = \sum_{y_j \in \Phi_b} \varepsilon_{y_j} r_{y_j}^{-\gamma} \tag{4.32}$$

where θ_{y_j} is the received SINR at BS y_j, H_{y_j} and $\exp(\chi_{y_j})$ are respectively the Rayleigh fading and shadowing component for link between device x_0 and BS y_j, $\varepsilon_{y_j} = H_{y_j} \exp(\chi_{y_j}) / I_{y_j}$, I_{y_j} refers to cumulative interference suffered at BS y_j.

It should be noted that formula (4.32) holds for slotted ALOHA system. However, we assume that such a conclusion is also applicable for pure ALOHA system without consid-

ering the implementation issue. The difference compared with slotted ALOHA case relies in that, for pure ALOHA based system with or without advanced transmission techniques (e.g., interleaving, robust channel coding, etc.) I_{y_j} in (4.32) is respectively replaced by the average or maximum interference during the packet transmission.

Using similar justification explained in Sec. 4.5.3, ε_{y_j} for $j = 0, 1, 2, \ldots$ constitute a series of random variable whose element is assumed to be identically independently distributed.

Let $P_{f,\mathrm{MRC}}$ be the network level packet loss rate in this case. According to capture effect:

$$P_{f,\mathrm{mrc}} = \mathbb{P}\{\Theta < \theta_T\} = F_\Theta(\theta_T), \tag{4.33}$$

where θ_T is the capture ratio, $F_\Theta(\theta)$ is the CDF of Θ. It is can be numerically computed from Laplace transform or characteristic function of Θ.

The Laplace transform of Θ is by definition as follows

$$\mathscr{L}_\Theta(s) = \mathbb{E}\left[e^{-s\Theta}\right] = \mathbb{E}\left[\exp(-s\sum_{y_j\in\Phi_b}\theta_{y_j})\right] = \mathbb{E}\left[\prod_{y_j\in\Phi_b}\mathbb{E}_\varepsilon\left[\exp(-s\varepsilon r_{y_j}^{-\gamma})\right]\right] \tag{4.34}$$

Actually, the mathematical operations for interference analysis used in [115] can be reused to simplify (4.34). For the sake of clarity, we detail the operations as follows:

Applying Campbell theorem to (4.34) and changing the order of integration and expectation operator, we have:

$$\begin{aligned}\mathscr{L}_\Theta(s) &= \exp\left\{-\int_0^{+\infty}\mathbb{E}_\varepsilon\left[1-\exp(-s\varepsilon r^{-\gamma})\right]2\pi\lambda_b r dr\right\}\\ &= \exp\left\{-\mathbb{E}_\varepsilon\left[\int_0^{+\infty}\left(1-\exp(-s\varepsilon r^{-\gamma})\right)2\pi\lambda_b r dr\right]\right\}\end{aligned} \tag{4.35}$$

Let us focus on the integral $D = \int_0^{+\infty}(1-\exp(-s\varepsilon r^{-\gamma}))\,2\pi\lambda_b r dr$:

$$\begin{aligned}D &\overset{(a)}{=} \pi\lambda_b\int_0^{+\infty}(1-\exp(-x))\,d\left(-x^{-\frac{2}{\gamma}}(s\varepsilon)^{\frac{2}{\gamma}}\right)\\ &\overset{(b)}{=} \pi\lambda_b\int_0^{+\infty}\exp(-x)x^{-\frac{2}{\gamma}}(s\varepsilon)^{\frac{2}{\gamma}}dx\\ &= \pi\lambda_b(s\varepsilon)^{\frac{2}{\gamma}}\Gamma(1-\frac{2}{\gamma}),\end{aligned} \tag{4.36}$$

where step (a) is obtained via a change of variable $x = s\varepsilon r^{-\gamma}$, step (b) is achieved via integration by parts, $\Gamma(\cdot)$ is gamma function.

Combining (4.35) and (4.36) , the Laplace Transform of Θ is finally simplified as:

$$\mathscr{L}_{\Theta}(s) = \exp(-\lambda_b \pi \mathbb{E}\left[\varepsilon^{\frac{2}{\gamma}}\right] \Gamma(1-\frac{2}{\gamma}) s^{\frac{2}{\gamma}}), \tag{4.37}$$

where $\mathbb{E}\left[\varepsilon^{\frac{2}{\gamma}}\right]$ is:

$$\mathbb{E}\left[\varepsilon^{\frac{2}{\gamma}}\right] = \mathbb{E}\left[(H\exp(\chi))^{\frac{2}{\gamma}}\right] \mathbb{E}\left[I^{-\frac{2}{\gamma}}\right] = \Gamma(1+\frac{2}{\gamma}) \exp(\frac{2\sigma^2}{\gamma^2}) \mathbb{E}\left[I^{-\frac{2}{\gamma}}\right] \tag{4.38}$$

Now the problem comes down to calculating the term $\mathbb{E}\left[I^{-\frac{2}{\gamma}}\right]$ (i.e. negative fractional moment calculation problem), which is a research subject in applied mathematical domain and planned as our future work. The most straightforward solution is to rely on Monte-Carlo method.

With substitution $s = -i\omega$ in (4.37) , the characteristic function (CF) of Θ is as follows:

$$\phi_{\Theta}(\omega) = \exp(-\lambda_b \pi \mathbb{E}\left[\varepsilon^{\frac{2}{\gamma}}\right] \Gamma(1-\frac{2}{\gamma}) \exp(-i\pi/\gamma) \omega^{\frac{2}{\gamma}}), \tag{4.39}$$

where $\omega \geq 0$, i is imaginary unit.

As a continuous random variable, the cumulative distribution function $F_{\Theta}(\theta)$ of total SINR Θ can be directly derived from its CF $\phi_{\Theta}(\omega)$. Applying mathematical techniques presented in Sec. 3.5 in Chapter. 3, we seek to calculate the Fourier transform of $e^{-\eta\theta} F_{\Theta}(x)$ where term $e^{-\eta\theta}$ is a damping function with $\eta > 0$.

$$\int_{-\infty}^{+\infty} e^{i\omega\theta} e^{-\eta\theta} F_{\Theta}(\theta)\, dx = \frac{1}{\eta - i\omega} \phi_{\Theta}(\omega + i\eta) \tag{4.40}$$

Applying Fourier inversion for (4.40), we obtain the expression for $F_{\Theta}(\theta)$ as follows:

$$\begin{aligned} F_{\theta}(\theta) &= \frac{e^{\eta\theta}}{2\pi} \int_{-\infty}^{+\infty} e^{-i\omega\theta} \frac{1}{\eta - i\omega} \phi_{Theta}(\omega + i\eta)\, d\omega \\ &= \frac{e^{\eta\theta}}{\pi} \Re\left\{ \int_{0}^{+\infty} e^{-i\omega\theta} \frac{1}{\eta - i\omega} \phi_{\Theta}(\omega + i\eta)\, d\omega \right\}, \end{aligned} \tag{4.41}$$

The packet loss rate $P_{f,\text{mrc}}$ in case of capture ratio θ_T can be obtained by substituting $\theta = \theta_T$ in (4.41). The latter can be computed using a single numerical integration.

4.5.4.1 A special case, $\gamma = 4$, without background noise

In this section, we study a special case where path loss exponent $\gamma = 4$ and ignore the impact of background noise. Note that the general form of Laplace transform of cumulative interference is given in (4.8), which can be simplified as follows in this case:

$$\mathscr{L}_I(s) = \exp\left\{-p\lambda_m \pi A \exp\left(\sigma^2/8\right) s^{1/2}\right\}. \tag{4.42}$$

Similarly, from (4.37) and (4.38), the Laplace transform of the output SIR Θ can be simplified:

$$\mathscr{L}_\Theta(s) = \exp(-\lambda_b \pi \exp(\frac{\sigma^2}{8})\Gamma(\frac{3}{2})\Gamma(\frac{1}{2})\mathbb{E}\left[I^{-\frac{1}{2}}\right] s^{\frac{1}{2}}), \tag{4.43}$$

where constant A is defined in (4.9) and depends on the ALOHA type.

When $\gamma = 4$, we observe that random variable I and Θ both follow Levy distribution [129]. The definition of Levy distribution is given as follows:

Definition 4.5.1. A non-negative random variable X follows Levy distribution if its probability density function $f_X(x)$ is:

$$f_X(x) = \sqrt{\frac{V}{2\pi}} \frac{\exp(-\frac{V}{2(x-U)})}{(x-U)^{\frac{3}{2}}}, \tag{4.44}$$

where $x \geq U$, U is the location parameter and V is the scale parameter. From 4.44, we can obtain CDF $F_X(x)$ and LT $\mathscr{L}_X(s)$ of X:

$$F_X(x) = 1 - \text{erf}(\sqrt{\frac{V}{2(x-U)}}), \tag{4.45}$$

$$\mathscr{L}_X(s) = \exp(-Us - \sqrt{2Vs}), \tag{4.46}$$

where $\text{erf}(x) = \frac{2}{\sqrt{\pi}} \int_0^{x^2} \exp(-t^2)dt$ refers to the error function.

By comparing (4.42) and (4.46), we find that RV I follows a Levy distribution with $U = 0$ and $\sqrt{V} = p\lambda_m \pi A \exp(\sigma^2/8)/\sqrt{2}$. Thus, the PDF of I is:

$$f_I(x) = \frac{p\lambda_m \pi A \exp(\frac{\sigma^2}{8})}{2\sqrt{\pi}} (\frac{1}{x})^{\frac{3}{2}} \exp(-\frac{\pi^4 p^2 A^2 \lambda_m^2 \exp^2(\frac{\sigma^2}{8})}{16x}), x \geq 0,$$

Hence, the negative fractional moment of I can be calculated:

$$\begin{aligned}\mathbb{E}\left[I^{-\frac{1}{2}}\right] &= \int_0^{+\infty} x^{-\frac{1}{2}} f_I(x)dx \\ &= \int_0^{+\infty} \frac{p\lambda_m \pi A \exp(\frac{\sigma^2}{8})}{2\sqrt{\pi}} (\frac{1}{x})^{-2} \exp(-\frac{\pi^4 p^2 A^2 \lambda_m^2 \exp^2(\frac{\sigma^2}{8})}{16x})dx \\ &= \frac{2}{\pi^{\frac{3}{2}} p\lambda_m A \exp(\frac{\sigma^2}{8})}\end{aligned} \tag{4.47}$$

By comparing (4.43) and (4.46), we observe that the RV Θ follows a Levy distribution with $U = 0$ and $\sqrt{V} = \frac{\Gamma(1/2)}{\sqrt{2}AL}$. By using (4.33), (4.45) and $\Gamma(1/2) = \sqrt{\pi}$, we obtain the closed-form expression of $P_{f,mrc}$, which is actually the CDF of Θ, as follows:

$$P_{f,\text{mrc}} = 1 - \text{erf}\left(\sqrt{\pi}/\left[2AL\sqrt{\theta_T}\right]\right), \tag{4.48}$$

where the constant A is given in (4.9).

4.5.5 Simulation Results and Discussion

To confirm the correctness of the proposed analytical model, we develop a simulator in which devices and BS are deployed according to PPP: at the beginning of each simulation, the number of devices and BS are determined and these nodes are uniformly placed in an disk area with radius 40. The interference on each BS is computed without any independence assumption. The background noise is neglected. The basic simulation settings are: $\gamma = 4$, $\sigma = 0$ or 8 dB, $\theta_T = 3$ dB, $p = 0.008$, $P_f^{\max} = 10\%$. The spatial device density λ_m varies from 0.2 to 2, and spatial BS density λ_b is fixed as 0.08. To calculate the 95% confidence interval, each simulation is repeated 50 times.

4.5.5.1 Packet loss Rate

Fig. 4.5, 4.6, 4.7 show the packet loss rate obtained from both simulation and analytical results, respectively for slotted ALOHA networks, pure ALOHA networks where average cumulative interference is considered, pure ALOHA where maximum cumulative interference is considered. In each figure, four cases are illustrated: nearest BS attach, best BS attach, selective combining macro reception diversity and maximum ratio combining macro reception diversity.

For the nearest and best BS attach cases, the simulation and analytical results fit well:i) this confirms the correctness of (4.21) (which is an approximation) and (4.14); ii) the upper

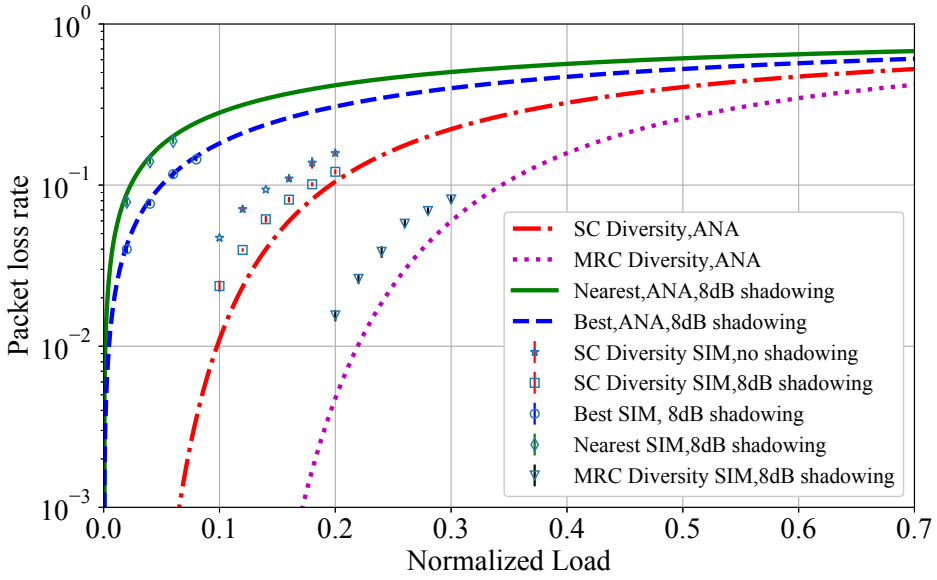

Fig. 4.5 Network packet loss rate with respect to normalized load $p\lambda_m/\lambda_b$ (ANA=analytical, SIM=simulation) for slotted ALOHA

bound proposed in Sec. 4.4.2 for maximum interference is a simple but accurate approximation (see Fig. 4.7). As proved by (4.14), the nearest BS attach with $\sigma = 0$ dB is identical to the best BS attach case. Our simulation confirms this, but we just plot the latter in Fig. 4.5, 4.6, 4.7 for the sake of clarity.

For both type of macro diversity (selective combining and maximum ratio combining), the packet loss rate in slotted ALOHA networks given by the analysis is lower than the rate obtained by simulations (see Fig. 4.5). The bias is larger without shadowing. The is due to the fact that the interference independence assumption does not always hold, especially at low load regime and without shadowing. When the load increases, diversity of interference increases, and the deviation between simulation and analysis is reduced. In the presence of shadowing, the randomness of interferences increases and the same trend is observed. Thus, shadowing effect can be leveraged to reduce packet loss rate if macro reception diversity is applied. With pure ALOHA and average interference (see Fig. 4.6), the lack of synchronization also increases the randomness of interferences, and the deviation is smaller than that in slotted ALOHA. With pure ALOHA and maximum interference (see Fig. 4.7), the interference independence assumption and upper bound approximation jointly reduce the deviation.

Actually, in realistic deployed M2M-dedicated networks, especially in urban areas, the shadowing effect is present. In addition, LPWAN apply macro diversity and pure ALOHA [24].

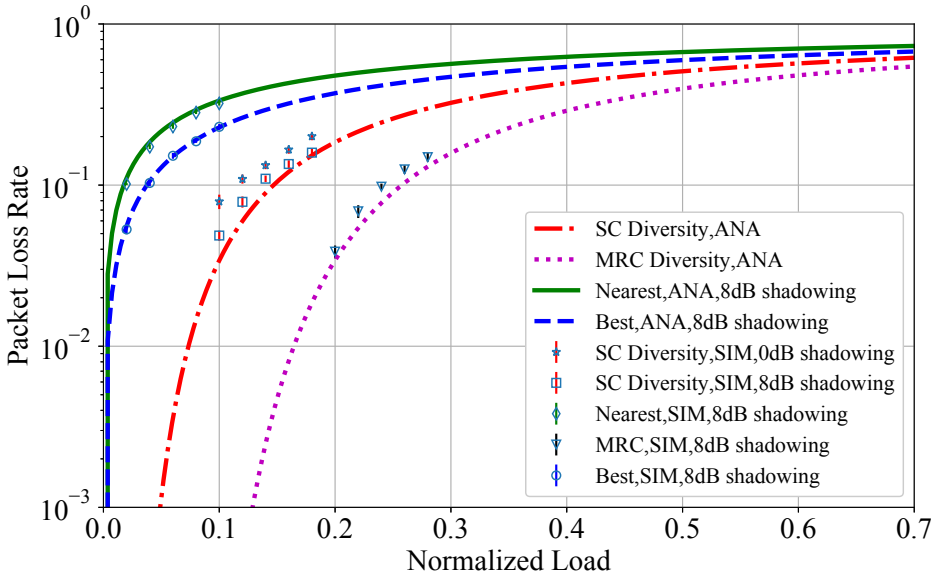

Fig. 4.6 Network packet loss rate with respect to normalized load $p\lambda_m/\lambda_b$ (ANA=analytical, SIM=simulation) for pure ALOHA with advanced transmission techniques.

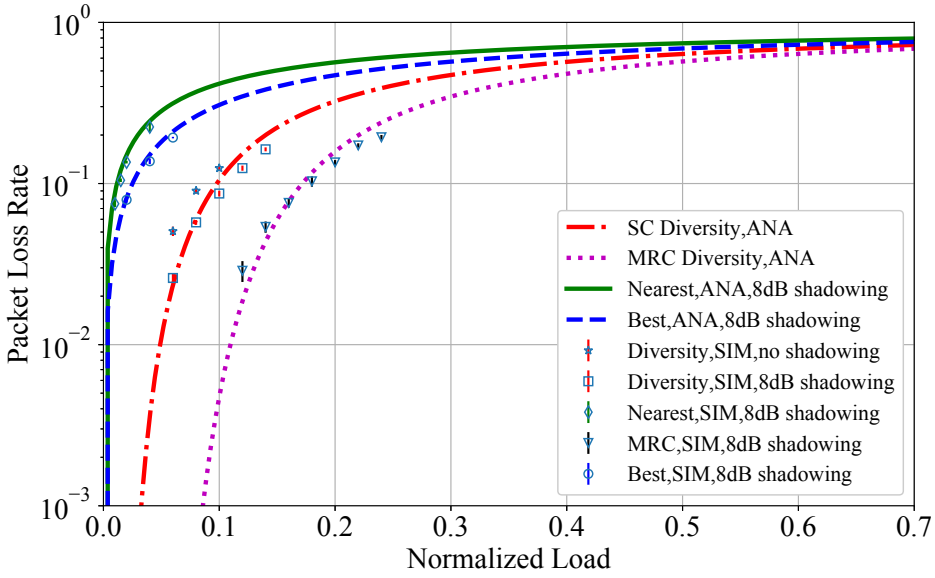

Fig. 4.7 Network packet loss rate with respect to normalized load $p\lambda_m/\lambda_b$ (ANA=analytical, SIM=simulation) for pure ALOHA without advanced transmission techniques.

The analytical model is relatively accurate around packet loss rate of 10%, which makes (4.28) suitable to analyze this kind of networks.

Table 4.1 Maximum normalized load under packet loss rate 10% and corresponding diversity gain with 8 dB shadowing

	Slotted ALOHA	Pure ALOHA Avg. Interference	Pure ALOHA Max. Interference
Best BS Attach	**0.05**	0.038	0.025
SC Macro Diversity	0.2	0.152	**0.1**
MRC Macro Diversity	0.344	0.258	**0.171**
SC Macro Diversity Gain		$\times$4.0	
MRC Macro Diversity Gain		$\times$6.8	

4.5.5.2 Maximum Normalized Load

From (4.21) and (4.28), the maximum normalized loads in different scenario are obtained and shown in Tab. 4.1. We observe that if using the same ALOHA type (either slotted or pure ALOHA) SC macro reception diversity and MRC macro reception diversity, respectively supports about 4.0 and 6.8 times devices as much as that served by best BS attach method in case of 8 dB shadowing. In addition, the maximum loads with SC macro diversity and MRC macro diversity for pure ALOHA in the worst case are respectively 0.1 and 0.171, which are respectively about 2 and 3.42 times the maximum load (0.05) for slotted ALOHA in best case. This means that for very cheap systems in which devices do not manage any downlink channel, the lack of synchronization is more than compensated by the macro diversity gain.

4.5.5.3 Spatial Throughput

Fig. 4.8 illustrates the spatial throughput comparison. We consider three categories: slotted ALOHA based best BS attach method, pure ALOHA based SC macro diversity and pure ALOHA based MRC macro diversity. In interval $[0,1.0]$, MRC macro diversity for pure ALOHA with average interference always has the best spatial through performance. In interval $[0,0.2]$, macro diversity for pure ALOHA in worst case (i.e. SC macro diversity and maximum interference) still outperforms the best BS attach method. In interval $[0.6,1]$ where network packet loss rate is very high, the best BS attach method for slotted ALOHA is better than SC macro diversity in pure ALOHA. In addition, we confirm that, the spatial throughput performances for all cases approach their respectively limit values.

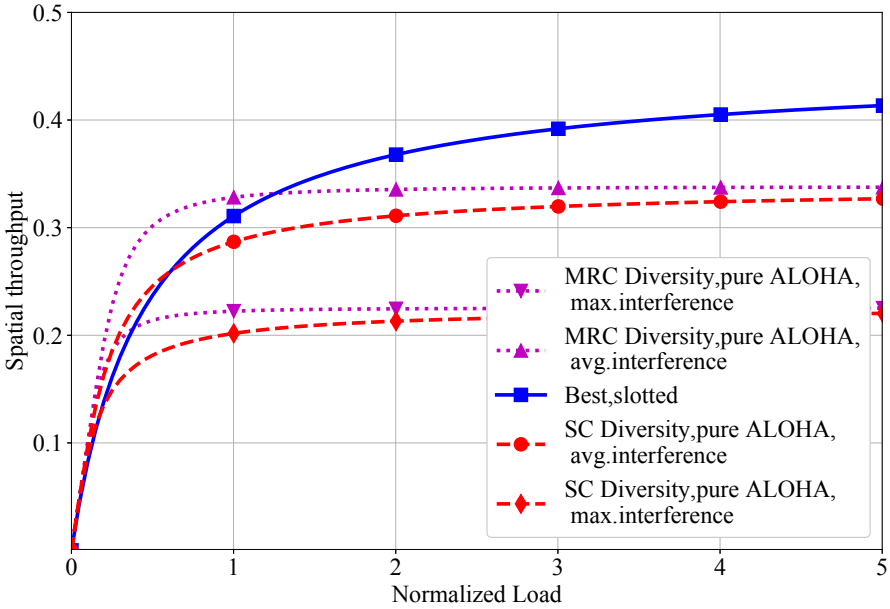

Fig. 4.8 Spatial throughput with respect to normalized load

4.6 Network Level Performance with Outage Probability Constraint

In Sec. 4.5, we study the network level performance metrics such as packet loss rate, throughput. These metrics are actually the average over the entire networks, which gives a global view about the quality of service in LPWAN networks but still have its limitations. With a target network level packet loss rate such as 10%, it is very possible that devices in the neighborhood of BS never fail while devices at the border of BS coverage area have packet loss rate higher than 10%.

In this section, we propose a new network performance indicator called *outage probability* that is associated with network level packet loss rate. Given a target packet loss rate, the outage probability here refers to the proportion of devices whose link level packet loss rate is superior to the target value. For example, the statement that a LPWAN network has outage probability of 10% with target network packet loss rate 1%, means that at most 10% of devices in the considered LPWAN network has a packet loss rate higher than 1%.

With the proposed outage probability, we can study the minimum BS spatial density λ_b if a LPWAN operator needs to guarantee a certain level of Grade of service (i.e. outage probability). We analyze the performance of BS attach method and selective combining

(SC) macro reception diversity with this proposed performance metric. These studies can help LPWAN operators to deploy their network in an efficient way. Note that retransmission is not considered.

4.6.1 Best BS Attach

4.6.2 With background noise, $\gamma = 4$

Consider a device at the origin whose distance to its best BS is r. If best BS attach method is applied, background noise is considered and path loss exponent γ is 4, the link level packet loss rate, according to the generalized model in Sec. 4.4.4, $p_{f,b}(r)$ is:

$$p_{f,b}(r) = 1 - \exp\left(-\eta_T r^4\right) \exp(-\varepsilon_T r^2), \tag{4.49}$$

where $\eta_T = \frac{\sigma_n^2 \theta_T}{P_t K}$ represents the impact of the background, $\varepsilon_T = p\lambda_m \pi A \theta_T^{\frac{1}{2}} e^{\frac{\sigma^2}{8}}$ reflects the impact of the cumulative interference from other transmitters. Note that the value of A depends on the type of ALOHA.

Still let $P_{f,\max}$ be the target network loss rate and $P_{\text{outage},b}$ be the outage probability (the subscript b refers to the best BS attach method). Since the link level packet loss rate $p_{f,b}(r)$ is a function of r, thus, the proportion of devices that have higher packet loss rate than $P_{f,\max}$, namely the outage probability $P_{\text{outage},b}$, can be expressed as follows:

$$\begin{aligned} P_{\text{outage},b} &= \int_0^{+\infty} \mathbb{1}_r\left[p_{f,b}(r) > P_{f,\max}\right] f(r) dr = \int_{r_c}^{+\infty} f(r) dr \\ &= 1 - \int_0^{r_c} f(r) dr = \exp(-\lambda_b e^{\frac{\sigma^2}{8}} \pi {r_c}^2), \end{aligned} \tag{4.50}$$

where $\mathbb{1}_r[\cdot]$ is a indicator function about r. The PDF of r, which is given in (4.4), is listed as follows:

$$f_r(r) = 2\pi\lambda_b e^{\frac{2\sigma^2}{\gamma^2}} \exp(-\lambda_b e^{\frac{2\sigma^2}{\gamma^2}} \pi r^2) r, r \in [0, +\infty],$$

r_c is the critical distance satisfying condition $p_{f,b} = P_{f,\max}$. The critical distance r_c is calculated by substituting $p_{f,b}(r_c) = P_{f,\max}$ into (4.49). Although there is no closed-form expression for critical distance r_c, the latter can be easily numerically calculated by leveraging the fact that $p_{f,b}(r)$ is a mono-increasing function with respect to r.

With the obtained r_c and a given outage probability, the minimum BS spatial density $\lambda_{b,\min}$ can be obtained by inversing (4.50):

$$\lambda_{b,\min} = -\ln(P_{\text{outage},b})\frac{1}{\pi \exp(\sigma^2/8) r_c^2}. \tag{4.51}$$

4.6.3 Without background noise

Now we consider an interference-limited LPWAN system in which the background is ignored. Applying the best BS attach method, the link level packet loss rate $p_{f,b}(r)$ is:

$$p_{f,b}(r) = 1 - \exp(-\varepsilon_T r^2), \tag{4.52}$$

where $\varepsilon_T = p\lambda_m \pi A \theta_T^{\frac{1}{2}} e^{\frac{\sigma^2}{8}}$. The critical distance r_c is thus:

$$r_c = \left[\ln(1 - P_{f,\max}) / \left(-p\lambda_m \pi A \theta_T^{\frac{1}{2}} e^{\frac{\sigma^2}{8}}\right)\right]^{1/2} \tag{4.53}$$

With substitution of (4.53) into (4.51), $\lambda_{b,\min}$ is as follows:

$$\lambda_{b,\min} = p\lambda_m \frac{\ln(P_{\text{outage},b}) A \theta_T^{1/2}}{\ln(1 - P_{f,\max})}. \tag{4.54}$$

From (4.54), we find that the network load $p\lambda_m$ has a linear relationship given an outage probability and a target network packet loss rate.

4.6.4 Selective Combining Macro Reception Diversity

Different from best BS attach method, whose link-level packet loss rate only depends on the distance to the nearest BS, the performance of SC macro reception diversity depends on a distance vector $r_i, i = 0, 1, 2....$ Thus, we need to know the characteristics of such a vector. However, the distance to the nearest BS r_0 has the most impact to SC macro reception diversity. Thus, to reduce the complexity and keep the tractability, for a given device, its packet loss rate can be approximately expressed in terms of r_0 (instead of the distance vector to all surrounding BS $r_i, i = 1, 2...$).

Let $p_{f,sc}(r_0)$ be link-level packet loss rate with respect to r_0. Recall that in case of SC macro reception diversity,

$$p_{f,sc}(r_0) \approx (1-p_s(r_0))\mathbb{E}\left[\prod_{r_i\in\Phi_b}(1-p_s(r_i))\right], \text{with } r_i \in [r_0,+\infty], \tag{4.55}$$

where r_i refers to the distance between the device and BS with label i. Note that r_i should be not less than r_0. The impact of other BS than the nearest one to the packet loss rate is thus reflected by term $\mathbb{E}\left[\prod_{r_i\in\Phi_b}(1-p_s(r_i))\right]$.

Term $\mathbb{E}\left[\prod_{r_i\in\Phi_b}(1-p_s(r_i))\right]$ in (4.55) is actually the Probability Generating FunctionaL (PGFL) of PPP Φ_b for BS, which states for some function $f(x)$ that:

$$\mathbb{E}\left[\prod_{x\in\Phi} f(x)\right] = \exp(-\lambda(\int_{\mathbb{R}^2}(1-f(x))dx))$$

Thus, it can be simplified as follows:

$$\begin{aligned}\mathbb{E}\left[\prod_{r_i\in\Phi_b}(1-p_s(r_i))\right] &= \exp\left\{-\int_{r_0}^{+\infty}\exp(-\eta_T r^4-\varepsilon_T r^2)2\pi\lambda_b e^{\frac{\sigma^2}{8}} r dr\right\} \\ &= \exp\left\{-\pi\lambda_b e^{\frac{\sigma^2}{8}}\int_{{r_0}^2}^{+\infty}\exp(-\eta_T r^2-\varepsilon_T r)dr\right\}\end{aligned} \tag{4.56}$$

With substitution of (4.56) into (4.55), we have:

$$p_{f,sc}(r_0) = (1-\exp(-\eta_T r_0^4-\varepsilon_T r_0^2))\exp\left\{-\pi\lambda_b e^{\frac{\sigma^2}{8}}\int_{{r_0}^2}^{+\infty}\exp(-\eta_T r^2-\varepsilon_T r)dr\right\} \tag{4.57}$$

By letting $p_{f,sc}(r_0) = P_{f,\max}$ and substituting (4.51) into (4.57), the critical distance r_c can be numerically calculated due to the fact that $p_{f,sc}(r_0)$ is a mono-increasing function (even though its closed-form expression does not exist). Then we can use formula (4.51) to calculate the minimum BS spatial density, given an outage probability and target network packet loss rate.

4.6.5 Numerical Results and Discussion

The system settings to get the numerical results are resumed in Tab. 4.2. Some explanations are given as follows: to evaluate the impact of the background noise to the system performance, we need to determine the values of P_t, K, σ_n^2. For one LPWAN device running on ISM band (e.g. with 868 MHz), from a regulatory point of view, the effective radiated power

Table 4.2 Parameter values for numerical results

Parameter Name	Parameter Notation	Value
Transmit power	P_t	14 dBm
Noise figure	NF	6 dB
Occupied bandwidth	B	200 kHz
Target network packet loss rate	$P_{\text{f, max}}$	10%
Outage probability	P_{outage}	1%, 10%
Device height	h_d	1.5 m
BS antenna height	h_{bs}	50 m
Noise power	σ_n^2	-115 dBm

(ERP) may not exceed 14 dBm (or 25 mW) in any direction [12], we thus assume that the transmit power P_t is set as 14 dBm.

About noise power level, we use the same formula given in [102]: $\sigma_n^2 = -174 + \text{NF} + 10\log(B)$, where NF is the noise figure, usually set as 6 dB, B is the bandwidth occupied by the transmitted packet. The occupied transmission band is assumed to be 200 kHz (e.g. LoRaWAN). Thus, σ_n^2 is -115 dBm.

In terms of propagation path-loss model, Okumura-Hata model is applied. In urban area, the path-loss between one device with antenna height $h_d = 1.5$ meters and a BS with height $h_{bs} = 50$ meters is [130]: $\text{Path\_Loss} = -10\log_{10}(K) + \gamma 10\log_{10}(r) = 123.6 + 33.8\log(r)$, where $\log_{10}(\cdot)$ is 10-based logarithm operator, r is in unit of kilometer. Thus, the constant $10\log_{10}(K)$ is -123.6 dB.

We consider a LPWAN network with target network packet loss rate 10%. With a given outage probability requirement, we calculate the minimum required BS spatial density (per km^2) with respect to the network load (per slot). The latter varies from 0.05 to 0.3. The numerical results are shown in Fig. 4.9 (with outage probability 10%) and Fig. 4.10 (with outage probability 1%).

From (4.54), we know that, if the background noise is neglected, there exists a linear relationship between network load (i.e. $p\lambda_m$) and minimum BS spatial density (i.e. λ_b) if target network packet loss rate and outage probability is given. This can be confirmed in Fig. 4.9 and Fig. 4.10. For slotted ALOHA based best Best BS attach with background noise, we unfortunately have no closed-form expression between minimum required BS density and network load. From these two figures, the relationship between minimum required BS density and network load can be assumed to be linear and we can use curve fitting techniques to get a closed form expression for the case with noise with high accuracy. In addition, It is not surprised that with background noise, the minimum required BS density is more larger.

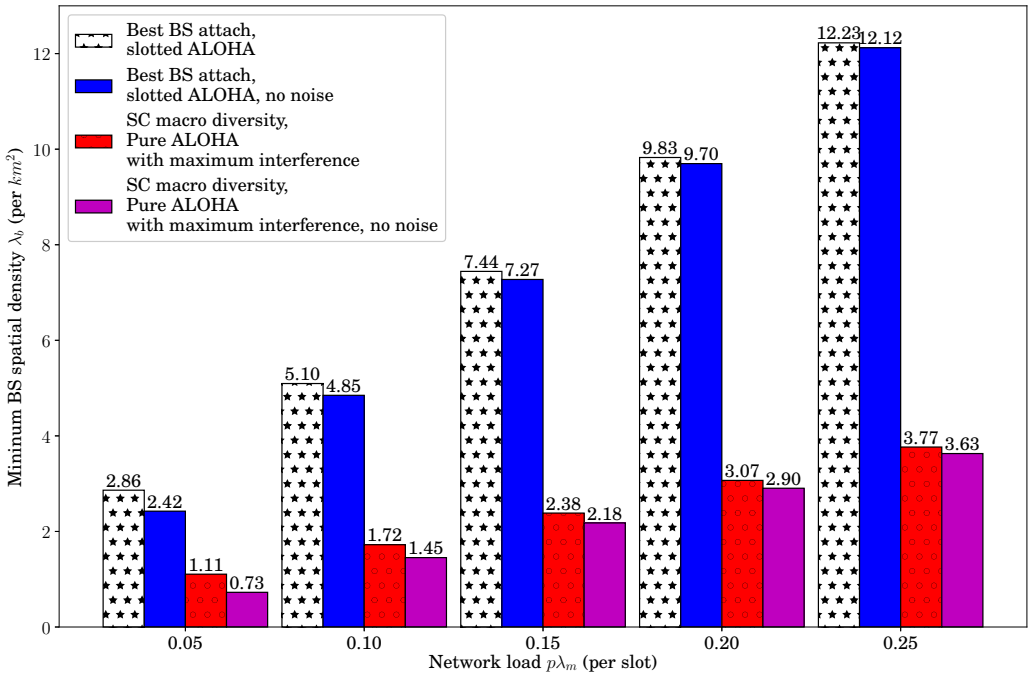

Fig. 4.9 Minimum BS spatial density with respect to network load. The target packet loss rate and outage probability threshold are both 10%.

From these two figures, we observe that as network load increases, the increase of minimum BS spatial density in case of macro diversity is significantly smaller than that in case of best BS attach. One straightforward explanation is: to guarantee a certain level of outage probability, as the load increases, the network should be more dense. The chance that one packet is received by several surrounding BS is thus much higher in a dense network. Thus, macro diversity has more obvious effect.

4.7 Network Level Performance with Retransmission Mechanism

In this section, we ignore the background noise and extend the network level performance analysis by taking into account retransmission mechanism. Let $N_{\max}$ be the maximum allowed number of transmissions. As a first step, we just consider the retransmission mechanism used by LPWAN systems that have no ACK mechanism (e.g. Sigfox): devices always transmit one packet $N_{\max}$ times no matter whether previous packet transmission is successful.

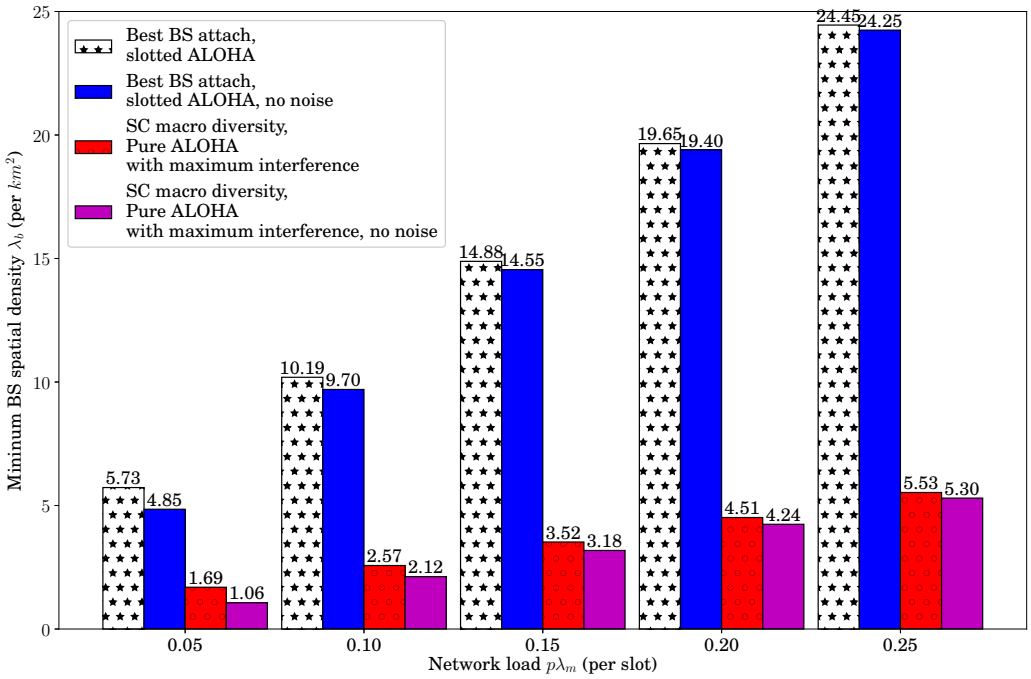

Fig. 4.10 Minimum BS spatial density with respect to network load. The target packet loss rate is 10% and outage probability threshold is 1%.

For LPWAN systems with ACK mechanism (LoRaWAN), the employed retransmission mechanism is completely the same as that use in slotted ALOHA cellular systems: a packet is retransmitted after a random interval until its delivery to BS or the reach of maximum allowed trials. The analysis about this kind of systems is planned as part of future works.

In case of retransmission, $p\lambda_m$ is the fresh space-time arrival packet intensity and $L = p\lambda_m/\lambda_b$ is referred to as the *fresh normalized load*. We assume that each retransmission takes place at random over long intervals following the previous transmission, therefore, the aggregate uplink packets stream still follows a PPP with aggregated space-time intensity λ_{agg}. Let $G = p\lambda_{\text{agg}}/\lambda_b = N_{\max}L$ be the *aggregated normalized load*.

According to Poisson's splitting property [93], the aggregate packet arrival process can be divided into N_{max} mutually independent Poisson arrivals processes. Let p_f be the failure probability of one transmission and P_f be the network level packet loss rate after N_{max} transmissions, namely $P_f = p_f^{N_{max}}$.

In the following section, we analyze the ALOHA performance for selective combining macro reception diversity.

4.7.1 Selective Combining based Macro Diversity

Let $P_{f,sc}$ and $p_{f,sc}$ respectively be the network packet loss rate and failure probability of one transmission. With macro reception diversity, one packet is failed if and only if none of BS has decoded it after $N_{\max}$ trials, $p_{f,sc}$ is obtained as follows:

$$\begin{aligned} p_{f,sc}(r) &= \left[1-\exp(-p\lambda_{\text{agg}}\pi A\theta_T^{\frac{2}{\gamma}}e^{\frac{2\sigma^2}{\gamma^2}}r^2)\right]^{N_{\max}}, \\ &= \left[1-\exp(-pN_{\max}\lambda_m\pi A\theta_T^{\frac{2}{\gamma}}e^{\frac{2\sigma^2}{\gamma^2}}r^2)\right]^{N_{\max}}, \\ &= \left[1-\exp(-N_{\max}\varepsilon_T r^2)\right]^{N_{\max}}, \end{aligned} \tag{4.58}$$

where $\varepsilon_T = p\lambda_m\pi A\theta_T^{\frac{2}{\gamma}}e^{\frac{2\sigma^2}{\gamma^2}}$. Using similar justification in Sec 4.5.3, we have:

$$P_{f,sc} = \mathbb{E}\left[\prod_{r_i\in\Phi_b}\left[1-\exp(-N_{\max}\varepsilon_T {r_i}^2)\right]^{N_{\max}}\right], \text{with } r_i\in[0,+\infty]. \tag{4.59}$$

where r_i is the distance between the device and BS with label i. By using PGFL of PPP, we have:

$$P_{f,sc} = \exp\left\{-2\pi\lambda_b e^{\frac{2\sigma^2}{\gamma^2}}\int_0^{+\infty}\left[1-\left(1-\exp(-N_{\max}\varepsilon_T r^2)\right)^{N_{\max}}\right]rdr\right\}. \tag{4.60}$$

Applying binomial theorem to (4.60):

$$\begin{aligned} P_{f,sc} &= \exp\left\{-2\pi\lambda_b e^{\frac{2\sigma^2}{\gamma^2}}\int_0^{+\infty}\left[-\sum_{i=1}^{N_{\max}}\binom{N_{\max}}{i}(-1)^i\exp(-iN_{\max}\varepsilon_T r^2)\right]rdr\right\} \\ &= \exp\left\{2\pi\lambda_b e^{\frac{2\sigma^2}{\gamma^2}}\sum_{i=1}^{N_{\max}}\int_0^{+\infty}\binom{N_{\max}}{i}(-1)^i\exp(-iN_{\max}\varepsilon_T r^2)rdr\right\} \\ &= \exp(\sum_{i=1}^{N_{\max}}\binom{N_{\max}}{i}(-1)^i\frac{1}{iA\theta_T^{2/\gamma}N_{\max}L}), \end{aligned} \tag{4.61}$$

where A is defined in (4.9), $\binom{N_{\max}}{i}$ is binomial coefficient.

4.7.2 Numerical Results and Discussions

From numerical results, we study the impact of retransmission mechanism that used by systems without ACK mechanism. The considered system uses pure ALOHA based selective

combining macro reception diversity with maximum interference. Let $N_{\max}$ respectively be $1,2,3,4$. The network packet loss rate is shown in Fig. 4.11. We observe that the packet loss rate degrades as $N_{\max}$ increases. The reason is that: the devices in the neighborhood of BS have more chance to deliver their packets. Even though they succeed in delivering the packets, they still transmit the same packet into the radio access network that aggravates the interference level, Thus, for other devices outside of BS neighborhood, especially for those at the border of BS, it is more difficult to deliver their packets. This kind of retransmission mechanism only brings benefit for those devices not far away from BS.

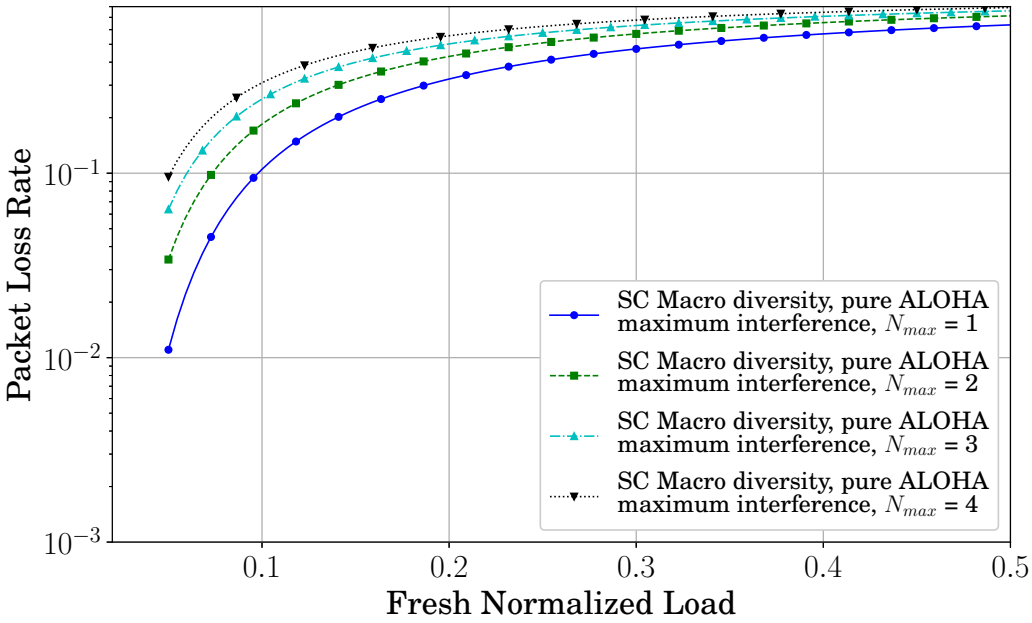

Fig. 4.11 Network packet loss rate with respect to fresh normalized load $p\lambda_m/\lambda_b$ for pure ALOHA. Each packet is always transmitted $N_{\max}$ times.

4.8 Summary

In this chapter, we have studied the (pure and slotted) ALOHA performance, in terms of packet loss rate and spatial throughput in LPWAN systems that are composed by multiple BS. In LPWAN networks, macro reception diversity is leveraged to improve system performance. The possible macro reception diversity forms are: selective combining and maximum ratio combining. We evaluate performance gain brought by macro diversity by taking traditional BS association policies: the geographical nearest BS attach and the best BS attach as the comparison reference. We have obtained closed-form expressions when the

background noise is neglected and given the integral form expressions when the background noise is considered.

The derived analytical model has been confirmed by simulation. Simulation results show that the established especially have a high level accuracy to evaluate the performance of LPWAN deployed in urban areas. From the analysis of the performance gain in one-shot random access case, we observe that systems with macro diversity benefit from shadowing effect and provides an important gain in all cases. For the analysis in cases with retransmission mechanism, we observe that the performance gain brought with macro diversity is limited compared with best attach method. From the analysis that take into account outage probability constraint, the macro diversity is more resistant to such a constraint.

Chapter 5

M2M-oriented network-integrated multiple-period polling service in LTE networks

5.1 Introduction

In previous chapters, the performance of MTC over LPWAN networks is analyzed. Although it is an attractive option to deploy M2M applications over LPWAN networks such as Sigfox or LoRaWAN, the operators have to maintain two separate infrastructures for their clients. Hence, due to the ubiquitous coverage area and mature infrastructure, the accommodation of MTC traffic over existing cellular networks is also attractive.

The 2G networks, such as GSM technology, are energy efficient and technically a very suitable choice for MTC. After decades development, it is a rather mature technology. With minimum reengineering work, they can well support MTC. However, M2M devices are expected to remain operational for decades while 2G networks are planed to be decommissioned within the next $5-15$ years. For example, AT&T decided to stop GSM-based service and refarm the spectrum occupied by GSM to LTE in 2017 [131]. For a long term view, 2G is not the most appropriate candidate for MTC. 3G is based on spectrum spreading technology and is not energy efficient, thus few research efforts are made to consider how to support MTC over 3G networks. 4G, now with wide deployment and still in its life circle, is a safe and appropriate choice. However, this technology was designed to solve mobile broadband demand for human beings and not for the particular requirements of MTC, which are quite different from human type communication (HTC). To efficiently support MTC, LTE has to be adapted with respect to MTC characteristics.

In this chapter, we present a proposal to efficiently handle large number of devices over future LTE networks. Inspired from the observation that a considerable partition of MTC traffic exhibit periodicity [29], we propose a multiple periodic polling service in LTE radio access network to serve a large number of MTC devices deployed for M2M periodic application, such as smart grid. Our proposal reduces the transmission overhead and thus improves the energy efficiency for MTC devices. It also reduces signaling overload in radio access network by avoiding random access. The proposed service can be integrated into LTE radio access network, fully compatible with the standard access mechanism and able to manage a large range of polling periods (typically from 1 minute to 28 days).

This chapter is organized as follows: Section 5.2 talks about related work, Section 5.3 gives an overview about the work-flow of MTC device periodic data report via random access method. Section 5.4 presents in detail our M2M-oriented multiple-period polling mechanism. Section 5.5 conducts a comparative performance analysis between our proposal and conventional LTE random access when handling MTC traffic. Section 5.7 is the conclusion part of this chapter.

5.2 Related work and motivation

Plenty of research efforts exist in the literature to remedy the random access overload and energy efficiency in M2M system. They can be categorized into orientations given in [19]: introduce separate access class for MTC devices, separate RACH resource for MTC, pull based schema, etc. As conventional random access used in LTE is not efficient for periodic MTC, some researchers consider to avoid random access by leveraging periodicity of most MTC traffic: A radio resource allocation method is proposed in [132] for reports with deadlines in GPRS/EDGE by avoiding random access and using a periodic structure to serve the devices such that the deadlines are met. The radio access control mechanism in GSM is reengineered in [133] to support massive smart metering. A M2M-dedicated uplink radio is proposed by [64]. The key idea is to periodically reserve dedicated resource pool for M2M traffic, but the authors have not indicated that how each device is scheduled to avoid collision in this resource pool. References [134, 63] propose a persistent radio resource method reserving periodically radio resource for devices without random access procedure, but none of these references gives implementation for LTE network.

In this chapter, we propose a network-integrated multiple-period polling service dedicated for periodic MTC traffic in LTE network. The motivations of this work are:i) as an all-IP architecture, LTE does not provide integrated service. Hence conventional MTC related polling services in LTE are at application level; ii) signaling overhead compared to

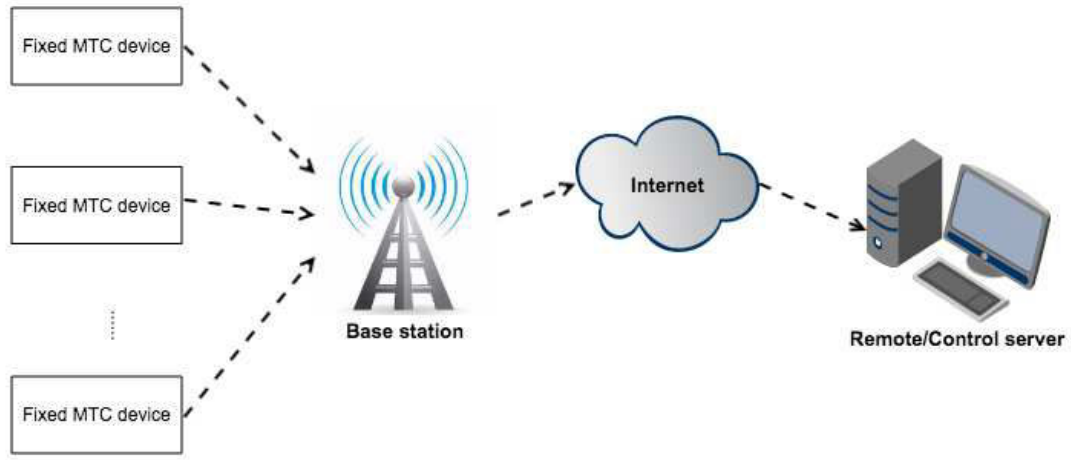

Fig. 5.1 Periodic M2M application work flow

the small payload of MTC traffic is too expensive; iii) the periodicity of MTC traffic is not well leveraged in the current version of LTE network. The key philosophy of the proposed service is: all devices with different report periods should sequentially use the same system resource without random access procedure under scheduling of the eNB, because each device has a deterministic comportment.

5.3 MTC device data upload procedure in LTE

We are only concerned about periodic MTC traffic whose work-flow is presented in a general way in Fig.5.1. It consists of user cases where low mobility or fixed devices[1] periodically report collected data with small payload (less than 200 bytes as in [34]) to remote servers. Consider a situation where a device stays in RRC_Idle state before starting its data reporting procedure. Deployed in current LTE network, to finish data transmission, a device should repetitively go through three procedures: contention-based random access procedure for establishment of RRC connection, data transmission and release of established RRC connection.

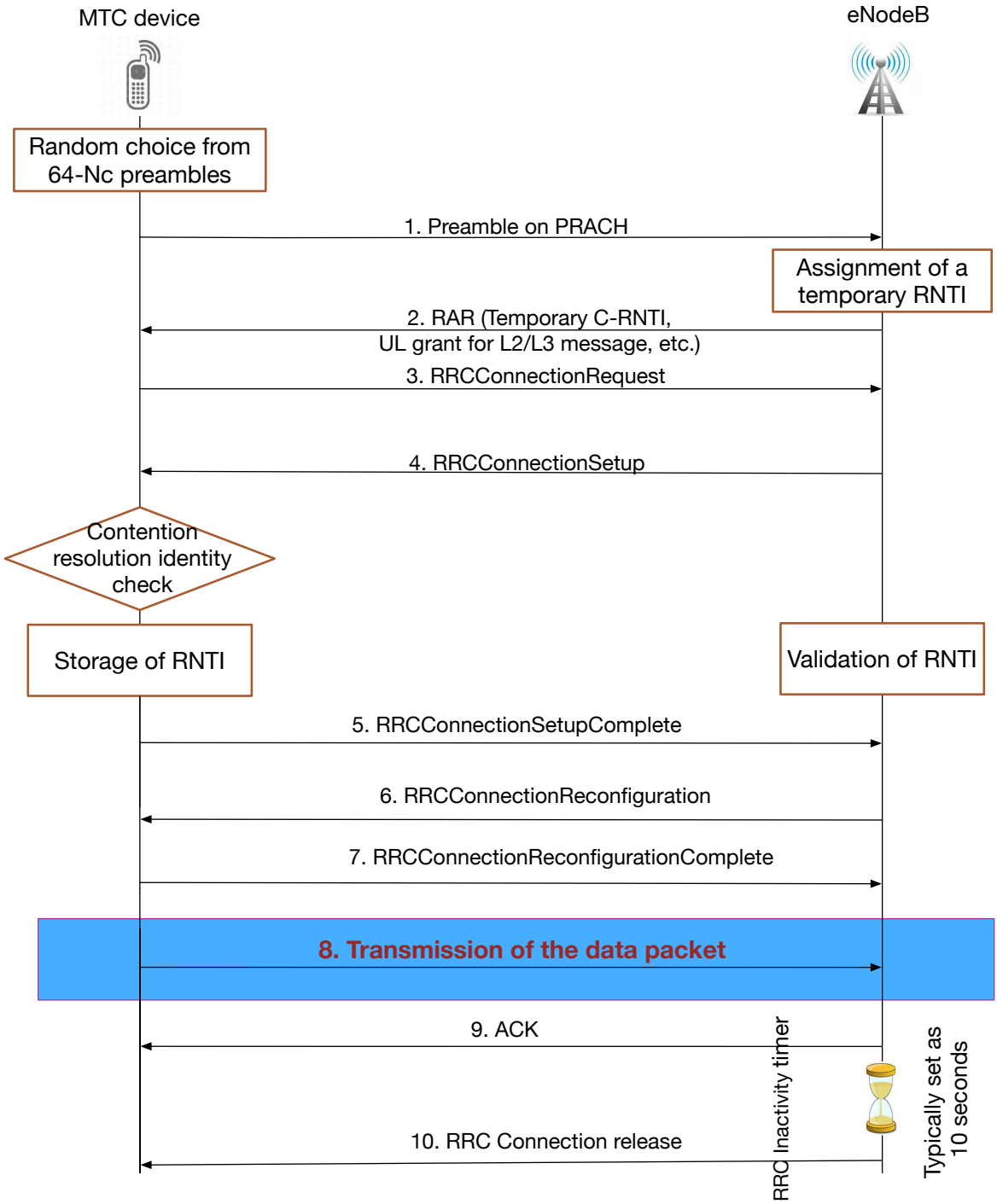

Fig. 5.2 Conventional random access and data upload procedure in LTE networks

5.3.1 Random access procedure

As illustrated in Fig. 5.2, the conventional random access procedure mainly consists of four steps presented as following.

Step 1: Preamble transmission

In this step, the UE randomly selects one from the $64 - N_c$ random access preambles and transmits the selected preamble at the next physical random access channel (PRACH) opportunity, where N_c is the number of preambles reserved for non-contention based random access. After the preamble transmission, the UE shall monitor the PDCCH channel and try to decode a Random Access Response identified by the RA-RNTI from the eNB.

Step 2: Random Access Response (RAR)

The RAR message generated by the eNB is decoded with UE-generated RA-RNTI and contains the identity of the detected preamble, uplink channel synchronization information, an initial uplink resource grant for the transmission of the step 3 message, an assignment of a temporary Cell Radio Network Temporary Identifier (C-RNTI) along with other information.

Step 3: L2/L3 message

In this step, the UE sends the messages related to RRC connection request for random access procedure and makes use of Hybrid Automatic Repeat reQuest (HARQ). It is addressed to the temporary C-RNTI allocated in RAR at step 2 and carries the contention resolution identity. The contention resolution identity is a locally unique identity of the UE, which is generally built with the S-TMSI. After the transmission of step 3, the UE wait for the contention resolution message.

Step 4: Contention Resolution Reception

The contention resolution message from the eNB is addressed to the temporary C-RNTI and contains contention resolution identity received in L2/L3 message. This is an echo mechanism: if the UE detects its own identity, it knows that its random access request is accepted by eNB. If not, UE can infer that collision happens in previous step. A collision is occurred if more than one UEs select and send the same preamble to eNB in step 1. Each of them receives the same RAR in step 2 and thus uses the same same temporary C-RNTI in step 3. Either none of devices receives contention solution message and all colliding UEs restart from step 1, or just one of them receives echo and finishes the random access procedure.

[1] Note that the terms device and UE are used interchangeably in the rest of this chapter.

5.3.2 Transmission of data packet

Since upload of MTC device data consists of a UE triggered service request procedure, L2/L3 message in the previous is a *RRCConnectionRequest* and Contention resolution message is *RRCConnectionSetup*. Subsequently the UE sends service request in message *RRCConnectionSetupComplete*. After an exchange of *RRCConnectionReconfiguration*, UE establishes a RRCConnection network and starts the data transmission.

5.3.3 RRC Connection Release

After transmission of data packet, UE goes back to RRC_Idle state after the expiration of RRC inactivity timer, eNB deletes complete UE context and releases the established RRC connection with UE. Thus, UE has to pass through above steps before getting a RNTI for the next reporting.

With above description, traditional RACH access method poses some challenges when handling MTC in particular periodic MTC traffic. First, massive device requests may lead to access network congestion. Second, the control signaling overhead for small payload (e.g. 100 bytes) is expensive, for example acquiring radio access network resources requires at least four messages exchanged between devices and network. Third, short transaction for small payload causes inefficient resource utilization. Taking the consumption of RNTI as an example: assuming a MTC device needs to send 100 bytes to remote server, with a robust modulation scheme, the transmission is usually finished in 100 ms, MTC device does not need to hold allocated RNTI until next reporting. However, the eNB has no way to determine whether device has data to transmit and takes back allocated RNTI after the expiration of related timer.

5.4 Network integrated M2M-oriental polling service

The main idea of our proposed periodic polling service is: the network provides a list of polling periods. MTC devices register to the network for an appropriate polling period by traditional random access procedure. Upon received requests, the eNB deterministically allocates RNTI and the phase number in the allocated polling period for each registered device. Afterwards, both the eNB and devices monitor LTE frames to determine their respective actions. When a transmission condition is verified for a certain device, the eNB directly allocates radio resources for the latter to poll the data. The qualified device directly sends its data via allocated resource without collision with other devices. Note that the radio resource allocation for data transmission may be of two types: either a semi-persistent allo-

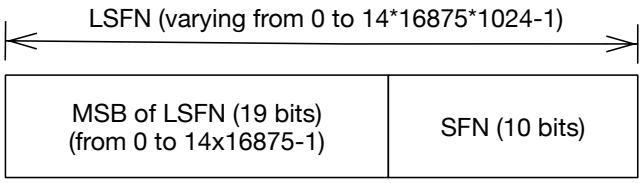

Fig. 5.3 Construction of LSFN

cation by which a fixed resource is periodically allocated to the registered MTC devices, or a flexible allocation where a standard packet access is used within the allocated polling window (detailed in Sec.5.4.1.4). Therefore, our proposed service consists of periodic polling mechanism and RNTI allocation algorithm. In this section, we first introduce several concepts introduced by our proposal. Second, we detail its periodic polling mechanism. Third, we present the RNTI allocation algorithm.

5.4.1 Terminology Related to the Proposed Service

5.4.1.1 LSFN

We propose to extend the frame counting mechanism of LTE known as SFN (System Frame Number) and define a counter called LSFN for Long SFN. It is used to helpi) the eNB to determine which target it should poll for data ii) a device to determine whether it is its turn to transmit data. The necessity for this extension is due to the fact that conventional LTE SFN varies from 0 to 1023 and each SFN value repeats every 10.24 sec. LSFN is constructed by extending 19 bits as MSB (Most significant bit) for current SFN. The value of LSFN is reset when it reaches $14\times16875\times1024$. The period is thus $14\times16875\times1024\times10$ ms, which is exactly 28 days and allows to define any process with period up to about one month. The 19 MSB of LSFN is broadcasted in a System Information Block every 10.24 sec. The relationship between LSFN and SFN is shown in Fig.5.3. Note that the LSFN indexing system does not modify the SFN-based mechanisms. Terminals other than those of periodic MTC applications still access network through conventional random access and use current LTE SFN system.

5.4.1.2 PRD-RNTI

PRD-RNTI is a kind of RNTI used to uniquely identify one MTC device in a polling window (detailed in 5.4.1.4). The range FFF4-FFFC (marked as reserved for future use in [135]) is thus allocated as PRD-RNTI. The same PRD-RNTI is allocated to several MTC devices

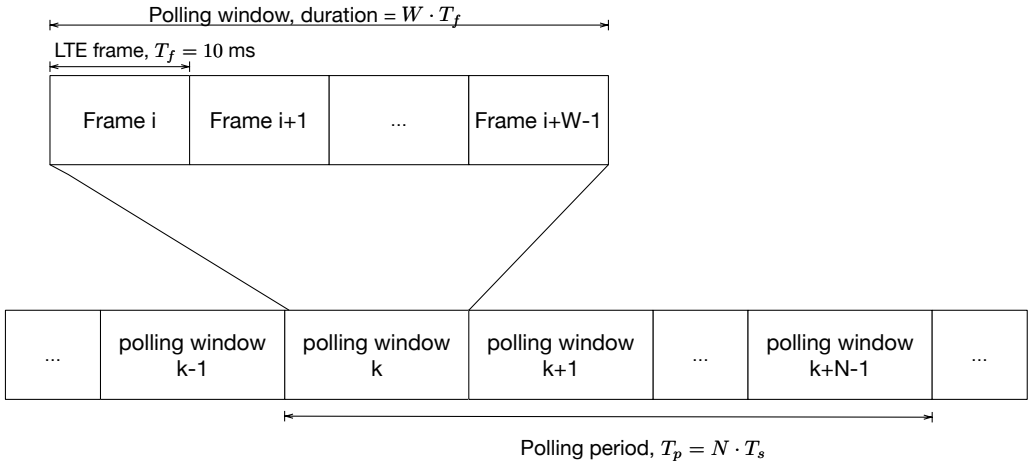

Fig. 5.4 Illustration of Polling window in time domain

but at different time. Hence, during a given period of time, the PRD-RNTI is allocated to only one device. As the allocation is deterministic, one device knows when it can use the PRD-RNTI and the network knows to which device the PRD-RNTI is used at any time. One PRD-RNTI can sequentially serve huge number of MTC devices.

5.4.1.3 Polling period

The polling period denoted by T_n is the time interval between two consecutive eNB-triggered polling procedures for the same MTC device. It is computed from the application report period T by:

$$T_n = 2^{\lfloor \log_2 \frac{T}{WT_f} \rfloor} \cdot W \cdot T_f = N_n \cdot W \cdot T_f \tag{5.1}$$

where $\lfloor x \rfloor$ means the maximum integer not greater than x, N_n is the number of polling window contained in period T_n, W is the number of LTE frame, T_f refers to LTE frame duration. As a network integrated service, the eNB uniquely supports polling periods satisfying (5.1).

5.4.1.4 Polling window

The polling window is a time interval which is reserved for data transmission of a unique MTC device. It is a configurable system parameter. Its duration is equal to W LTE frame and should ensure that the device can deliver its data even in case of retransmission due to the HARQ mechanism. The relationship between polling window and LTE frame is illustrated in Fig.5.4.

5.4.2 Multiple-period polling mechanism

Different with traditional RACH method for network access, the eNB in our proposed periodic polling mechanism allocates system resource (i.e. RNTI) to a certain registered MTC device when LSFN satisfies some predefined rules, since periodic MTC application comportment is deterministic. It consists of two stages: registration stage and polling stage.

5.4.2.1 Registration stage

Let consider one MTC device m asking for periodic polling service. It first sends a polling activation request including the polling period T_n by traditional random access procedure. If the request is accepted, the network then sends back a confirmation message with i) the number of polling windows N_n that corresponds to the polling period; ii) a phase value ϕ_m between 0 and $N_n - 1$; iii) a PRD-RNTI value. Once the registration stage is finished, eNB updates its internal data for periodic polling service and registered device m can use allocated PRD-RNTI with following rules:

$$\text{PRD-RNTI for device } m \text{ when} \lfloor \frac{LSFN}{W} \rfloor \bmod N_n = \phi_m \tag{5.2}$$

5.4.2.2 Periodic polling stage

At this stage, for each LTE frame, the eNB manipulates LSFN value and determines current polling window is reserved for which MTC device by checking stored rules like in (5.2). Still taking device m as an example, once rule (5.2) is satisfied, the eNB allocates radio resource for the device holding the PRD-RNTI, namely device m. As to device m, it also monitors the value of LSFN. If the MTC device has no specific action, it can switch to a low consumption mode in order to spare energy. As soon as rule (5.2) is checked then the device m listens to the PDCCH during all the polling window. It is up to the eNB to allocate uplink radio resource in order to allow the data transmission of the MTC device. Note that the PRD-RNTI is allocated to only one device during a given polling window. Standard system resource allocation mechanisms can be used without any risk of collision. This procedure is illustrated in Fig. 5.5.

5.4.3 RNTI allocation algorithm

Algorithm 1 serves for allocating resource such as PRD-RNTI and phase value (refers to a series of polling windows) for each registered device. Some notations about our algorithm: the eNB provides N different polling periods denoted by T_n, where $n = 0, 1, ..., N-1$

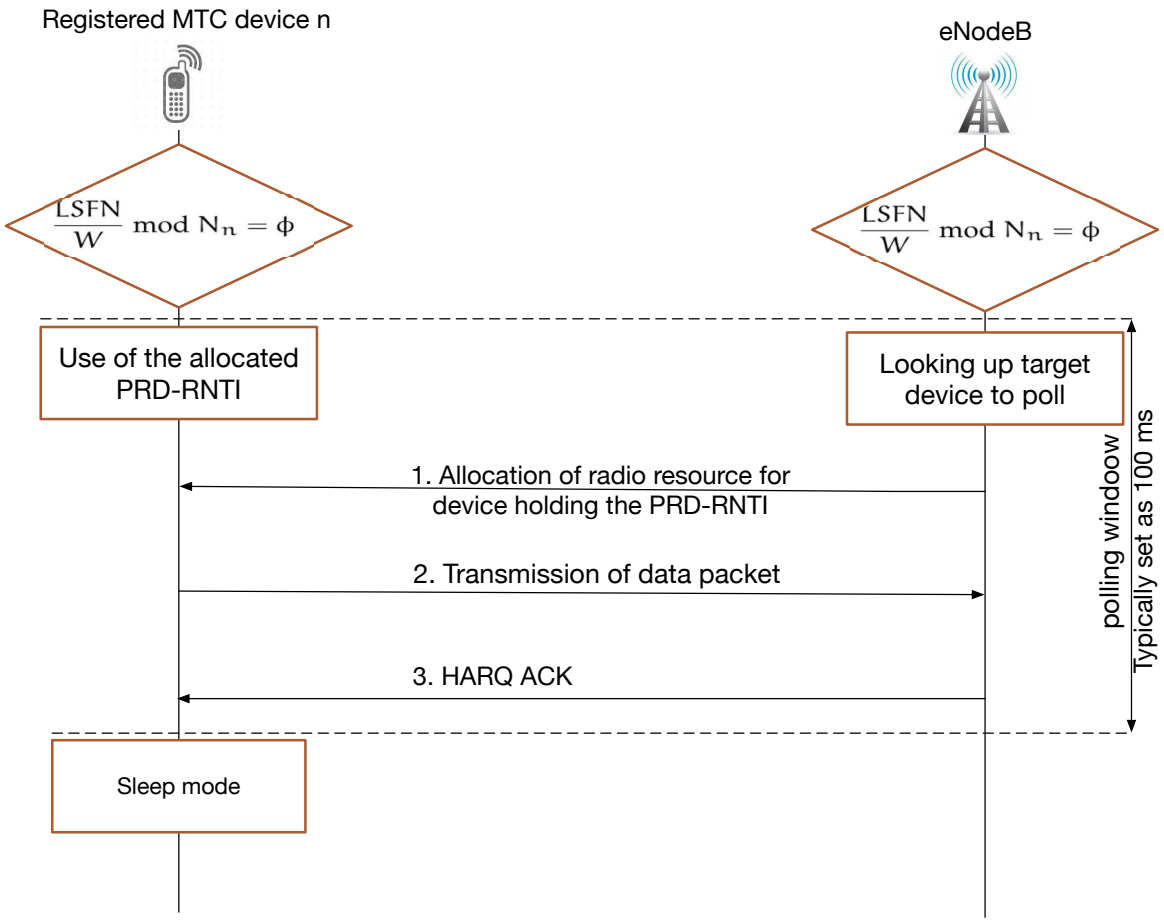

Fig. 5.5 Proposed polling service work flow

and $T_n = 2T_{n-1}$. The number of polling windows in polling period T_n is denoted by N_n. All devices are regrouped into N groups according to polling periods with ascending order. The number of devices waiting for polling window allocation in group n is denoted by g_n. Each PRD-RNTI provides a limited number of polling windows. The cardinality of available polling windows set when allocating for devices in group i is denoted by $C_{PRD-RNTI,i}$. When there are no available polling windows, a new PRD-RNTI should be taken from PRD-RNTI set. The Algorithm 1 first takes an available PRD-RNTI and initiates $C_{PRD-RNTI,0}$ as N_0. A loop structure from line 4 to 18 is used to process all requests on the basis of group. In iteration i for phase value allocation of group i, algorithm first calculates available polling windows $C_{PRD-RNTI,i}$ by a recursive relation $C_{PRD-RNTI,i} = 2C_{PRD-RNTI,i-1}$, since the number of polling window contained in a polling period $N_i = 2N_{i-1}$. If the number of devices remaining to be processed is still more than 0, algorithm enters in while-loop (line 8 to 17) for allocating each device a polling window. In this while-loop, first check if it

needs take a new PRD-RNTI. Then the algorithm calculates the allocated phase value ϕ for $\min(g_i, C_{PRD-RNTI,i})$ devices then updates $C_{PRD-RNTI,i}$ and g_i.

Algorithm 1 RNTI allocation algorithm

procedure ALLOCATION($g_0, g_1, g_2, ..., g_N$)
  $PRD-RNTI \leftarrow pop\ PRD-RNTI\ set$
  $C_{PRD-RNTI,0} \leftarrow N_0$
  for $i = 0; i < N; i++$ **do**
    if $i > 0$ **then**
      $C_{PRD-RNTI,i} \leftarrow 2C_{PRD-RNTI,i-1}$
    end if
    while $g_i > 0$ **do**
      if $C_{PRD-RNTI,i} = 0$ **then**
        $PRD-RNTI \leftarrow pop\ PRD-RNTI\ set$
      end if
      for $j = 0; j < min(g_i, C_{PRD-RNTI,i}); j++$ **do**
        $\phi_j \leftarrow \lfloor \frac{LSFN}{W} \rfloor \mod N_n$
      end for
      $C_{PRD-RNTI,i} \leftarrow C_{PRD-RNTI,i} - \min(g_i, C_{PRD-RNTI,i})$
      $g_i \leftarrow g_i - \min(g_i, C_{PRD-RNTI,i})$
    end while
  end for
end procedure

5.4.4 An example

Let take an example to illustrate the proposed RNTI allocation algorithm. Supposing an eNB supports 4 different polling periods whose notations are $T_0 = 4T_s, T_1 = 8T_s, T_2 = 16T_s, T_3 = 32T_s$, T_s is duration of a polling window. All devices are regrouped into four groups $0, 1, 2, 3$. Each group consists of two devices so $g_0 = 2, g_1 = 2, g_2 = 2, g_3 = 2$ and each device is respectively identified as $a_0, a_1, b_0, b_1, c_0, c_1, d_0, d_1$. To allocate polling window for these devices, first take value $FFF4$ from PRD-RNTI set. For group 0 with polling period $4T_s$, the available polling windows is $N_0 = 4$. Allocate respectively polling windows satisfying $\phi_{a_0} = 0, \phi_{a_1} = 1$ for a_0, a_1. Since there are just two devices to be served in group 0, it still remains 2 polling windows after allocation. Then for group 1, at this time available polling window number is 4 , polling windows that satisfy $\phi_{b_0} = 2, \phi_{b_1} = 3$ are respectively allocated to b_0, b_1. So after allocation for group 1, $C_{PRD-RNTI,i=1}$ is updated as 2. With the same philosophy, allocation is done for groupes $2, 3$. The RNTI and phase value allocation result is shown in Fig.5.6 and resumed in Tab. 5.1.

Table 5.1 Polling window allocation resume

group name	number of device	identity	polling period	phase value
0	2	$4T_s$	a_0	0
			a_1	1
1	2	$8T_s$	b_0	2
			b_1	3
2	2	$16T_s$	c_0	6
			c_1	7
3	2	$32T_s$	d_0	14
			d_1	15

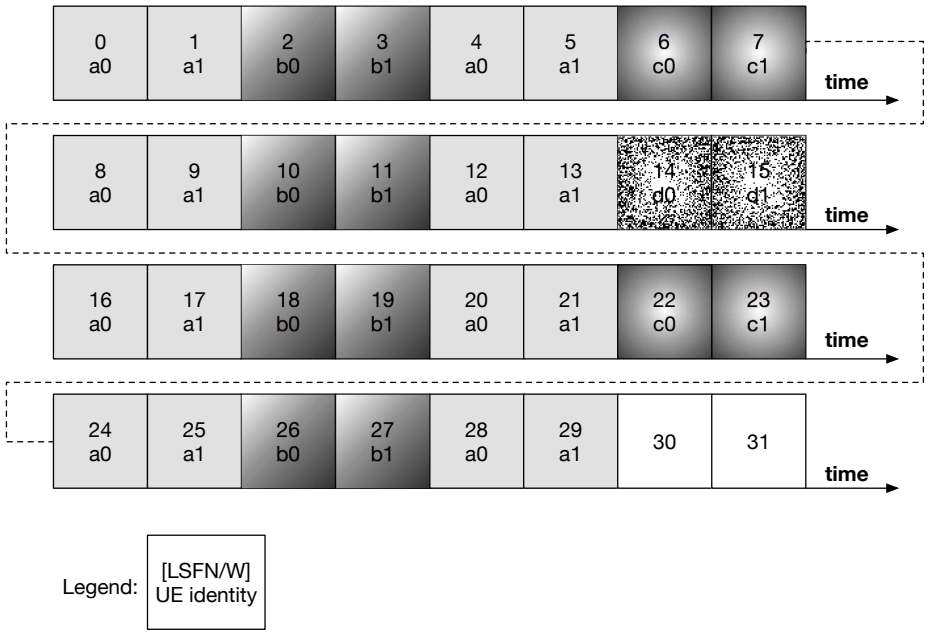

Fig. 5.6 Illustration of RNTI allocation result

5.5 Performance Analysis

A comparative performance analysis between traditional LTE random access and our proposal (network integrated M2M-orientated polling service) is presented in this section. We focus on the consumption of Resource Block (RB) (used for data transmission and signaling) and the minimum number of RNTI, for both methods.

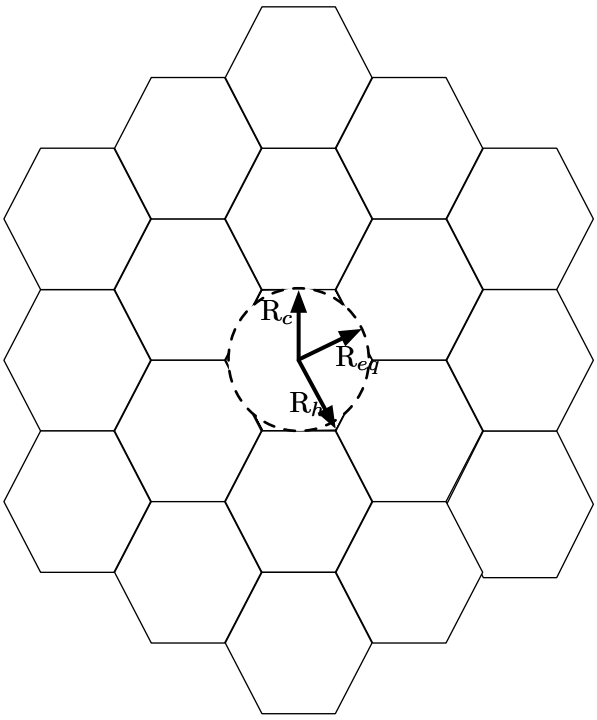

Fig. 5.7 The studied hexagonal grid network topology

5.5.1 System model

We consider a regular hexagonal network whose topology is illustrated in Fig. 5.7, where R_h refers to the hexagonal radius and R_c denotes the half distance between two adjacent eNBs. We assume that all the eNBs have omnidirectional antenna so that each eNB covers a single cell. All eNB transmit with the same power.

The amount of MTC devices served by each eNB, denoted by N_d, is assumed to be very large. These devices are static and periodically sending data to remote servers. The device reporting period T is assumed to be a random variable whose distribution can be of any type. To reduce the reporting collision rate, the report moment for each device is chosen uniformly between time interval $[0,T]$.

Fractional power control is taken into account in this model. The path-loss is partially compensated by the power control scheme. The power compensation factor is denoted by α. Okumura-Hata model [130] is applied to model the propagation attenuation. Fading and shadowing are assumed to be averaged out. Thus, the received power can be expressed as follows:

$$P_r = \rho \left[K \left(\frac{1}{r} \right)^{\gamma} \right]^{1-\alpha} \tag{5.3}$$

where ρ is target received power, r is the distance between the receiver and the transmitter, where K is a unitless constant which depends on the antenna characteristics and the average channel attenuation, γ is the path loss exponent. Note that all the eNB transmit with the same power without applying power control, hence for downlink transmission, $\alpha = 0$. For uplink transmission, and α varies between $[0, 1]$.

In fact, performance analysis for a regular hexagonal grid network has no closed form expressions, however, such networks can be well approximated by the fluid model proposed in [136] (circle in discontinuous lines in Fig. 5.7). The key idea of such a model consists in replacing a given fixed finite number of interfering sources by an equivalent continuum of transmitters. For example, when analyzing downlink interference, a limited area hexagonal network, which has a fixed number of eNB, now can be approximately replaced by a network with eNB density ρ_m.These eNBs are spatially uniformly distributed in the network. The eNB density ρ_m is the ratio between the number of eNB and the network coverage area.

5.5.2 Lower bound of RNTI Consumption

Let $C_{\min}$ be the low bound of RNTI required in the coverage zone of an eNB.

5.5.2.1 Our proposal

In a system with our proposed multiple period polling service, the number of occupied RNTI (i.e. PRD-RNTI) depends on the amount of device N_d served by the eNB and polling period.

Recall that eNB provides M available polling periods. The polling period is denoted by T_n, where $T_n = 2^n \cdot W \cdot T_f$. The number of devices with the same polling period is denoted by g_n. For polling period T_n, there exist 2^n available polling windows. Thus with g_n device, it needs at least $\frac{g_n}{2^n}$ RNTI to satisfy all devices. Similarly, it should provide at least C_{min} RNTI satisfying the following formula:

$$C_{\min} = \sum_{n=0}^{M} \frac{g_n}{2^n} \tag{5.4}$$

5.5.2.2 Random access method

Once that RNTI is allocated, it will be occupied within time duration T_{timer}, which is the expiration time of RRC inactivity timer. Let C_{RNTI} be the total occupied RNTI number within T_{timer}.

Lemma 5.5.1. *Given that each MTC device reporting period is T whose distribution can be of any type, the number of deployed devices in a cell is N_d, C_{RNTI} follows distribution and*

its intensity can be approximated by

$$\lambda_{C_{RNTI}} = N_d T_{timer} \mathbb{E}\left[\frac{1}{T}\right], \tag{5.5}$$

Proof. The arguments of the statement that C_{RNTI} approximately follows Poisson distribution are as follows:

- Each MTC device independently chooses a random moment during its reporting period to transmit data.
- The expectation of reporting period T is much larger than duration of random access procedure, thus the probability that one device occupies one RNTI (i.e. transmits a packet) is small.
- A large number of MTC devices are deployed in each eNB coverage area.

Thus, the aggregated traffic of all the deployed MTC devices and the occupied RNTI number, follow a Poisson distribution.

Let $\lambda_{C_{\mathrm{RNTI}}}$ be the intensity of C_{RNTI}. The void probability $\mathbf{P}\{C_{\mathrm{RNTI}} = 0\}$ is thus equal to $\exp(-\lambda_{C_{\mathrm{RNTI}}})$, which allows to estimate $\lambda_{C_{\mathrm{RNTI}}}$. Recall that N_d is the amount of M2M devices deployed in each cell. Hence, the locations of M2M devices form a Binomial Point Process (BPP). Given that N_d is large enough, the locations of devices can be well approximated by a two-dimensional Poisson Point Process Φ_m with spatial intensity $\lambda_m = N_d/\pi R_{eq}^2$ (refer to Fig. 5.7).

Consider a given M2M device with index i. Its reporting period is T_i. The probability p that one RNTI is occupied by this device is T_{timer}/T_i. The void probability is thus:

$$\mathbf{P}\{C_{\mathrm{RNTI}} = 0\} = \mathbb{E}\left[\prod_{r_i \in \Phi_m} 1 - \frac{T_{\mathrm{timer}}}{T_i}\right], \tag{5.6}$$

where r_i refers to the distance between the considered device and the eNB located at the origin, T_i is a random variable whose distribution is unknown. The subscript i can be omitted

for the sake of readability. According to Campbell theory, (5.6) can be further simplified:

$$\begin{aligned}\mathbf{P}\{C_{\text{RNTI}}=0\} &= \mathbb{E}_{\Phi_m}\left[\prod_{r\in\Phi_m}\mathbb{E}_T\left[1-\frac{T_{\text{timer}}}{T}\right]\right]\\ &= \exp\left\{-\mathbb{E}_T\left[\int_0^{R_{eq}}\frac{T_{\text{timer}}}{T}2\pi r\lambda_m dr\right]\right\}\\ &= \exp\left\{-\lambda_m\pi R_{eq}^2 T_{\text{timer}}\mathbb{E}_T\left[\frac{1}{T}\right]\right\}\\ &= \exp\left\{-N_d T_{\text{timer}}\mathbb{E}_T\left[\frac{1}{T}\right]\right\}. \end{aligned} \tag{5.7}$$

From (5.7), we deduce that the average of C_{RNTI}, i.e., the intensity of corresponding Poisson distribution, is:

$$\lambda_{C_{\text{RNTI}}} = N_d T_{\text{timer}}\mathbb{E}\left[\frac{1}{T}\right], \tag{5.8}$$

□

Recall that C_{RNTI} follows poisson distribution, the minimum number of RNTI required C_{min} should satisfy the probability where C_{RNTI} is less than C_{min} is greater than a predefined threshold, for example 0.99. Thus, the low bound of required RNTI C_{min} can be calculated as follows:

$$\begin{aligned}C_{\text{min}} &= \min\{\mathbf{P}\{C_{RNTI} < C_{min}\} \geq \text{Threshold}\}\\ &= \min\left\{X : \sum_{n=0}^{X}\frac{\lambda^n}{n!}e^{-\lambda} \geq \text{Threshold}\right\}\end{aligned} \tag{5.9}$$

5.5.3 Resource Blocks Consumption

RB consumption is analyzed for message transmission from step.3 to step 10 in Fig. 5.2. The cases of downlink and uplink transmission are separately considered within the approximated fluid model, because the interference analysis is different for uplink and downlink. Since M2M application is uplink-centric, the packet transmission in the uplink convey both collected data and signaling messages, while the transmission in the downlink only contains signaling. It should be noted that just RRC layer signaling messages is considered. Signaling related to control information related to RB allocations are ignored.

Let L be the message size (at MAC layer) to be transmitted. We assume that the considered message should be transmitted within unit Transmission Time Interval (TTI, 1 ms

Table 5.2 Transport block size with respect to TBS index and number of RB pair. Source: [18, Tab. 7.1.7.2.1-1]

I_{TBS}	N_{RB}											
	1	2	3	4	5	6	7	8	9	10	⋯	100
0	16	32	56	88	120	152	176	208	224	256	⋯	2992
1	24	56	88	144	176	208	224	256	328	344	⋯	3624
2	32	72	144	176	208	256	296	328	376	424	⋯	4584
3	40	104	176	208	256	328	392	440	504	568	⋯	5736
4	56	120	208	256	328	408	488	552	632	696	⋯	7224
⋯	⋯	⋯	⋯	⋯	⋯	⋯	⋯	⋯	⋯	⋯	⋯	⋯
26	712	1480	2216	2984	3752	4392	5160	5992	6712	7480	⋯	75376

in LTE). Let $N_{\text{RB}}(L)$ be the number of RB pairs required to satisfy this requirement. We evaluate the average number of RB pairs $\overline{N_{\text{RB}}}(L)$ with which a given device can transmit this message within unit TTI in a hexagonal cell.

Since $N_{\text{RB}}(L)$ depends on the transport block size (TBS) that one pair of RB can support. TBS itself is determined by the modulation coding scheme (MCS) that the device chooses. We assume that the device always selects the MCS which carries the most bits. The MCS (indicated by TBS index) and TBS are given in Tab. 5.2. We assume that the TBS and the number of RB pair have a linear relationship, thus we take the second column in Tab. 5.2 to calculate the capacity per RB pair.

5.5.3.1 Downlink Resource Block Consumption

Given that one message should be transmitted within one TTI, the downlink data rate should be greater than a threshold and there exists a minimum SINR requirement so that a given MCS can be used. Recall that the channel gain only depends on the distance between receiver and transmitter r (fading and shadowing are averaged out), SNR Θ is a function with respect to r. Thus, the problem comes down to how to calculate the SNR threshold for each MCS and find the function between Θ and r.

We use a modified Shannon formula adjusted by simulation results proposed in [137]. This formula is as follows:

$$S = \beta B \eta \log_2 \left(1 + \frac{\Theta}{\Theta_{\text{ref}}}\right), \tag{5.10}$$

where S (with unit of bits per second) is the date rate, β adjusts for the system bandwidth (BW) efficiency of LTE , Θ_{ref} adjusts for the SNR implementation efficiency of LTE. Param-

eter B refers to the RB bandwidth, Θ is the received SNR. The factor η is a correction factor. By inversing (5.10), we obtain the SNR threshold with respect to the data rate as follows:

$$\Theta = \Theta_{\text{ref}} \left(2^{\frac{S}{\beta B \eta}} - 1 \right). \tag{5.11}$$

In terms of downlink SNR, due to scheduling algorithm and OFDMA multiplexing, the eNB during a given TTI only transmits to a certain device. Thus, there is no intra-cell interference. The interfering sources are other transmitting eNB. Actually, no closed form expression between SNR and distance is available in the case of hexagonal cell. However, we can use one approximated expression with high accuracy in a fluid model. Proposed in [136], SNR Θ can be expressed as follows:

$$\Theta = \frac{\gamma - 2}{2\pi \rho_{\text{eNB}} r^{\gamma}} (2R_c - r)^{\gamma - 2}, \tag{5.12}$$

where ρ_{eNB} is the eNB density in the fluid model, R_c is the half intersite distance in the fluid model, γ is the path-loss exponent.

To approximate the hexagonal network by a fluid model, according to [136], with substitution $\rho_{\text{eNB}} = 2/(3\sqrt{3}R_h^2)$, $R = \sqrt{3}R_h/2$ into (5.12), we have:

$$\begin{aligned} \Theta &= \frac{\sqrt{3}(\gamma - 2)}{4\pi} \frac{(1 - \frac{r}{\sqrt{3}R_h})^{\gamma - 2}}{(\frac{r}{\sqrt{3}R_h})^{\gamma}}, \\ &= \frac{\sqrt{3}(\gamma - 2)}{4\pi} \frac{(1 - \sqrt{\frac{\sqrt{3}}{2\pi}} \frac{r}{R_{eq}})^{\gamma - 2}}{(\sqrt{\frac{\sqrt{3}}{2\pi}} \frac{r}{R_{eq}})^{\gamma}}, \end{aligned} \tag{5.13}$$

From (5.13), we deduce that N_{RB} is a function of L and $\frac{r}{R_{eq}}$, denoted as $N_{\text{RB}}(L, \frac{r}{R_{eq}})$.

Numerically inversing (5.13) with SNR threshold obtained via (5.11), we obtain the maximum distance to cell center that one device can be located if it needs to satisfy the SNR threshold. Combing MCS and TBS mapping table, the coverage area of a eNB can be divided into a series of M rings in which the device can use the same amount of RBs. Hence, $N_{\text{RB}}(L, \frac{r}{R_{eq}})$ is a increasing step function with respect to relative location $\frac{r}{R_{eq}}$ if L is given.

Now we integrate $N_{\text{RB}}(L, r/R_h)$ on a disk cell with radius R_{eq} equivalent to a hexagonal one to obtain the average number of RB pair consumption $\overline{N_{\text{RB}}}(L)$. The area of a cell is $1/\rho_{\text{eNB}} = \pi R_{eq}^2$ with $R_{eq} = R_c\sqrt{2\sqrt{3}/\pi} = R_h\sqrt{3\sqrt{3}/(2\pi)}$. As the eNBs are uniformly distributed over the equivalent disk, the probability density (PDF) of r is: $f_r(x) = 2x/R_{eq}^2, x \in$

$[0, R_{eq}]$. Hence, $\overline{N_{\mathrm{RB}}}(L)$ can be expressed as follow:

$$\begin{aligned}\overline{N_{\mathrm{RB}}}(L) &= \int_0^{R_{eq}} N_{\mathrm{RB}}(L, \frac{r}{R_{eq}}) \frac{2r}{R_{eq}^2} dr \\ &= \int_0^{R_{eq}} N_{\mathrm{RB}}(L, \frac{r}{R_{eq}}) d(\frac{r}{R_{eq}})^2, \end{aligned} \tag{5.14}$$

Recall that $N_{\mathrm{RB}}(L, \frac{r}{R_{eq}})$ is a step function that can be written as M linear combination of indicator functions of intervals. Let $N_{\mathrm{RB}}(L, \frac{r}{R_{eq}}, i)$ be the possible discrete values, $\left(\frac{r}{R_{eq}}\right)_{\mathrm{u,i}}$ and $\left(\frac{r}{R_{eq}}\right)_{\mathrm{l,i}}$ be the upper and low bound of interval with index $i, i = 0, 1, ..., M-1$. Thus, integral in (5.14) can be further written as follows:

$$\overline{N_{\mathrm{RB}}}(L) = \sum_{i=0}^{M} N_{\mathrm{RB}}(L, \frac{r}{R_{eq}}, i) \left[\left(\frac{r}{R_{eq}}\right)_{\mathrm{u,i}}^2 - \left(\frac{r}{R_{eq}}\right)_{\mathrm{l,i}}^2 \right], \tag{5.15}$$

5.5.3.2 Uplink Resource Block Consumption

Similar methodology presented in previous section can be applied to estimate the average number of RB pairs consumption for packet transmission in the uplink direction. The only difference relies in that function between SNR received at the eNB Θ_{uplink} and distance r between device and eNB is different from (5.13), since the fractional power control is taken into account in the uplink channel.

Due to the packet scheduling algorithms and SC-FDMA multiplexing, within a given TTI, only one device is transmitting to its attached eNB. The interfering sources are those transmitting devices in other cells and internal interference is null. Thus, the device density in the fluid model ρ_m is identical to that of eNB. In reference [138], uplink interference analysis with fractional power control in LTE network is conducted within fluid model. The SNR expression for the uplink is as follows:

$$\Theta_{\mathrm{uplink}} = \frac{r^{-\gamma(1-\alpha)}}{2\pi\rho_m \sum_{n=1}^{\infty} (2nR_c)^{\alpha\gamma+2-\gamma} I_n(\alpha, \gamma)}, \tag{5.16}$$

where γ is the path loss exponent, R_c is the half inter-site distance, α is the power compensation factor that is adjusted between $[0, 1]$, $I_n(\alpha, \gamma) = \int_0^{\frac{1}{2n}} x^{\alpha\gamma} \left[(1-x)^{1-\gamma} + (1+x)^{1-\gamma}\right] dx$.

To approximate the hexagonal network by a fluid model, with substitution $\rho_m = 2/(3\sqrt{3}R_h^2)$, $R_c = \sqrt{3}R_h/2$ into (5.16), we have:

$$\Theta_{\text{uplink}} = \frac{\sqrt{3}(\sqrt{\frac{\sqrt{3}}{2\pi}}\frac{r}{R_{eq}})^{-\gamma(1-\alpha)}}{4\pi\sum_{n=1}^{\infty} n^{\alpha\gamma+2-\gamma} I_n(\alpha,\gamma)}. \tag{5.17}$$

From (5.11), (5.17) and TBS and MCS mapping table, we can get the step function $N_{\text{RB}}(L,v)$ for uplink data transmission, and use (5.15) to calculate average value.

5.5.4 Uplink Energy efficiency ratio

The uplink energy efficiency is defined as the ratio between the data packet size (at MAC layer) and the consumed energy during a uplink reporting procedure. Note that the consumed energy is composed by two parts: consumption by uplink signaling messages and data packet. Let $\overline{EE}_{\text{con}}$ and $\overline{EE}_{\text{polling}}$ respectively be the energy efficiency for the conventional mechanism in LTE and energy efficiency of our proposal.

For the case of conventional mechanism, N_s refers to the the total number of uplink messages to delivery one packet. Let L_0 be the data packet size of interest, and $L_j, j = 1,...,N_s-1$ be the size of uplink signaling messages j involved in this data packet transmission.

For a packet L_j, given that data rate is given by (5.10) and the occupied pair number of RB is $N_{\text{RB}}(L_j, r/R_{eq})$. Due to the fractional power control, the transmit power on one single pair of RB is the production of the target received power ρ and $\left[K^{-1}r^{\gamma}\right]^{\alpha}$. Thus using conventional mechanism, the energy efficiency for a device with distance r to its eNB is:

$$\text{EE}_{\text{con}} = L_0 / \left[\sum_{j=0}^{N_s} N_{\text{RB}}(L_j, r/R_{eq}) \frac{\rho(K^{-1}r^{\gamma})^{\alpha} L_j}{\beta B\eta \log_2\left(1+\frac{\Theta}{\Theta_{\text{ref}}}\right)}\right] \tag{5.18}$$

Average on the disk cell, the average energy efficiency $\overline{\text{EE}}_{\text{con}}$ is:

$$\overline{EE}_{\text{con}} = \int_0^{R_{eq}} L_0 / \left[\sum_{j=0}^{N_s} N_{\text{RB}}(L_j, r/R_{eq}) \frac{\rho(K^{-1}r^{\gamma})^{\alpha} L_j}{\beta B\eta \log_2\left(1+\frac{\Theta}{\Theta_{\text{ref}}}\right)}\right] \frac{2r}{R_{eq}^2} dr \tag{5.19}$$

Table 5.3 Parameter Values for Numerical Results

Parameter Name	Parameter Notation	Value
Reporting period	T	1 min, 24 hours
Polling window	W	10
RRC inactivity timer	T_{timer}	10 seconds
LTE frame duration	T_f	10 ms
Path-loss exponent	γ	4.0
Power compensation factor	α	0.1
RB bandwidth	B	180 KHz
Bandwidth efficiency	β	0.83
SNR efficiency	θ_{ref}	1.25
Correction factor	η	1.0
Number of served devices eNB	N_d	$20000, 30000, ..., 50000$

As to our proposal, the number of uplink signaling messages is 0. From (5.19), $\overline{\text{EE}}_{\text{polling}}$ is obtained by letting $N_s = 1$:

$$\overline{EE}_{\text{polling}} = \int_0^{R_{eq}} 1/\left[N_{\text{RB}}(L_0, r/R_{eq}) \frac{\rho (K^{-1} r^{\gamma})^{\alpha}}{\beta B \eta \log_2 \left(1 + \frac{\Theta}{\Theta_{\text{ref}}}\right)} \right] \frac{2r}{R_{eq}^2} dr \tag{5.20}$$

From (5.19) and (5.20), we obtain the uplink energy efficiency ratio via numerical integration.

5.6 Numerical results and Discussions

We conduct a numerical analysis to compare the proposed service and conventional mechanism. The LTE system total bandwidth is assumed to be 10 MHz. Since there is no consensus about distribution of reporting period T, we thus assume that T is distributed between 1 min and 24 hours. The number of LTE frames W contained in A polling window is set as 10. RRC inactivity timer is set as 10 seconds. For parameters used in (5.10): bandwidth efficiency β, SNR efficiency Θ_{ref}, correction factor η, they are respectively set as 0.83, 1.25, 1, as in reference [137]. The power compensation factor α is 0.1. The values of aforementioned system parameters are resumed in Tab. 5.3.

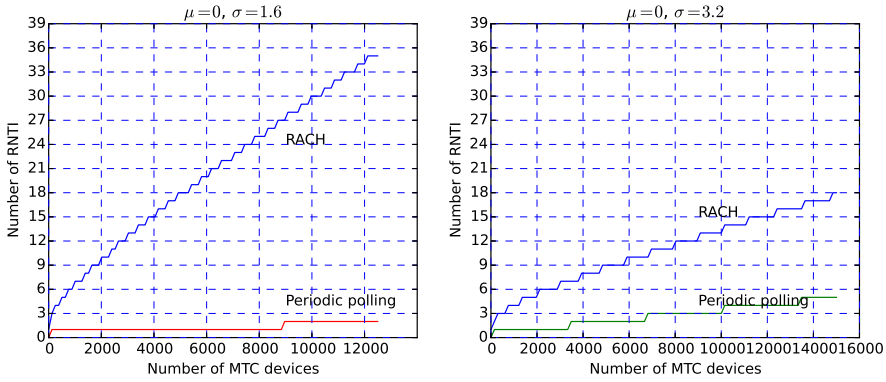

Fig. 5.8 Comparison of RNTI required for case of log-normal distribution

5.6.1 RNTI consumption

5.6.1.1 Log-normal distribution

We suppose that logarithm of user-defined reporting period T (unit of hour), namely $\ln T$, is a random variable respecting normal distribution $N(\mu, \sigma^2)$. The mean of $\ln T$ is 0. The probability of T in interval from 1 min to 24 hours is greater than 68.27% and less than 95%. Thus, we take 0 for μ and σ should be in range $[1.6, 3.2]$. To reduce complexity of problem, we make some approximation when estimating the mean of T: regarding all reporting periods less than 1 min as 1 min and all periods great than 24 hours as 24 hours. Supposing number of LTE frame in a single polling window W is set as 10. To cover the range from 1 min to 24 hours, the minimum supported polling period in our proposal is set as 51.2 sec and the maximum supported polling period as 104857.6 sec , almost 29.13 hours. According to Eq.5.1, the supported polling period list is 51.2 sec, 102.4 sec, 204.8 sec, 409.6 sec, ..., 52428.8 sec, 104857.6 sec. Polling period T_n is thus a discrete random variable. Given distribution of each polling period and total MTC device in system model, the consumption of PRD-RNTI in RACH and periodic polling case could be estimated by formula 5.4 and 5.9. Two cases where $\mu = 0, \sigma = 1.6$ and $\mu = 0, \sigma = 3.2$ are shown in Fig.5.8.

5.6.1.2 Uniform distribution

We suppose in this case that the user-defined reporting period T respects uniform distribution between 1 min and 24 hours. Obviously the mean of T is equal to 12 hours. Given total device number and the repartition of each polling period it is not difficult to get the probability distribution for each eNB supported polling period and estimate device repartition, and

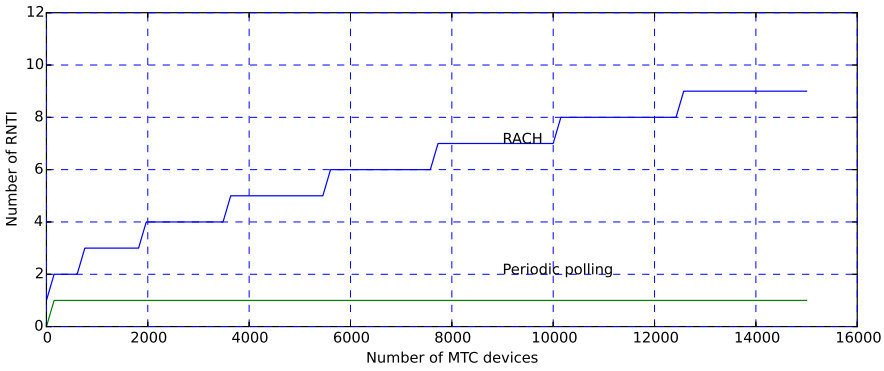

Fig. 5.9 Comparison of RNTI required for case of uniform distribution

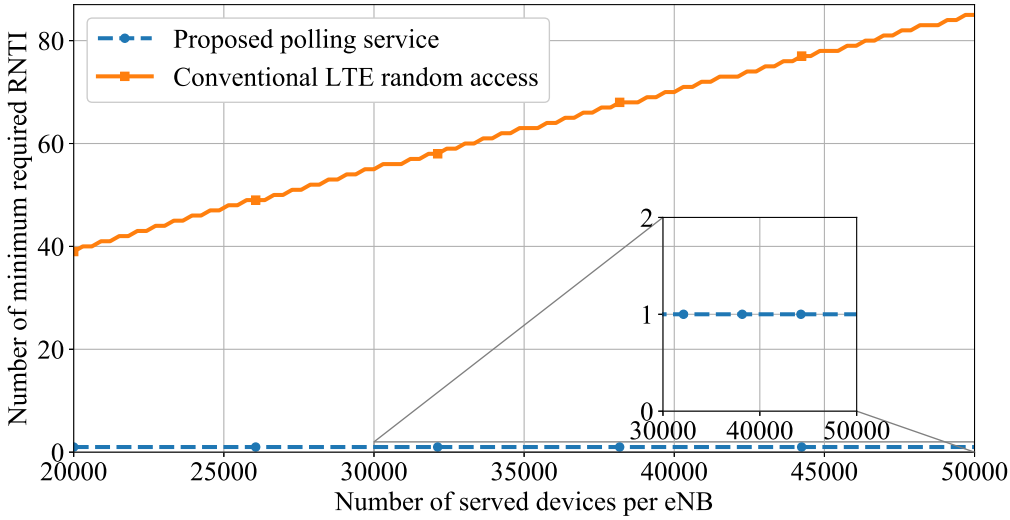

Fig. 5.10 Comparison of RNTI required for the traffic model proposed by 3GPP

further estimate the minimum required RNTI for both case according to formula (5.4) and (5.9). The comparison result is shown in Fig.5.9.

5.6.1.3 Traffic Model [6, Annex E]

In [6, Annex E], 3GPP gives a device reporting distribution to study the performance of MTC over cellular networks. It is assumed that inter-arrival time periodicity for MAR periodic is: 1 day (40%), 2 hours (40%), 1 hour (15%), and 30 minutes (5%).

To cover the range from 30 minutes to 24 hours, According to Eq. (5.1), the supported polling period list is 1638.4, 3276.8, 6553.6, 13107.2, 26214.4, 52428.8, 104857.6. The RNTI consumption of two methods within such a traffic model is illustrated in Fig. 5.10.

From Fig. 5.8, Fig. 5.9 and Fig. 5.10, we confirm that the distribution of reporting period T has a significant impact on RNTI consumption. For distribution that spreads out over the reporting range, such as uniform distribution, the RNTI consumption economization compared to the conventional LTE random access is smaller than in case where distribution is centered such as truncated lognormal distribution.

5.6.2 Resource Block Pairs Consumption

To get the exact RRC messages payload size, we do a realistic experiment to capture the exchange traffic between a UE and eNB. The economized bytes number, in uplink and downlink, are resumed in Table. 5.4. The bytes related to security and integrity are ignored. The PDCP protocol header occupies 1 bytes, RLC header occupies 1 bytes. The header of MAC layer is a little complicated. Normaly MAC header takes 2 bytes, however, before contention resolution stage, the MAC layer should contain a random number as temporary UE identifier (6 bytes) and an associated subheader (1 bytes).

The size of data packet application layer payload is assumed to follow a truncated Pareto distribution with shape parameter 2.5. The application payload size range is $[20, 200]$ (unit bytes) , and packet header size is 29 bytes [6, Annex E]. Thus, we assume that total data packet size varies in the interval of $[50, 230]$ bytes.

Table 5.4 RRC messages exchanged between UE and the eNB (unit: bit)

RRC Message Name	Payload Size	MAC Header	RLC Header	PDCP Header	Downlink	Uplink
ConnectionSetupRequest	48	72	8	8		136
ConnectionSetup	320	72	8	8	408	
ConnnectionSetupComplete	56	16	8	8		88
ConnectionReconfiguration	632	16	8	8	664	
ConnectionReconfigurationComplete	16	16	8	8		48
ConnectionRelease	16	16	8	8	48	
Economized Bytes Number					1120	272

5.6.2.1 Downlink RB pairs consumption

Only signaling messages consume RB in the downlink. We take the message RRC *ConnectionReconfiguration* as example, to estimate the average amount of RB pairs are consumed within one TTI for the downlink channel in a hexagonal cell.

The information of transport block size that one pair of RB can carry and their corresponding TBS index is taken from [18, Tab. 7.1.7.2.1-1] and placed into the left two

Table 5.5 SNR threshold and distance for message *ConnectionReconfiguration*

TBS Index	TBS (unit: bits)	SINR Threshold (in decimal)	Maximum relative distance	Number of RB Pairs
4	60	0.40	1.000	12
5	72	0.50	0.983	10
6	88	0.63	0.948	8
7	112	0.85	0.904	6
8	128	1.01	0.878	6
9	148	1.23	0.850	5
10	164	1.43	0.829	5
11	188	1.74	0.801	4
12	220	2.22	0.767	4
13	244	2.63	0.744	3
14	276	3.25	0.716	3
15	300	3.78	0.696	3
16	316	4.17	0.684	3
17	348	5.03	0.659	2
18	388	6.31	0.631	2
19	420	7.52	0.610	2
20	452	8.93	0.590	2
21	500	11.47	0.561	2
22	532	13.50	0.543	2
23	564	15.86	0.525	2
24	596	18.60	0.508	2
25	628	21.78	0.492	2
26	740	37.47	0.438	1

columns in Tab. 5.5. The SNR threshold and the corresponding maximum relative distance, respectively obtained from (5.11) and (5.13), are resumed in Tab. 5.5. Since RRC *ConnectionReconfiguration* contains 664 bits (i.e. 83 bytes, resumed in Tab. 5.4), the required number of RB pairs is shown in the right most column of Tab. 5.5).

Aggregating according to the consumed RB pairs number, we obtain Tab. 5.6. According to Tab. 5.6, the relative distance (r/R_{eq}) can be divided into a series of interval in which the eNB consume the same amount of RB. Apply (5.15), the average number of RB pairs, consumed by one device in a hexagonal cell within one TTI to transmit RRC *ConnectionReconfiguration* message, is thus 2.85.

Similar methodology can be used to estimate the RB consumption for other signaling messages: 1.91 pairs of RB for *ConnectionSetup* message, 1.0 pair of RB for *Connection-*

Table 5.6 RB pairs number and relative distance interval for message *ConnectionReconfiguration*

Relative Distance(r/R_{eq}) Interval	RB
$[0.000, 0.438]$	1
$[0.438, 0.659]$	2
$[0.659, 0.744]$	3
$[0.744, 0.801]$	4
$[0.801, 0.850]$	5
$[0.850, 0.904]$	6
$[0.904, 0.948]$	8
$[0.948, 0.983]$	10

Release. In total, the conventional random access requires on average 5.76 pairs of RB for downlink signaling message transmission.

5.6.2.2 Uplink RB pairs consumption

By using similar methodology and (5.15) for uplink signaling RB consumption, we obtain that message *ConnectionSetupRequest* , *ConnectionSetupComplete*, *ConnectionReconfigurationComplete* respectively consumes 1 pairs of RBs. By varying the packet size from 50 bytes to 200 bytes, the RB pairs consumed for data packet can be calculated. The uplink and download signaling overhead (i.e. the ratio between the number of RB used for signaling and for data packet) are obtained and shown in Fig. 5.11. As the packet size increases, the signaling overhead progressively reduces. However, it is known that MTC features with small payload. It is very possible that the number of RB pairs used for signaling is greater than that used for data packet.

We also evaluate the average RB pair consumption per TTI, respectively by uplink, downlink signaling and data transmission. The applied traffic model is the one recommended by 3GPP and detailed in Sec. 5.6.1.3. The result is shown in 5.12. We observe that average RB consumption per TTI is rather small. The reason is that, according to formula (5.8), the equivalent charges in this traffic model is at rather low level and thus occupy just a small of all available RBs.

5.6.3 Uplink Energy Efficiency Ratio

We calculate the energy efficiency for our polling service and conventional LTE random access mechanism. The ratio between two methods are shown in Fig. 5.13. We observe that

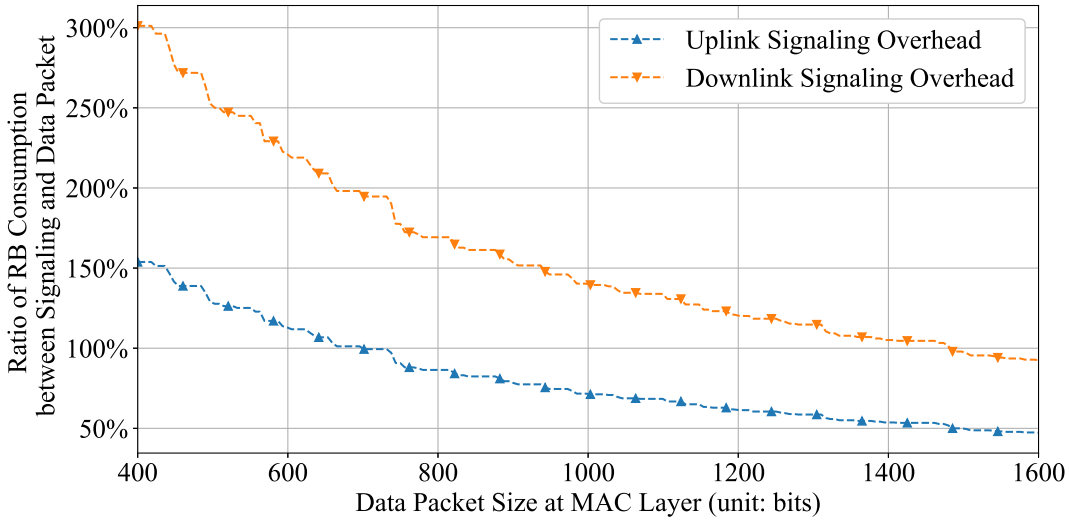

Fig. 5.11 Signaling overhead in terms of consumed RB pair number with respect to uplink reporting packet size

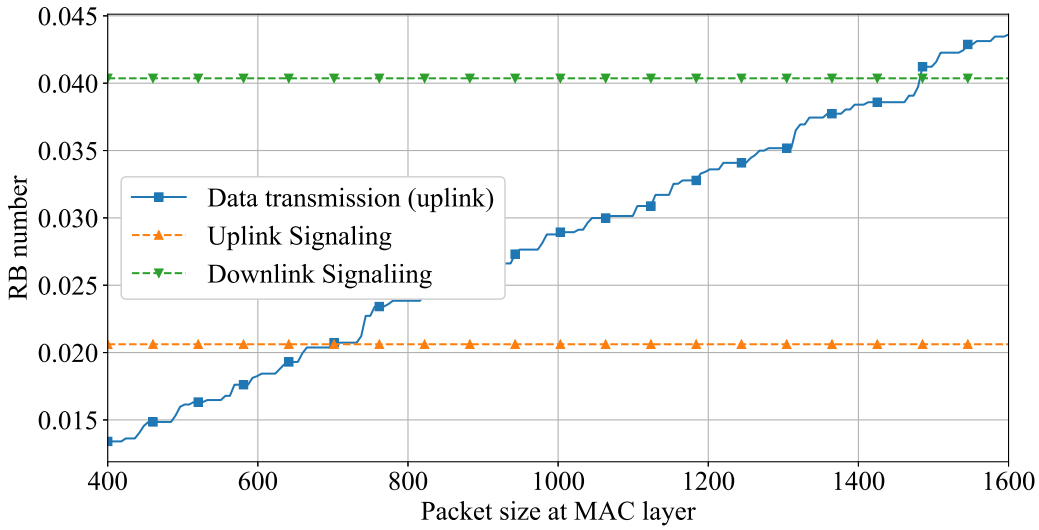

Fig. 5.12 Average RB occupation ratio within a traffic model [6, Annex E]

the energy efficiency of our proposal is at least 1.15 times of that in conventional LTE when data packet size is less than 600 bits, the energy efficiency gain approaches to one with the augmentation of data packet size.

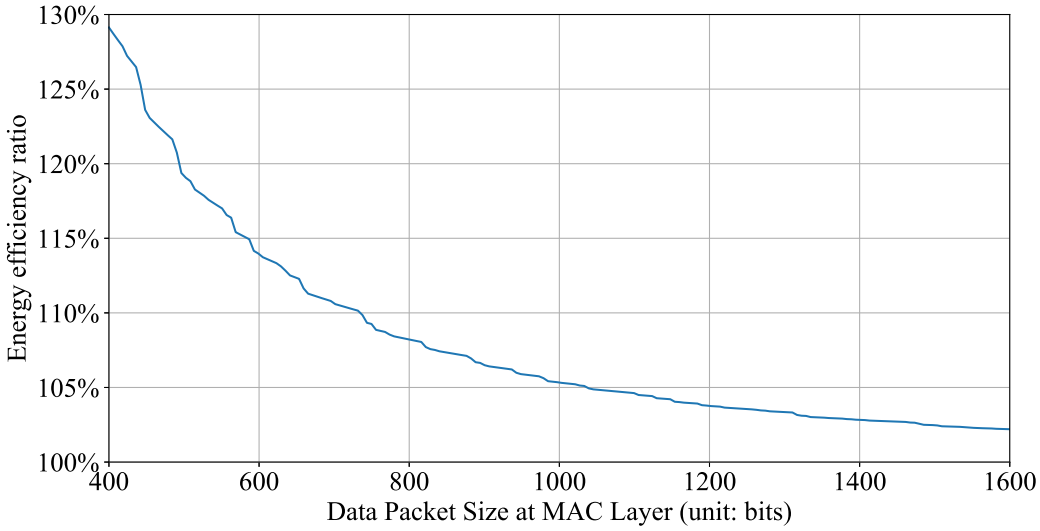

Fig. 5.13 Energy efficiency ratio with respect to uplink reporting packet size

5.7 Summary

In this chapter, we propose a multiple-period polling service, which can can be integrated into LTE radio access network and avoid random access procedure once the registration stage is done.

With our proposal, the RNTI consumption is largely reduced. The reason is that the proposed polling service leverages the periodicity feature exhibited by MTC traffic and make a large number of devices use a same RNTI in a sequential manner. For conventional LTE random access mechanism, a RNTI is occupied until the expiration of RRC inactivity timer. The RNTI economization depends on RRC inactivity timer setting and device reporting period distribution. Due to the lack of statistics about device uplink reporting period, we assume that the latter is in range between 1 minutes and 1 day, and evaluate the RNTI consumption by assuming that the reporting period follows:1) truncated lognormal distribution; 2) uniform distribution.

The proposed polling serve reduces the RB consumption for downlink and uplink. The reason is that RRC signaling messages are not needed within our proposal. By comparing Fig. 5.2 and Fig. 5.5, we observe that the conventional LTE random access mechanism needs to send *RRC ConnectionRequest*, *RRC ConnectionSetupComplete* and *RRC ConnectionReconfigurationComplete* in the uplink, and *RRC ConnectionSetup*, *RRC ConnectionReconfiguration* and *RRC Connection release* in the downlink. The aforementioned signaling size (at MAC layer) are obtained by a realistic measurement and resumed in Table. 5.4. RB

consumption per uplink reporting for downlink and uplink, are respectively 5.76 and 3. By varying the data packet size (at MAC layer) from 50 bytes to 200 bytes, we observe that the signaling overhead is 300% for a reporting packet of size 50 bytes.

In this work, we just consider the radio interface, the effort for reducing signaling overhead in the core network, especially on the S1 interface, can be expected in future work.

Chapter 6

Conclusions and Future Work

In this chapter, we summarize our major contributions and discuss future research directions.

6.1 Major Contributions

The objective of this thesis is study how future wireless networks efficiently handle the massive MTC traffic. The radio access mechanism used in Radio Access Network (RAN) of wireless networks is the main part to satisfy the MTC related requirements such as energy efficiency and thus is the focus of this thesis. The studies have been done from two aspects: performance study and adaption to widely deployed LTE networks. The meaning of performance evaluation study lies in that they can give the scientific community the networks design guidelines satisfying MTC special requirements. Concretely, the main contributions can be summarized as follows:

6.1.1 A Survey about energy efficiency for M2M-included wireless networks

In this survey, we provide a global view of the network technologies for M2M in wireless networks. The main contributions of this survey is to review, compare and categorize the proposals related to energy issues of cellular M2M mainly over the period from 2011 to 2016. We also present the development of LPWAN networks. Finally, we observe that the cooperative relaying, the design of energy efficient signaling and operation, the new radio resource allocation schemes, and the energy efficient random access procedure are the main research directions. Besides, it is also necessary and meaningful to leverage mathematical tools, such as game theory, stochastic geometry, etc., for topology-aware modeling, analysis and design of future M2M-included wireless networks.

6.1.2 Performance of transmit power diversity and imperfect power control in S-ALOHA based LPWAN networks

The S-ALOHA (i.e. slotted-ALOHA) protocol is recently regaining interest in the study of Low Power Wide Area Networks (LPWAN). We study the impact of transmit power diversity strategy with imperfect power control to the performance of S-ALOHA based LPWAN. The performance metrics that we care about are packet loss rate, throughput, energy efficiency and average number of transmissions.

To this end, we propose a low complexity but still accurate analytical model, and conduct the analysis for three kinds of networks: ideal networks with perfect power control, wide band systems with imperfect power control and narrow band networks with imperfect power control. The proposed model is able to facilitate the dimensioning and design of S-ALOHA based LPWAN. The comparison between simulation and analytical results confirms the accuracy of the proposed model.

From the established analytical model, we obtain some design guidelines about S-ALOHA based LPWAN. For example, in wide band systems with capture ratio 3 dB, the imperfect power control has a positive impact to identical transmit power diversity strategy but bring negative impact to incremental and decremental strategies. To design a LPWAN system that prefers lower packet loss rate and support more devices, incremental transmit power diversity strategy is a good choice. To design a system that has low latency requirement and has no energy efficiency constraint, decremental diversity strategy is recommended. In narrow band systems that suffer from Rayleigh fading, impact of imperfect power control to the system is slight compared with case of wide band systems. The advantage of decremental strategy in terms of delay is no more significant. Thus, the identical transmit power strategy is the most suitable one.

6.1.3 Performance analysis of macro reception diversity in large-scale ALOHA Network

In cellular networks, the packet is sent in unicast mode: the destination Base Station (BS) is indicated by the terminal. However, it also could be sent in broadcast mode, and benefit from macro reception diversity. Due to its advantages, BS reception diversity has been applied by some LPWAN Networks, such as Sigfox and LoRaWAN [24].

In this work, we first present two possible forms of macro reception diversity: selective combining and maximum ratio combining. Basing on available stochastic geometry research efforts, we then derive the simple closed-form formulas, covering both pure and slotted ALOHA, about network packet loss and spatial throughput. These formulas are very

useful to analyze LPWAN networks (especially in urban areas) and to quantify the gain brought by macro diversity. Through simulations, the accuracy of the proposed model is confirmed. We observe that systems with macro reception diversity can benefit from shadowing effect. With path loss exponent 4, packet loss rate constraint 10% and 8 dB shadowing, the capacity of pure ALOHA with selective combining macro diversity and maximum ratio combining are respectively at least 2 and 3.42 times as much as that in systems in which a device transmits only to the best BS.

Then we extend the study to analyze a new network performance indicator called outage probability that is associated with a target network loss rate. From numerical results, we observe that with 10% outage probability associated with network packet loss rate 10%, selective macro diversity still support 80% of system capacity in case without outage probability constraint, while best BS attach method only achieves 40% of that in case without outage probability constraint.

6.1.4 A periodic polling service in LTE network to support periodic M2M traffic

As a first step, we analyze traditional random access procedure and identify its inefficiency for M2M periodic uplink reporting use case. We then propose a polling service for periodic M2M traffic that avoids access contention. This service can be easily integrated into LTE radio access network, fully compatible with the standard access mechanism and able to manage a large range of polling periods (typically from 1 minute to 28 days). This proposed service reduces the transmission overhead related to signaling and thus improves the energy efficiency for MTC devices. It also reduces access network overload in radio access network by avoiding random access.

Traditional random access mechanism and our proposal are compared in terms of RNTI (Radio Network Temporary Identifier) and RB (Resource Block) consumption. The numerical results show that with the proposed service one eNodeB (eNB) can easily support up to 15000 MTC devices without network access collision. In terms of RB consumption per uplink reporting, our proposal avoids 5.76 pairs of RB consumption for downlink and 3 pairs of RB for uplink.

6.2 Future Works

6.2.1 Optimum transmit power diversity strategy and topology-aware modeling

The performance evaluation about transmit power diversity can be extended from the following directions: First, consider more sophisticated transmit power diversity strategy. We just analyze a simple transmit power diversity strategy in this thesis: the power increment factor is a constant. It would be interesting to consider the case in which the power increment factor is a random variable. The objective is to find the optimum distribution of such a random variable. To solve this problem, it require the mathematical tools such as game theory and convex optimization. Second, conduct the analysis in topology-aware model with stochastic geometry. In this work, we has not taken into account the impact of devices and BS spatial distribution. Using stochastic geometry, we can get a more accurate analysis, especially for energy efficiency evaluation, we can compare the performance in this case with the results presented in this thesis.

6.2.2 Extension of analysis about macro reception diversity

The performance analysis about macro reception diversity can be extended from the following directions: First, consider energy efficiency as performance indicator apart from packet loss rate and spatial throughput. Second, analyze and design more efficient retransmission mechanism. We did not consider the retransmission mechanism with ACK and we observe that the retransmission mechanism used by LPWAN systems without ACK brings negative impact to the system performance. This is due to the spatial distribution of devices. Maybe we can apply the transmit power diversity in LPWAN when design more efficient retransmission mechanism. Third, use more realistic point process for macro reception diversity evaluation. In this these, we just used the elementary point process: homogeneous Point point process (PPP), which has limitation for the performance evaluation of realistic networks. It would be interesting to conduct performance evaluation in more realistic point process such as Hard core point process (HCPP).

6.2.3 Advanced RNTI or radio resource allocation algorithm

In this thesis, we propose a polling service for LTE radio access network. we propose a RNTI allocation algorithm and profit the existing LTE radio resource allocation algorithms. First point that we can extend is to propose more advanced RNTI allocation algorithms. The

presented algorithm is based the power of 2, which is not efficient. One possible research direction is to use graph theory to design a tree-based allocation algorithm. It will also be interesting to design energy efficient radio resource allocation algorithm for M2M. One promising idea is to exploit how to apply the available algorithms about machine learning, deep learning in radio resource allocation field.

References

[1] Q. Song, X. Lagrange, and L. Nuaymi, "Evaluation of macro diversity gain in long range ALOHA networks," *IEEE Communications Letters*, 2017.

[2] Q. Song, X. Lagrange, and L. Nuaymi, "An analytical model for S-ALOHA performance evaluation in M2M networks," in *2017 IEEE International Conference on Communications (ICC)*, pp. 1–7, May 2017.

[3] Q. Song, L. Nuaymi, and X. Lagrange, "Survey of radio resource management issues and proposals for energy-efficient cellular networks that will cover billions of machines," *EURASIP Journal on Wireless Communications and Networking*, vol. 2016, no. 1, pp. 1–20, 2016.

[4] Q. Song, L. Nuaymi, and X. Lagrange, "Evaluation of multiple access strategies with power control error and variable packet length in M2M," in *Wireless Communications and Networking Conference Workshops (WCNCW), 2016 IEEE*, pp. 379–384, IEEE, 2016.

[5] Q. Song, X. Lagrange, and L. Nuaymi, "An efficient M2M-oriented network-integrated multiple-period polling service in LTE network," in *IEEE 82nd Vehicular Technology Conference, VTC Fall 2015, Boston, MA, USA, September 6-9, 2015*, pp. 1–6, 2015.

[6] 3GPP, "Cellular system support for ultra-low complexity and low throughput internet of things (CIoT)," TR 45.820, 3rd Generation Partnership Project (3GPP), Sept. 2015.

[7] Cisco, "Cisco visual networking index: Global mobile data traffic forecast update, 2016–2021," February 2017.

[8] OECD, "Machine-to-machine communications: Connecting billions of devices," *OECD Digital Economy Papers, No. 192*, 2012.

[9] ETSI, "Machine-to-machine communications (M2M); functional architecture," TS 102 690, ETSI, Oct. 2011.

[10] oneM2M, "Functional architecture," Tech. Rep. TS 0001, V.1.6.1, Jan. 2015.

[11] 3GPP, "System improvements for machine-type communications," TS 23.888 V11.0.0, Sept. 2012.

[12] N. Sornin, M. Luis, T. Eirich, and T. Kramp, "LoRaWAN specification," Tech. Rep. V.1.0, LoRa Alliance, Jan. 2015.

[13] Y. Chen and Y. Yang, "Cellular based machine to machine communication with unpeer2peer protocol stacks.," in *VTC Fall*, IEEE, 2009.

[14] 3GPP, "Service requirements for machine-type communications,," TS 22.368 V11.0.0, Dec. 2010.

[15] F. Ghavimi and H.-H. Chen, "M2m communications in 3gpp lte/lte-a networks: Architectures, service requirements, challenges, and applications," *Communications Surveys Tutorials, IEEE*, vol. 17, pp. 525–549, Secondquarter 2015.

[16] Y. Mehmood, C. Görg, M. Muehleisen, and A. Timm-Giel, "Mobile M2M communication architectures, upcoming challenges, applications, and future directions," *EURASIP Journal on Wireless Communications and Networking*, vol. 2015, no. 1, p. 250, 2015.

[17] B. Moyer, "Low power, wide area: A survey of longer-range IoT wireless protocols," 2015. [Online; accessed 13-October-2015].

[18] 3GPP, "LTE;Evolved Universal Terrestrial Radio Access (E-UTRA);Physical layer procedures," TS 36.213, 3rd Generation Partnership Project (3GPP), 04 2015.

[19] 3GPP, "Study on RAN improvements for machine-type communication," TS 37.868 V11.0.0, Dec. 2010.

[20] Ericsson, "More than 50 billion connected devices," white paper, Febrary 2011.

[21] M. Shafiq, L. Ji, and A. L. et al, "A first look at cellular machine-to-machine traffic: Large scale measurement and characterization," *SIGMETRICS Perform. Eval. Rev.*, June 2012.

[22] "Lora Alliance." [Online; accessed 14-October-2015].

[23] R. Ratasuk, N. Mangalvedhe, A. Ghosh, and B. Vejlgaard, "Narrowband LTE-M system for M2M communication," in *Vehicular Technology Conference (VTC Fall), 2014 IEEE 80th*, pp. 1–5, IEEE, 2014.

[24] S. Farrell, "LPWAN Overview," Internet-Draft draft-ietf-lpwan-overview-03, Internet Engineering Task Force, May 2017. Work in Progress.

[25] Y. Chen and W. Wang, "Machine-to-machine communication in LTE-A.," in *VTC Fall*, pp. 1–4, IEEE, 2010.

[26] H. Tullberg, P. Popovski, and et al., "METIS system concept: The shape of 5G to come," in *IEEE Communications Magazine*, 2015.

[27] K. Zheng, F. Hu, and W. W. et al, "Radio resource allocation in LTE-Advanced cellular networks with M2M communications," *Communications Magazine, IEEE*, vol. 50, pp. 184–192, July 2012.

[28] J. N. Al-Karaki and A. E. Kamal, "Routing techniques in wireless sensor networks: a survey," *Wireless communications, IEEE*, vol. 11, no. 6, pp. 6–28, 2004.

[29] J. Costa and G. Miao, "Context-aware machine-to-machine communications," in *INFOCOM Workshops*, April 2014.

[30] L. M. Borges, F. J. Velez, and A. S. Lebres, "Survey on the characterization and classification of wireless sensor network applications," *Communications Surveys & Tutorials, IEEE*, vol. 16, no. 4, pp. 1860–1890, 2014.

[31] R. Ratasuk, J. Tan, and A. Ghosh, "Coverage and capacity analysis for machine type communications in LTE," in *Vehicular Technology Conference (VTC Spring), 2012 IEEE 75th*, pp. 1–5, May 2012.

[32] 3GPP, "Smart grid traffic behaviour discussion," TSG-RAN R2-102340, 2012.

[33] J. Poncela, J. Moreno-Roldan, M. Aamir, and B. Alvi, "M2M challenges and opportunities in 4G," *Wireless Personal Communications*, pp. 1–14, 2015.

[34] "Health informatics - PoC medical device communication - part 00101: Guide–guidelines for the use of rf wireless technology," Dec. 2008.

[35] R. Ratasuk, A. Prasad, Z. Li, A. Ghosh, and M. Uusitalo, "Recent advancements in M2M communications in 4G networks and evolution towards 5G," in *Intelligence in Next Generation Networks (ICIN), 2015 18th International Conference on*, pp. 52–57, IEEE, 2015.

[36] S. Lien, K. Chen, and Y. Lin, "Toward ubiquitous massive accesses in 3GPP machine-to-machine communications.," *IEEE Communications Magazine*, 2011.

[37] D. Boswarthick, O. Hersent, and O. Elloumi, *M2M communications : a system's approach*. Oxford: Wiley-Blackwell, 2012.

[38] J. Chou, "Machine-to-machine (M2M) communications using short message services (SMS)," may 2014. EP Patent App. EP20,110,869,333.

[39] L. Andres, A. Luis, and A. Jesus, "Is the random access channel of LTE and LTE-A suitable for M2M communications? a survey of alternatives," *IEEE Communications Surveys and Tutorials*, pp. 4–16, 2014.

[40] 3GPP, "Study on facilitating machine to machine communication in 3GPP systems," TR 22.868, Mar. 2007.

[41] 3GPP, "Study on provision of low-cost machine type communication (MTC) user equipments (UEs) based on LTE," Tech. Rep. 36.888 V12.0.0, 3rd Generation Partnership Project (3GPP), Jun. 2013.

[42] "The ICT EXALTED project (2010)."

[43] A. Bartoli, M. Dohler, J. Hernández-Serrano, A. Kountouris, and D. Barthel, "Low-power low-rate goes long-range: the case for secure and cooperative machine-to-machine communications," in *NETWORKING 2011 Workshops*, pp. 219–230, Springer, 2011.

[44] A. Gotsis, A. Lioumpas, and A. Alexiou, "Evolution of packet scheduling for machine-type communications over LTE: algorithmic design and performance analysis," in *Workshops Proceedings of the Global Communications Conference, GLOBECOM 2012, 3-7 December 2012, Anaheim, California, USA*, 2012.

[45] "LOLA (achieving low-latency in wireless communications)." [Online; accessed 14-October-2015].

[46] IEEE, "IEEE 802.16p machine-to-machine (M2M) system requirements document," ts, Sept. 2011.

[47] 3GPP, "Architecture enhancements to facilitate communications with packet data networks and applications," Tech. Rep. TS 23.682 V 12.4.0, July 2015.

[48] Nokia, "LTE-M – optimizing LTE for the internet of things," white paper, 2015.

[49] F. Rayal, "Shaping cellular IoT connectivity: Emerging technologies in wide-area connectivity," 2015.

[50] R. Y. Kim, "Snoop based group communication scheme in cellular machine-to-machine communications," in *Information and Communication Technology Convergence (ICTC), 2010 International Conference on*, pp. 380–381, IEEE, 2010.

[51] C. Tu, C. Ho, and C. Huang, "Energy-efficient algorithms and evaluations for massive access management in cellular based machine to machine communications," in *Vehicular Technology Conference (VTC Fall), 2011 IEEE*, pp. 1–5, Sept 2011.

[52] C. Ho and C. Huang, "Energy-saving massive access control and resource allocation schemes for M2M communications in ofdma cellular networks," *Wireless Communications Letters, IEEE*, vol. 1, pp. 209–212, June 2012.

[53] A. Azari and G. Miao, "Energy efficient MAC for cellular-based M2M communications," in *Signal and Information Processing (GlobalSIP), 2014 IEEE Global Conference on*, pp. 128–132, Dec 2014.

[54] C. Pereira and A. Aguiar, "Towards efficient mobile M2M communications: Survey and open challenges," *Sensors*, vol. 14, no. 10, pp. 19582–19608, 2014.

[55] M. Gupta, S. Jha, A. Koc, and R. Vannithamby, "Energy impact of emerging mobile internet applications on LTE networks: issues and solutions," *Communications Magazine, IEEE*, vol. 51, pp. 90–97, February 2013.

[56] T. Tirronen, A. Larmo, J. Sachs, B. Lindoff, and N. Wiberg, "Reducing energy consumption of LTE devices for machine-to-machine communication," in *Globecom Workshops (GC Wkshps), 2012 IEEE*, pp. 1650–1656, IEEE, 2012.

[57] 3GPP, "Study on machine-type communications (MTC) and other mobile data applications communications enhancements," TS 23.887 V12.03, 3GPP, 2013.

[58] S. Jha, A. Koc, and et al., "Power saving mechanisms for M2M communication over LTE networks," in *Communications and Networking (BlackSeaCom), 2013 First International Black Sea Conference on*, July 2013.

[59] H. Chao, Y. Chen, and J. Wu, "Power saving for machine to machine communications in cellular networks," in *GLOBECOM Workshops (GC Wkshps), 2011 IEEE*, Dec. 2011.

[60] S. Jha, A. Koc, and R. Vannithamby, "Device power saving mechanisms for low cost MTC over LTE networks," in *Communications Workshops (ICC), 2014 IEEE International Conference on*, June 2014.

[61] A. Aijaz and A. Aghvami, "On radio resource allocation in LTE networks with machine-to-machine communications," in *Proceedings of the 77th IEEE Vehicular Technology Conference, VTC Spring 2013, Dresden, Germany, June 2-5, 2013*, 2013.

[62] A. Aijaz, M. Tshangini, M. Nakhai, and et al., "Energy-efficient uplink resource allocation in LTE networks with M2M/H2H co-existence under statistical QoS guarantees," *IEEE Transactions on Communications*, 2014.

[63] Y. Zhang, "Tree-based resource allocation for periodic cellular M2M communications," *Wireless Communications Letters, IEEE*, Dec 2014.

[64] G. Madueno, C. Stefanovic, and P. Popovski, "Reliable reporting for massive M2M communications with periodic resource pooling," *Wireless Communications Letters, IEEE*, Aug 2014.

[65] S. Lien and K. Chen, "Massive access management for QoS guarantees in 3GPP machine-to-machine communications," *IEEE Communications Letters*, March 2011.

[66] K. Ko, M. Kim, and et al., "A novel random access for fixed-location machine-to-machine communications in OFDMA based systems.," *IEEE Communications Letters*, no. 9, pp. 1428–1431, 2012.

[67] X. M. Zhang, Y. Zhang, F. Yan, and A. V. Vasilakos, "Interference-based topology control algorithm for delay-constrained mobile ad hoc networks," *IEEE Transactions on Mobile Computing*, vol. 14, no. 4, pp. 742–754, 2015.

[68] Y. Niu, Y. Li, D. Jin, L. Su, and A. V. Vasilakos, "A survey of millimeter wave communications (mmWave) for 5G: opportunities and challenges," *Wireless Networks*, vol. 21, no. 8, pp. 2657–2676, 2015.

[69] Y. Niu, C. Gao, Y. Li, L. Su, D. Jin, and A. V. Vasilakos, "Exploiting device-to-device communications in joint scheduling of access and backhaul for mmWave small cells," *IEEE Journal on Selected Areas in Communications*, vol. 33, no. 10, pp. 2052–2069, 2015.

[70] S. Plass, M. Berioli, and R. Hermenier, "Concept for an M2M communications infrastructure via airliners," in *Future Network & Mobile Summit (FutureNetw), 2012*, pp. 1–8, IEEE, 2012.

[71] 3GPP, "Evolved universal terrestrial radio access (EUTRA); user equipment (UE) procedures in idle mode (release 11)," TS 36.304 V11.3.0, 3GPP, Mar. 2013.

[72] A. G. Gotsis, N. T. Koutsokeras, and P. Constantinou, "Radio resource allocation and packet scheduling strategies for single-cell OFDMA packet networks," in *Vehicular Technology Conference, 2007. VTC-2007 Fall. 2007 IEEE 66th*, pp. 1847–1851, IEEE, 2007.

[73] D. López-Pérez, X. Chu, A. V. Vasilakos, and H. Claussen, "On distributed and coordinated resource allocation for interference mitigation in self-organizing LTE networks," *IEEE/ACM Transactions on Networking (TON)*, vol. 21, no. 4, pp. 1145–1158, 2013.

[74] M. Ding, D. Lopez-Perez, R. Xue, A. V. Vasilakos, and W. Chen, "Small cell dynamic TDD transmissions in heterogeneous networks," in *Communications (ICC), 2014 IEEE International Conference on*, pp. 4881–4887, IEEE, 2014.

[75] A. S. Lioumpas and A. Alexiou, "Uplink scheduling for machine-to-machine communications in LTE-based cellular systems," in *GLOBECOM Workshops (GC Wkshps), 2011 IEEE*, pp. 353–357, IEEE, 2011.

[76] D. T. Wiriaatmadja and K. W. Choi, "Hybrid random access and data transmission protocol for machine-to-machine communications in cellular networks," *IEEE Transactions on Wireless Communications*, vol. 14, no. 1, pp. 33–46, 2015.

[77] B. Yang, G. Zhu, W. Wu, and Y. Gao, "M2M access performance in LTE-A system," *Transactions on Emerging Telecommunications Technologies*, vol. 25, no. 1, pp. 3–10, 2014.

[78] M. Hasan, E. Hossain, and D. Niyato, "Random access for machine-to-machine communication in LTE-advanced networks: issues and approaches," *Communications Magazine, IEEE*, vol. 51, pp. 86–93, June 2013.

[79] W. Xu and G. Campbell, "A near perfect stable random access protocol for a broadcast channel," in *Communications, 1992. ICC '92*, Jun 1992.

[80] H. S. Dhillon, H. C. Huang, and et al., "Power-efficient system design for cellular-based machine-to-machine communications," *Wireless Communications, IEEE Transactions on*, 2013.

[81] C. S. Bontu, S. Periyalwar, and M. Pecen, "Wireless wide-area networks for internet of things: An air interface protocol for iot and a simultaneous access channel for uplink iot communication," *Vehicular Technology Magazine, IEEE*, vol. 9, no. 1, pp. 54–63, 2014.

[82] M. Khoshkholgh, Y. Zhang, K. Shin, V. Leung, and S. Gjessing, "Modeling and characterization of transmission energy consumption in machine-to-machine networks," in *Wireless Communications and Networking Conference (WCNC), 2015 IEEE*, pp. 2073–2078, IEEE, 2015.

[83] C. Goursaud and J.-M. Gorce, "Dedicated networks for IoT: PHY/MAC state of the art and challenges," *EAI endorsed transactions on Internet of Things*, 2015.

[84] N. Abramson, "The ALOHA system: another alternative for computer communications," in *Proceedings of the November 17-19, 1970, fall joint computer conference*, pp. 281–285, ACM, 1970.

[85] R. O. LaMaire, A. Krishna, and M. Zorzi, "On the randomization of transmitter power levels to increase throughput in multiple access radio systems," *Wireless Networks*, vol. 4, no. 3, pp. 263–277, 1998.

[86] E. Altman, D. Barman, A. Benslimane, and R. El Azouzi, "Slotted aloha with priorities and random power," in *NETWORKING 2005. Networking Technologies, Services, and Protocols; Performance of Computer and Communication Networks; Mobile and Wireless Communications Systems*, pp. 610–622, Springer, 2005.

[87] X. Yang, A. O. Fapojuwo, and E. E. Egbogah, "Performance analysis and parameter optimization of random access backoff algorithm in LTE," in *Vehicular Technology Conference (VTC Fall), 2012 IEEE*, pp. 1–5, IEEE, 2012.

[88] J. J. Nielsen, D. M. Kim, G. C. Madueno, N. K. Pratas, and P. Popovski, "A tractable model of the LTE access reservation procedure for machine-type communications," in *2015 IEEE Global Communications Conference (GLOBECOM)*, pp. 1–6, IEEE, 2015.

[89] G. Bianchi, "Performance analysis of the IEEE 802.11 distributed coordination function," *IEEE Journal on selected areas in communications*, vol. 18, no. 3, pp. 535–547, 2000.

[90] S. Zozor, Z. Li, Q. Lampin, and J.-M. Brossier, "Time-frequency ALOHA-like random access: A scalability study of low-power wide-area networks for IoT using stochastic geometry," *arXiv preprint arXiv:1606.04791*, 2016.

[91] C. Goursaud and Y. Mo, "Random unslotted time-frequency ALOHA: Theory and application to IoT UNB networks," in *2016 23rd International Conference on Telecommunications (ICT)*, pp. 1–5, IEEE, 2016.

[92] M. E. Bayrakdar, S. Atmaca, and A. Karahan, "A slotted ALOHA-based cognitive radio network under capture effect in Rayleigh fading channels," *Turkish Journal of Electrical Engineering & Computer Sciences*, vol. 24, no. 3, pp. 1955–1966, 2016.

[93] S. P. Meyn and R. L. Tweedie, *Markov chains and stochastic stability*. Springer Science & Business Media, 2012.

[94] D. Dardari, V. Tralli, and R. Verdone, "On the capacity of slotted Aloha with rayleigh fading: the role played by the number of interferers," *IEEE Communications Letters*, vol. 4, no. 5, pp. 155–157, 2000.

[95] S. M. Ross, *Introduction to probability models*. Academic press, 2014.

[96] A. H. Nuttall, "Numerical evaluation of cumulative probability distribution functions directly from characteristic functions," tech. rep., DTIC Document, 1969.

[97] W. C. Y. Lee, *Mobile Communications Design Fundamentals*. New York, NY, USA: John Wiley & Sons, Inc., 2nd ed., 1992.

[98] S. Asmussen, J. L. Jensen, and L. Rojas-Nandayapa, "On the Laplace transform of the Lognormal distribution," *Methodology and Computing in Applied Probability*, vol. 18, no. 2, pp. 441–458, 2016.

[99] R. M. Corless, G. H. Gonnet, D. E. Hare, D. J. Jeffrey, and D. E. Knuth, "On the lambertw function," *Advances in Computational mathematics*, vol. 5, no. 1, pp. 329–359, 1996.

[100] J. Gil-Pelaez, "Note on the inversion theorem," *Biometrika*, vol. 38, no. 3-4, pp. 481–482, 1951.

[101] A. Hirsa, *Computational methods in finance*. CRC Press, 2012.

[102] O. Georgiou and U. Raza, "Low power wide area network analysis: Can LoRa scale?," *IEEE Wireless Communications Letters*, vol. 6, no. 2, pp. 162–165, 2017.

[103] M. Haenggi, *Stochastic geometry for wireless networks*. Cambridge University Press, 2012.

[104] D. J. Daley and D. Vere-Jones, *An introduction to the theory of point processes: volume II: general theory and structure*. Springer Science & Business Media, 2007.

[105] B. François and B. Bartłomiej, "Stochastic geometry and wireless networks. volume i. theory," *NoW PublishersBreda*, 2009.

[106] F. Baccelli, B. Błaszczyszyn, *et al.*, "Stochastic geometry and wireless networks: Volume II Applications," *Foundations and Trends® in Networking*, vol. 4, no. 1–2, pp. 1–312, 2010.

[107] H. ElSawy, E. Hossain, and M. Haenggi, "Stochastic geometry for modeling, analysis, and design of multi-tier and cognitive cellular wireless networks: A survey," *IEEE Communications Surveys & Tutorials*, vol. 15, no. 3, pp. 996–1019, 2013.

[108] M. Haenggi, J. G. Andrews, F. Baccelli, O. Dousse, and M. Franceschetti, "Stochastic geometry and random graphs for the analysis and design of wireless networks," *IEEE Journal on Selected Areas in Communications*, vol. 27, no. 7, 2009.

[109] S. N. Chiu, D. Stoyan, W. S. Kendall, and J. Mecke, *Stochastic geometry and its applications*. John Wiley & Sons, 2013.

[110] F. Baccelli, M. Klein, M. Lebourges, and S. Zuyev, "Géométrie aléatoire et architecture de réseaux," *Annals of Telecommunications*, vol. 51, no. 3, pp. 158–179, 1996.

[111] F. Baccelli, M. Klein, M. Lebourges, and S. Zuyev, "Stochastic geometry and architecture of communication networks," *Telecommunication Systems*, vol. 7, pp. 209–227, Jun 1997.

[112] F. Baccelli, B. Blaszczyszyn, and P. Muhlethaler, "An Aloha protocol for multihop mobile wireless networks," *IEEE Transactions on Information Theory*, vol. 52, no. 2, pp. 421–436, 2006.

[113] T. D. Novlan, H. S. Dhillon, and J. G. Andrews, "Analytical modeling of uplink cellular networks," *IEEE Transactions on Wireless Communications*, vol. 12, no. 6, pp. 2669–2679, 2013.

[114] M. Gharbieh, H. ElSawy, A. Bader, and M.-S. Alouini, "Tractable stochastic geometry model for IoT access in LTE networks," in *Global Communications Conference (GLOBECOM), 2016 IEEE*, pp. 1–7, IEEE, 2016.

[115] M. Haenggi and R. K. Ganti, *Interference in large wireless networks*. Now Publishers Inc, 2009.

[116] B. Błaszczyszyn and P. Mühlethaler, "Stochastic analysis of non-slotted ALOHA in wireless ad-hoc networks," in *INFOCOM, 2010 Proceedings IEEE*, pp. 1–9, IEEE, 2010.

[117] R. K. Ganti and M. Haenggi, "Spatial and temporal correlation of the interference in aloha ad hoc networks," *IEEE Communications Letters*, vol. 13, no. 9, 2009.

[118] T. T. Vu, *Spatial models for cellular network planning*. PhD thesis, Télécom ParisTech, 2012.

[119] T.-T. Vu, L. Decreusefond, and P. Martins, "An analytical model for evaluating outage and handover probability of cellular wireless networks," *Wireless personal communications*, vol. 74, no. 4, pp. 1117–1127, 2014.

[120] J. G. Andrews, A. K. Gupta, and H. S. Dhillon, "A primer on cellular network analysis using stochastic geometry," *arXiv preprint arXiv:1604.03183*, 2016.

[121] Y.-P. E. Wang, X. Lin, A. Adhikary, A. Grovlen, Y. Sui, Y. Blankenship, J. Bergman, and H. S. Razaghi, "A primer on 3GPP narrowband internet of things," *IEEE Communications Magazine*, vol. 55, no. 3, pp. 117–123, 2017.

[122] U. Raza, P. Kulkarni, and M. Sooriyabandara, "Low power wide area networks: An overview," *IEEE Communications Surveys & Tutorials*, vol. 19, no. 2, pp. 855–873, 2017.

[123] H. S. Dhillon and J. G. Andrews, "Downlink rate distribution in heterogeneous cellular networks under generalized cell selection," *IEEE Wireless Communications Letters*, vol. 3, no. 1, pp. 42–45, 2014.

[124] P. Madhusudhanan, J. G. Restrepo, Y. Liu, T. X. Brown, and K. R. Baker, "Downlink performance analysis for a generalized shotgun cellular system," *IEEE Transactions on Wireless Communications*, vol. 13, no. 12, pp. 6684–6696, 2014.

[125] J. G. Andrews, F. Baccelli, and R. K. Ganti, "A tractable approach to coverage and rate in cellular networks," *IEEE Transactions on Communications*, vol. 59, no. 11, pp. 3122–3134, 2011.

[126] B. Błaszczyszyn and P. Mühlethaler, "Interference and SINR coverage in spatial non-slotted Aloha networks," *Annals of telecommunications*, vol. 70, no. 7-8, pp. 345–358, 2015.

[127] G. E. Crooks, "Logistic approximation to the logistic-normal integral," tech. rep., Citeseer, 2009.

[128] J. G. Proakis, *Digital Communications 5th Edition*. McGraw Hill, 2007.

[129] J. P. Nolan, *Stable Distributions - Models for Heavy Tailed Data*. Boston: Birkhauser, 2018. In progress, Chapter 1 online at http://fs2.american.edu/jpnolan/www/stable/stable.html.

[130] X. Lagrange, P. Godelewski, and S. Tabbane, "Réseaux GSM: des principesa la norme," 2000.

[131] AT&T, "Frequently asked questions regarding 2G sunset," 2014. [Online; accessed 27-October-2015].

[132] G. C. Madueno, C. Stefanovic, and P. Popovski, "How many smart meters can be deployed in a GSM cell?," in *Communications Workshops (ICC), 2013 IEEE International Conference on*, pp. 1263–1268, IEEE, 2013.

[133] G. C. Madueno, Č. Stefanović, and P. Popovski, "Reengineering GSM/GPRS towards a dedicated network for massive smart metering," in *Smart Grid Communications (SmartGridComm), 2014 IEEE International Conference on*, pp. 338–343, IEEE, 2014.

[134] C. You and Y. Zhang, "A radio resource scheduling scheme for periodic M2M communications in cellular networks," in *Wireless Communications and Signal Processing (WCSP)*, 2014.

[135] 3GPP, "Evolved universal terrestrial radio access (E-UTRAN);medium access control(MAC)," TS 36.321 V11.2.0, 3GPP, Mar. 2013.

[136] J.-M. Kelif, M. Coupechoux, and P. Godlewski, "A fluid model for performance analysis in cellular networks," *EURASIP Journal on Wireless Communications and Networking*, vol. 2010, no. 1, p. 435189, 2010.

[137] P. Mogensen, W. Na, I. Z. Kovács, F. Frederiksen, A. Pokhariyal, K. I. Pedersen, T. Kolding, K. Hugl, and M. Kuusela, "LTE capacity compared to the shannon bound," in *Vehicular Technology Conference, 2007. VTC2007-Spring. IEEE 65th*, pp. 1234–1238, IEEE, 2007.

[138] M. Coupechoux and J.-M. Kelif, "How to set the fractional power control compensation factor in LTE?," in *Sarnoff Symposium, 2011 34th IEEE*, pp. 1–5, IEEE, 2011.

Appendix A

Proof of Lemmas and theorems used in this thesis

Sum of a random number of random variables

Theorem A.0.1. *Consider a compound random number $S = \sum_{i=1}^{N} X_i$, where X_i are independent identically distributed, N follows Poisson distribution and is independent from X_i. Let S be 0 if $N = 0$. The Laplace transform of compound random variable S is $\mathscr{L}\{S\}(\theta) = \exp\lambda(\mathscr{L}\{X\}(\theta) - 1)$.*

Proof. The Laplace transform of S is:

$$\mathscr{L}\{S\}(\theta) = \mathbb{E}\left[e^{-\theta S}\right] = \sum_{n\geq 0} \mathbb{E}\left[e^{-\theta S}|N = n\right]\mathbb{P}(N = n)$$

We have $\mathbb{E}\left[e^{-\theta S}|N = 0\right] = 1$, moreover, for $n \geq 1$,

$$\mathbb{E}\left[e^{-\theta S}|N = n\right] = \prod_{i=1}^{n} \mathbb{E}\left[e^{-\theta X_i}\right] = (\mathscr{L}\{X\}(\theta))^n$$

The probability generating function $G_N(z)$ of N is:

$$G_N(z) = \sum_{n\geq 0} z^n \mathbb{P}(N = n)$$

With substitution $z = \mathscr{L}\{X\}(\theta)$, we have:

$$\mathscr{L}\{S\}(\theta) = \sum_{n\geq 0} (\mathscr{L}_X[\theta])^n \mathbb{P}(N = n) = G_N(\mathscr{L}\{X\}(\theta))$$

If N follows Poisson distribution with mean λ, its probability generating function $G_N(z) = e^{\lambda(z-1)}$. Thus the corresponding Laplace transform is as follows:

$$\mathscr{L}\{S\}(\theta) = \exp\lambda\left(\mathscr{L}\{X\}(\theta) - 1\right) \tag{A.1}$$

□

Laplace transform of the product of two random variables

Theorem A.0.2. *Let X be a random variable of log-normal distribution, $\log(X) \sim N\left(0, \sigma^2\right)$, Y be an exponential distribution random variable with mean μ, the Laplace transform of random variable $Z = XY$ is:*

$$\mathscr{L}\{f_Z(z)\}(s) = \frac{1}{1 + (\mu s)^{1/\sqrt{1+\pi\sigma^2/8}}}, s > 0 \tag{A.2}$$

Proof. The density function $f_X(x)$ is as follows:

$$f_X(x) = \frac{1}{\sqrt{2\pi}\sigma x} \exp\left\{-\frac{\ln^2(x)}{2\sigma^2}\right\}, x > 0$$

The probability density function$f_Y(y)$ is:

$$f_Y(y) = \frac{1}{\mu_Y} \exp -\frac{y}{\mu_Y}, y \geq 0$$

For random variable $Z = XY$. Its probability density function $f_Z(z)$ is as follows:

$$f_Z(z) = \int_0^\infty f_X(x) f_Y\left(\frac{z}{x}\right) \frac{1}{x} dx, z > 0$$

The Laplace transform of Z is as follows:

$$\begin{aligned}
\mathscr{L}\{f_Z(z)\}(s) &= \int_0^{+\infty} e^{-sz} f_Z(z)\, dz \\
&= \int_0^{+\infty} \frac{f_X(x)}{x} \left[\int_0^\infty e^{-sz} f_Y\left(\frac{z}{x}\right) dz\right] dx \\
&= \int_0^{+\infty} \frac{f_X(x)}{\mu x} \left[\int_0^\infty e^{\left\{-z\left(s+\frac{1}{\mu x}\right)\right\}} dz\right] dx
\end{aligned}$$

It just need to consider the case where $s \geq 0$, thus

$$\mathscr{L}\{f_Z(z)\}(s) = \int_0^{+\infty} \frac{1}{\mu x s + 1} \cdot \frac{1}{\sqrt{2\pi}\sigma x} \exp\left\{-\frac{\ln^2(x)}{2\sigma^2}\right\} dx$$

With substitution $\ln(x) = t, x = e^t, t \in \mathbb{R}$, thus

$$\begin{aligned}\mathscr{L}\{f_Z(z)\}(s) &= \int_{-\infty}^{+\infty} \frac{1}{\mu s e^t + 1} \cdot \frac{1}{\sqrt{2\pi}\sigma} \exp\left\{-\frac{t^2}{2\sigma^2}\right\} dt \\ &= \int_{-\infty}^{+\infty} \frac{\phi(t)}{1 + \exp - \left(\frac{t - \frac{\ln(\mu s)}{\sigma}}{\frac{1}{\sigma}}\right)} dt, \end{aligned} \tag{A.3}$$

where $\phi(t)$ is the standard normal distribution probability density function.

The term $\left\{1 + \exp - \left(\frac{t - \frac{\ln(\mu s)}{\sigma}}{\frac{1}{\sigma}}\right)\right\}^{-1}$ is a logistic function. The logistic function can be closely approximated by the error function via the following formula [127].

$$\frac{1}{1 + \exp(-\frac{x}{\alpha})} \approx \frac{1}{2} + \frac{1}{2}\mathrm{erf}(\frac{\sqrt{\pi}}{4\alpha}x) = \Phi\left(\sqrt{\frac{\pi}{8}}\frac{x}{\alpha}\right), \tag{A.4}$$

where $\Phi(t)$ is the cumulative distribution function of standard normal distribution.

With approximation formula (A.4), formula (A.3) can be further simplified:

$$\begin{aligned}\mathscr{L}\{f_Z(z)\}(s) &= \int_{-\infty}^{+\infty} \Phi\left(\sqrt{\frac{\pi}{8}}\sigma\left(t - \frac{\ln(\mu s)}{\sigma}\right)\right)\phi(t)\,dt \\ &= Pr\left\{X_1 \leq \sqrt{\frac{\pi}{8}}\sigma\left(X_2 - \frac{\ln(\mu s)}{\sigma}\right)\right\} \\ &= Pr\left\{X_1 - \sqrt{\frac{\pi}{8}}\sigma X_2 \leq -\frac{\ln(\mu s)}{2}\sqrt{\frac{\pi}{2}}\right\}\end{aligned}$$

where X_1, X_2 are independent standard normal random variable. Obviously, $X_1 - \sqrt{\frac{\pi}{8}}\sigma X_2 \sim \mathscr{N}\left(0, 1 + \frac{\pi}{8}\sigma^2\right)$. Hence,

$$\begin{aligned}\mathscr{L}\{f_Z(z)\}(s) &= Pr\left\{\frac{X_1 - \sqrt{\frac{\pi}{8}}\sigma X_2}{\sqrt{1 + \frac{\pi}{8}\sigma^2}} \leq -\frac{\ln(\mu s)}{\sqrt{\frac{8}{\pi} + \sigma^2}}\right\} \\ &= \frac{1}{2} + \frac{1}{2}\mathrm{erf}\left\{-\frac{\ln(\mu s)}{\sqrt{\frac{16}{\pi} + 2\sigma^2}}\right\}\end{aligned} \tag{A.5}$$

Applying (A.4) for (A.5), we have:

$$\begin{aligned}\mathscr{L}\{f_Z(z)\}(s) &\approx \frac{1}{1+\exp\left\{\left(1+\frac{\pi\sigma^2}{8}\right)^{-\frac{1}{2}}\ln(\mu s)\right\}} \\ &= \frac{1}{1+(\mu s)^{1/\sqrt{1+\pi\sigma^2/8}}}, s>0\end{aligned}$$

□

Integral computation details with background noise (Chapter 5)

Lemma A.0.3. *Consider an integral* $M=\int_0^{+\infty}\exp(-Ur^2-Vr)dr$ *where* $U\geq 0, V\geq 0$, $\mathrm{erf}(\cdot)$ *we finally arrive at:*

$$M=\frac{\sqrt{\pi}}{2}\sqrt{\frac{1}{U}}\exp(\frac{V^2}{4U})\left[1-\mathrm{erf}(\frac{V}{2\sqrt{U}})\right] \tag{A.6}$$

Proof. The mathematical operations are detailed as follows:

$$\begin{aligned}M &= \int_0^{+\infty}\exp(-Ur^2-Vr)dr \\ &= \exp(\frac{V^2}{4U})\int_0^{+\infty}\exp(-U(r^2+\frac{V}{U}r+\frac{V^2}{4U^2}))dr \\ &= \exp(\frac{V^2}{4U})\int_0^{+\infty}\exp(-U(r+\frac{V}{2U})^2)dr \\ &= \exp(\frac{V^2}{4U})\int_{\frac{V}{2U}}^{+\infty}\exp(-Uz^2)dz \\ &= \frac{1}{\sqrt{U}}\exp(\frac{V^2}{4U})\int_{\frac{V}{2\sqrt{U}}}^{+\infty}\exp(-z^2)dz \\ &= \frac{1}{\sqrt{U}}\exp(\frac{V^2}{4U})\left[\int_0^{+\infty}\exp(-z^2)dz-\int_0^{\frac{V}{2\sqrt{U}}}\exp(-z^2)dz\right] \\ &= \frac{1}{\sqrt{U}}\exp(\frac{V^2}{4U})\left[\frac{\sqrt{\pi}}{2}-\int_0^{\frac{V}{2\sqrt{U}}}\exp(-z^2)dz\right]\end{aligned} \tag{A.7}$$

Recall the error function is defined as follows:

$$\operatorname{erf}(x) = \frac{2}{\sqrt{\pi}} \int_0^x \exp(-t^2) dt \tag{A.8}$$

Thus,

$$\begin{aligned} M &= \frac{1}{\sqrt{U}} \exp(\frac{V^2}{4U}) \left[\frac{\sqrt{\pi}}{2} - \frac{\sqrt{\pi}}{2} \operatorname{erf}(\frac{V}{2\sqrt{U}}) \right] \\ &= \frac{\sqrt{\pi}}{2} \sqrt{\frac{1}{U}} \exp(\frac{V^2}{4U}) \left[1 - \operatorname{erf}(\frac{V}{2\sqrt{U}}) \right] \end{aligned} \tag{A.9}$$

□

Appendix B

Mécanismes d'accès radio pour la télécommunication de type machine massive dans les réseaux sans fil à longue portée

B.1 Contexte de la thèse

La télécommunication de type machine (MTC), aussi connue sous le nom de M2M, est une technologie émergente permettant aux terminaux de communiquer mutuellement sans intervention humaine (ou seulement limitée). Ce mode de communication sans fil devrait devenir plus populaire au cours de la prochaine décennie et faire partie intégrante des futurs réseaux sans fil [14][19].

MTC présente beaucoup de caractéristiques spécifiques: occupation souvent plus importante (par rapport à la liaison descendante) sur la liaison montante, une transmission courte mais plus fréquente, un grand nombre de périphériques et des difficultés pour changer de batterie [21]. Les caractéristiques susmentionnées posent des problèmes aux systèmes sans fil déployés actuels pour gérer le trafic de MTC. Par exemple, un grand nombre de dispositifs déployés peut rapidement congestionner le réseau d'accès radio, ce qui entraîne un taux élevé de collision et de retransmission et une faible efficacité énergétique. Cependant, ces terminaux n'ont généralement pas d'alimentation électrique et ne peuvent pas être facilement remplacés par une nouvelle batterie. Par conséquent, comment la meilleure façon de servir efficacement une quantité énorme d'appareils est une préoccupation primordiale pour les opérateurs de réseaux mobiles.

De nos jours, les efforts de recherche pour MTC dans les futurs réseaux sans fil, peuvent être classés en deux catégories:

- Conception des réseaux à longue portée dédiés au M2M, c'est-à-dire les nouveaux LPWAN (Low Power Wide Area Network). Un exemple représentatif est le LoRaWAN [12] proposé par LoRa Alliance [22];
- Évolution des réseaux sans fil existants, qui consiste à adapter les réseaux cellulaires 3GPP pour supporter le trafic MTC en plus du trafic H2H, par exemple le LTE-M [23].

Peu importe la direction de la recherche, la performance du mécanisme d'accès radio, utilisé dans les réseaux d'accès, est d'une importance vitale pour réduire le taux de collision et obtenir efficacité énergétique plus élevée. Par conséquent, la performance et le choix du mécanisme d'accès radio dans les réseaux sans fil compatibles M2M est le principal objectif de nos études.

B.2 Contributions

Les contributions de cette thèse sont résumées dans les points suivants:

- Nous faisons état de l'art sur les études liées à l'efficacité énergétique des MTC de la littérature. La contribution principale de cette enquête est de passer en revue, classifier les travaux de recherche existants dans différentes catégories, et de comparer les avantages et les inconvénients entre les catégories. Nous parlons également les progrès de l'étude liée au LPWAN.
- Nous étudions l'impact de la diversité de puissance d'émission dans les systèmes LPWAN en slotted-ALOHA. La diversité de puissance d'émission consiste à varier la puissance d'émission entre différentes transmissions. Dans ce travail, nous considérons également le contrôle de puissance imparfait et analysons les performance dans trois scénarios différents. Quelques directives de conception sont obtenues en manipulant le modèle analytique établi.
- Nous étudions les performances du système LPWAN avec la diversité de la réception macros. Par la géométrie stochastique, nous obtenons des formules simples de forme fermée pour le taux de perte de paquets et le débit spatial, qui étaient inconnus auparavant. Ces formules sont très utiles pour analyser les réseaux LPWAN (en particulier dans les zones urbaines) et pour quantifier le gain de capacité du système. En rassemblant plusieurs résultats disponibles sur l'analyse de l'ALOHA pure, nous obtenons finalement un cadre de synthèse pour étudier le RAN de LPWAN.

- En termes d'adaptations au RAN des réseaux LTE, nous analysons d'abord le mécanisme d'accès aléatoire conventionnel dans LTE et identifions les inefficacités existantes. Nous proposons ensuite un service d'interrogation multipériodique pour les cas d'utilisation M2M périodiques. Le service proposé est comparé au mécanisme d'accès aléatoire conventionnel inclus dans le système LTE dans un modèle fluide. Les résultats numériques montrent que le service proposé réduit considérablement la consommation des ressources système telles que l'identificateur temporaire de réseau radio (RNTI), le bloc de ressources (RB) et a une efficacité énergétique supérieure en raison de l'évitement de la procédure d'accès aléatoire et des messages de signalisation associés.

B.3 Analyse de la diversité de la puissance d'émission dans S-ALOHA LPWAN

Le protocole S-ALOHA a récemment regagné de l'intérêt dans les études des réseaux LPWAN. Nous étudions l'impact de la stratégie de diversité de puissance d'émission avec un contrôle de puissance imparfait sur les performances de LPWAN à base de S-ALOHA. Les mesures de performance qui nous intéressent sont le taux de perte de paquets, le débit, l'efficacité énergétique et le nombre moyen de transmissions.

Pour cela, nous proposons un modèle analytique peu complexe mais également précis, et conduisons l'analyse pour trois types de réseaux:

- Système avec contrôle de puissance parfait et sans fading;
- Système large bande avec contrôle de puissance imparfait;
- Système bande étroite avec contrôle de puissance imparfait.

Le modèle proposé est capable de faciliter le dimensionnement et la conception de LPWAN à base de S-ALOHA. La comparaison entre la simulation et les résultats analytiques confirme l'exactitude du modèle proposé. À partir du modèle analytique établi, nous obtenons quelques lignes directrices sur la conception de LPWAN à base de S-ALOHA. Par exemple, la Fig. B.1 montre que, dans les systèmes à bande large avec un taux de capture de 3 dB, le contrôle de puissance imparfait a un impact positif sur la stratégie de diversité de puissance de transmission identique mais a un impact négatif sur les stratégies incrémentales et décrémentales. Pour concevoir un système LPWAN ayant comme contrainte un taux de perte de paquets inférieur et qui prend en charge plus de périphériques, la stratégie de diversité de puissance de transmission incrémentale est un bon choix. Pour concevoir un

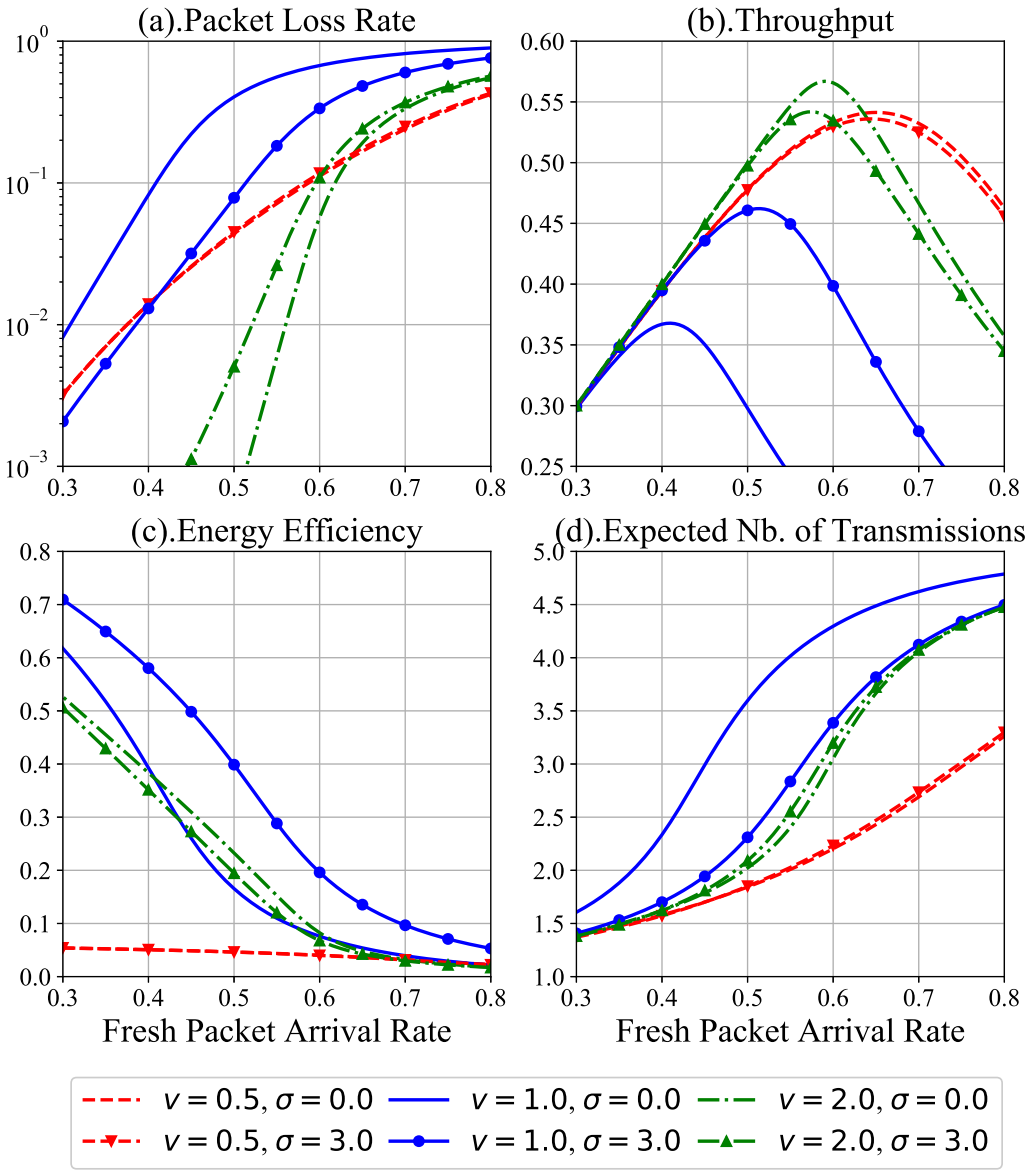

Fig. B.1 Comparaison de performances entre différentes stratégies de diversités de puissance de transmission dans des systèmes à large bande. SINR seuil 3 dB

système à faible latence et sans contrainte d'efficacité énergétique, une stratégie de diversité décroissante est recommandée. Dans les systèmes à bande étroite qui souffrent d'un évanouissement de Rayleigh, l'impact d'un contrôle de puissance imparfait sur le système est faible comparé au cas des systèmes à large bande. L'avantage de la stratégie décrémentale en termes de délai n'est plus significatif. Ainsi, la stratégie de puissance d'émission identique lors d'une retransmission est la plus appropriée.

B.4 Analyse de la diversité macro dans les réseaux LPWAN

Dans les réseaux cellulaires, le paquet est envoyé en mode unicast: la station de base cible est indiquée par le terminal. Cependant, il pourrait également être envoyé en mode broadcast, et bénéficier de la diversité de réception macro. En raison de ses avantages, la diversité de réception macro a été appliquée par certains réseaux LPWAN, tels que Sigfox et LoRaWAN [24]. Dans ce travail, nous présentons d'abord deux formes possibles de diversité

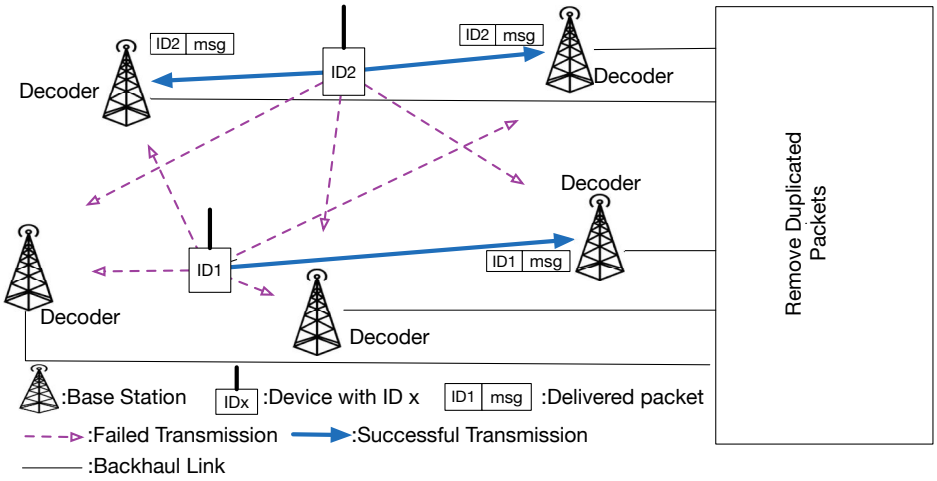

Fig. B.2 Illustration de diversité de réception macro de type combinaison sélective (SC). Chaque BS est équipée d'une fonction de décodage de paquet. Le paquet décodé est envoyé au coeur du réseau et ce dernier est en charge des paquets dupliqués

de réception macro: la combinaison sélective (Fig. B.2) et la combinaison de ratio maximum (Fig. B.3). A la base des efforts de recherche en géométrie stochastique disponibles, nous dérivons ensuite les formules simples de forme fermée, couvrant pure-ALOHA et slotted-ALOHA, sur la perte de paquets et le débit spatial. Ces formules sont très utiles pour analyser les réseaux LPWAN (en particulier dans les zones urbaines) et pour quantifier le gain apporté par la diversité macro. Avce des simulations, la précision du modèle proposé est confirmée. Nous observons que les systèmes avec la diversité de réception macro peut

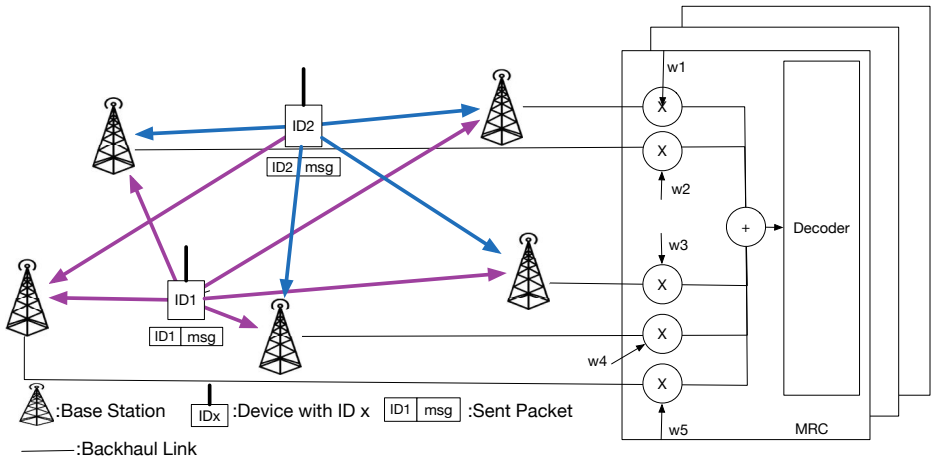

Fig. B.3 Illustration de diversité de réception macro de type combinaison de taux maximum (MRC)

bénéficier de l'effet d'ombrage. Avec un exposant de l'affaiblissement sur le trajet 4, une contrainte de taux de perte de paquets 10% et 8 dB d'ombrage, la capacité de l'ALOHA pur avec diversité macro de type combinaison sélective et de type combinaison de ratio maximum sont respectivement au moins 2 et 3,42 fois plus élevés que dans les systèmes dans lesquels un terminal ne transmet qu'à la meilleure BS.

Ensuite, nous étendons l'étude pour analyser un nouvel indicateur de performance du réseau appelé 'probabilité d'outage' qui est associée à un taux de perte de réseau cible. A partir des résultats numériques, nous constatons qu'avec une probabilité d'outage de 10% associée à un taux de perte de paquets réseau de 10%, la macro diversité sélective supporte encore 80% de capacité système par rapport au cas sans contrainte de probabilité d'outage.

B.5 Service d'interrogation multi-périodes dédié à M2M périodique dans les réseaux LTE

De nos jours, une grande partie du trafic MTC présente une périodicité [29]. Malheureusement, la procédure traditionnelle d'accès aléatoire de LTE n'est pas suffisament efficace pour traiter ce genre de trafic. Nous proposons un service d'interrogation multiple-période. Ce service peut être intégré au réseau d'accès radio LTE, entièrement compatible avec le mécanisme d'accès standard et est capable de gérer une large palette de périodes d'interrogation (typiquement de 1 minute à 28 jours).

Le service proposé est composé de deux phases: la phase d'enregistrement et la phase d'interrogation. Pendant la phase d'enregistrement, un terminal envoie sa période de report-

ing et demande l'activation du service d'interrogation auprès de l'eNB. La phase d'enregistrement se fait par une procédure d'accès aléatoire conventionnelle. Après réception d'une telle requête, l'eNB répond avec un message de confirmation qui comprend l'allocation de la fenêtre d'interrogation et du règle d'interrogation. Une fois la phase d'enregistrement terminée, le terminal est en phase d'interrogation périodique. A cette phase, pour chaque trame LTE, l'eNB manipule la numéro de trame système et détermine que la fenêtre d'interrogation courante est réservée pour quel terminal MTC en vérifiant les règles d'interrogation stockées. Quant au terminal, il surveille également la valeur de LSFN. Si le terminal MTC n'a pas d'action spécifique, il peut passer en mode veille afin d'économiser de l'énergie. Dès que le besoin existe, le terminal écoute le PDCCH pendant toute la fenêtre d'interrogation. Il appartient à l'eNB d'allouer des ressources radio de liaison montante afin de permettre la transmission de données du terminal MTC. Notons que l'identifier temporaire de réseau est alloué à un seul terminal pendant une fenêtre d'interrogation donnée. Les mécanismes d'allocation de ressources système standard peuvent être utilisées sans risque de collision. Cette procédure est illustrée dans la Fig. B.4. Le mécanisme traditionnel d'accès aléatoire et notre proposition sont comparés en termes de consommation RNTI (Radio Network Temporary Identifier) et RB (Resource Block). Les résultats numériques montrent qu'avec le service proposé, un eNodeB (eNB) peut facilement prendre en charge dispositifs contenant jusqu'à 15000 MTC sans collision d'accès au réseau. En ce qui concerne la consommation de RB, notre proposition économise $5,76$ paires de RB pour la liaison descendante et 3 paires de RB pour la liaison montante.

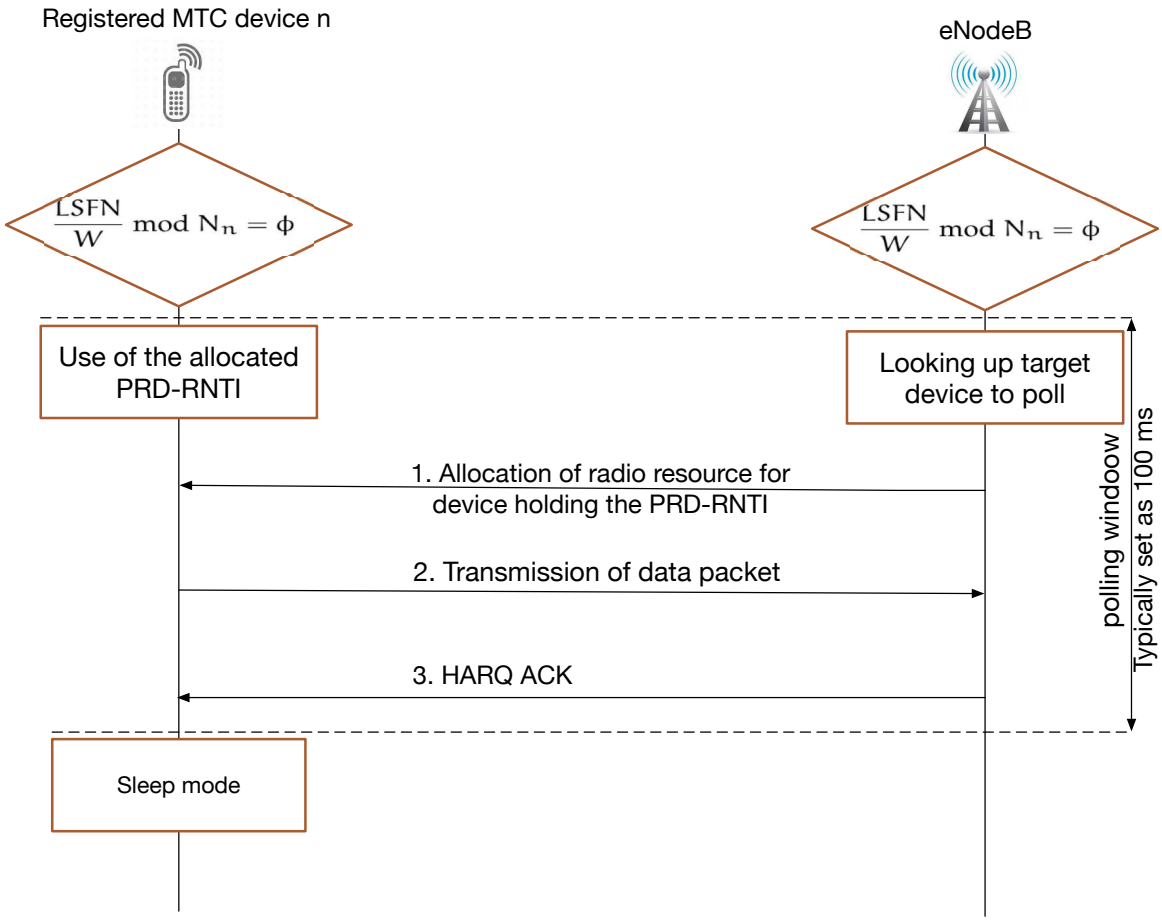

Fig. B.4 Illustration du service d'interrogation proposé

Résumé

En tant qu'étape importante vers une société intelligente, hormis la communication d'humain à humain (H2H), les réseaux sans fil de l'avenir devraient prendre en charge la communication machine-à-machine (également connue sous le nom de MTC). Ce dernier est un nouveau paradigme de communication dans lequel les terminaux peuvent parler les uns avec les autres sans ou avec peu d'intervention humaine. Avec la prolifération rapide des applications M2M, un grand nombre de terminaux seront déployés dans de nombreux types d'applications telles que le comptage intelligent, l'automatisation de l'industrie, la télésanté, etc.

Cependant, les réseaux sans fil actuels ne sont toujours pas prêts pour écouler correctement le trafic des MTC. La raison en est double. Tout d'abord, l'évolution du réseau sans fil vise à augmenter le débit et à réduire le délai. Deuxièmement, les caractéristiques spéciales des MTC, telles qu'un nombre très élevé de terminaux déployés, une petite charge utile mais une transmission fréquente, un emplacement souvent d'installation défavorable, etc., font que les exigences de H2H ne sont pas partagés par la plupart des cas d'utilisation M2M.

À partir de l'état de l'art, nous distinguons deux orientations de recherche possibles pour gérer efficacement le trafic M2M: Low Power Wide Area Network (LPWAN) et adaptation des réseaux cellulaires existants. Pour les deux pistes, les mécanismes d'accès radio, utilisés dans le réseau d'accès radio (RAN) sont d'une importance vitale pour assurer le succès de MTC. De ce point de vue, le mécanisme d'accès radio est le principal objectif de nos études. Dans cette thèse, nous présentons les contributions couvrant les aspects susmentionnés.

Les contributions de cette thèse sont résumées dans les points suivants:

Nous faisons état de l'art sur les études liées à l'efficacité énergétique des MTC de la littérature. La contribution principale de cette enquête est de passer en revue, classifier les travaux de recherche existants dans différentes catégories, et de comparer les avantages et les inconvénients entre les catégories. Nous parlons également des progrès de l'approche basée sur les LPWAN.

Nous étudions l'impact de la diversité du niveau de puissance d'émission et du contrôle de puissance imparfait sur les systèmes LPWAN en slotted-ALOHA. Quelques directives de conception perspicaces sont obtenues en manipulant le modèle analytique établi.

Nous étudions les performances du système LPWAN avec la diversité de la réception macro. En utilisant la géométrie stochastique, nous établissons des formules simples de forme fermée pour le taux de perte de paquets et le débit spatial. Ces formules sont très utiles pour analyser les réseaux LPWAN (en particulier dans les zones urbaines) et pour quantifier le gain de capacité du système. En rassemblant plusieurs résultats disponibles sur l'analyse de l'ALOHA pure, nous obtenons finalement un cadre de synthèse pour étudier le RAN de LPWAN.

En termes d'adaptations au RAN des réseaux LTE, nous analysons d'abord le mécanisme d'accès aléatoire conventionnel dans LTE et identifions les inefficacités existantes. Nous proposons ensuite un service d'interrogation multipériodique pour les cas d'utilisation M2M périodiques. Le service proposé est comparé au mécanisme d'accès aléatoire conventionnel en LTE dans un modèle fluide. Les résultats numériques montrent que le service proposé réduit considérablement la consommation des ressources système telles que l'identificateur temporaire de réseau radio (RNTI), le bloc de ressources (RB) et a une efficacité énergétique supérieure en raison de l'évitement de la procédure d'accès aléatoire et des messages de signalisation associés.

Mots clefs : M2M, ALOHA, LPWAN, Macro reception diversity, LTE

Abstract

As a key step toward a smart society, apart from the Human-to-Human (H2H) communication, the future wireless networks, are expected to accommodate Machine-to-Machine Communication (also known as Machine Type Communication (MTC)). The latter is a new communication paradigm in which the devices can talk with each other without or with little human intervention. With the rapid proliferation of M2M applications, a huge number of devices will be deployed in many types of use cases such as smart metering, industry automation, e-health, etc.

However, the current wireless networks are still not ready to hold traffic from MTC. The reason is twofold. First, the evolution of the wireless network seeks for higher throughput and lower latency. Second, the special features that MTC exhibits, such as huge number of deployed devices, small payload but frequent transmission, adverse installation location, etc., lead to that the requirements by H2H are no longer required by most of M2M use cases.

From the state-of-the-art work, we find that two possible research orientations to efficiently handle M2M traffic: Low Power Wide Area Network (LPWAN) and adaption of the existing cellular networks. For both of them, the radio access mechanisms, used in Radio Access Network (RAN), is vitally important to make MTC a promising technology. From this view, radio access mechanism is the main focus of our studies. In this thesis, we present the contributions covering the aforementioned aspects: performance evaluation of ALOHA-based LPWAN networks, and a polling service that is an extension to RAN of LTE networks for periodic M2M traffic.

The contributions of this thesis are summarized on the following axis:

We make a survey about the energy efficiency related studies in the literatures. The main contribution in this survey is to review, classify the existing research works into different categories, and compare the pros and cons between categories. We also review the advances of the LPWAN related study.

We study the impact of transmit power level diversity and imperfect power control to the slotted ALOHA based LPWAN systems. Some insightful design guidelines are obtained by manipulating the established analytical model.

We study the performance of LPWAN system with macro reception diversity. By stochastic geometry, we get simple closed-form formulas for the packet loss rate and spatial throughput, which were unknown before. These formulas are very useful to analyze LPWAN networks (especially in urban areas) and to quantify the system capacity gain. By gathering several available results about the analysis of non slotted ALOHA, we finally get a synthesis framework to study the RAN of LPWAN.

In terms of adaptations to RAN of LTE networks, we first analyze the conventional random access mechanism in LTE and identify the existing inefficiencies. We then propose a multiple period polling service for periodic M2M use cases. The proposed service is compared with conventional random access mechanism in LTE in a fluid model. The numerical results show that the proposed service dramatically reduces the consumption of system resources such as Radio Network Temporary Identifier (RNTI), Resource Block (RB) and has a higher energy efficiency due to the avoidance of random access procedure and related signaling messages.

Keywords: M2M, ALOHA, LPWAN, Macro reception diversity, LTE

IMT Atlantique
Bretagne-Pays de la Loire
École Mines-Télécom

N° d'ordre : 2017IMTA0047

IMT Atlantique Bretagne-Pays de la Loire - www.imt-atlantique.fr

Campus de Brest
Technopôle Brest-Iroise
CS 83818
29238 Brest Cedex 03
T +33 (0)2 29 00 11 11
F +33 (0)2 29 00 10 00

Campus de Nantes
4, rue Alfred Kastler - La Chantrerie
CS 20722
44307 Nantes Cedex 3
T +33 (0)2 51 85 81 00
F +33 (0)2 51 85 81 99

Campus de Rennes
2, rue de la Châtaigneraie
CS 17607
35576 Cesson Sévigné Cedex
T +33 (0)2 99 12 70 00
F +33 (0)2 99 12 70 08